Editors' Suggestion

Crystallographic splitting theorem for band representations and fragile topological photonic crystals

A. Alexandradinata, ¹ J. Höller, ² Chong Wang, ³ Hengbin Cheng, ^{4,5} and Ling Lu^{4,6}

(Received 8 January 2020; accepted 19 August 2020; published 9 September 2020)

The fundamental building blocks in band theory are band representations—bands whose infinitely numbered Wannier functions are generated (by action of a space group) from a finite number of symmetric Wannier functions centered on a point in space. This paper aims to simplify questions on a multirank band representation by splitting it into unit-rank bands via the following crystallographic splitting theorem: Being a rank-N band representation is equivalent to being splittable into a finite sum of bands indexed by $\{1, 2, \dots, N\}$, such that each band is spanned by a single, analytic Bloch function of k, and any symmetry in the space group acts by permuting $\{1, 2, \dots, N\}$. We prove this theorem for all band representations (of crystallographic space groups) whose Wannier functions transform in the integer-spin representation; in the half-integer-spin case, the only exceptions to the theorem exist for three-spatial-dimensional space groups with cubic point groups. Applying this theorem, we develop computationally efficient methods to determine whether a given energy band (of a tight-binding or Schrödinger-type Hamiltonian) is a band representation and, if so, how to numerically construct the corresponding symmetric Wannier functions. Thus we prove that rotation-symmetric topological insulators in Wigner-Dyson class AI are fragile, meaning that the obstruction to symmetric Wannier functions can be removed by addition of band representations to the filled-band subspace. An implication of fragility is that its boundary states, while robustly covering the bulk energy gap in finite-rank tight-binding models, can be destabilized if the Hilbert space is expanded to include all symmetry-allowed representations. These fragile insulators have photonic analogs that we identify; in particular, we prove that an existing photonic crystal built by Yihao Yang et al. [Nature 565, 622 (2019)] is fragile topological with removable boundary states, which disproves a widespread perception of "topologically protected" boundary states in time-reversal-invariant, gapped photonic/phononic crystals. As a final application of our theorem, we derive various symmetry obstructions on the Wannier functions of topological insulators; for certain space groups, these obstructions are proven to be equivalent to the nontrivial holonomy of Bloch functions.

DOI: 10.1103/PhysRevB.102.115117

I. INTRODUCTION

Solid-state physicists have predominantly held that to know a band is to specify its properties in the space of crystal momentum k [1–4]. The crystallographic space-group symmetry of a band is specified by the different representations of little groups (in k space) [5,6], their compatibility relations [7–11], and associated energy degeneracies [12–16].

As pioneered by Zak [17,18], a real-space formulation of bands specifies how a space group G transforms an infinite set of exponentially localized Wannier functions distributed over a real-space lattice. Zak proposed that the fundamental building blocks of bands are *band representations* (BRs): bands whose infinitely numbered Wannier functions are generated (by action of G) from a finite number of symmetric Wannier functions centered at a point in space (known as a Wyckoff position). An intuitive example of a BR is the Hilbert space of any tight-binding lattice model. Unfortunately, it is generally

difficult to identify if an energy band (of a tight-binding or Schrödinger-type Hamiltonian) is a BR because one would not *a priori* know the Wyckoff position or the symmetry representation of the Wannier functions.

Such an identification would confer the following advantages: (i) one may utilize comprehensive databases for the *k*-space symmetry representations and compatibility relations of BRs, which have been tabulated in the Bilbao crystallographic server [19]; (ii) some BRs exhibit symmetry-fixed Berry-Zak phases [20,21] which are measurable in transport [21] and cold-atomic experiments [21–23]; and (iii), conversely, *not* being a BR manifests in various physical implications, which may include nontrivial *k*-space holonomy [20,21,24–26], quantum entanglement [11,27–31], and robust boundary states [32–39].

Following Zak's *real-space* definition of BRs, one may heuristically test if an energy band—given numerically by a set of Bloch functions on a *k* mesh—is a BR. Namely,

¹Department of Physics and Institute for Condensed Matter Theory, University of Illinois at Urbana-Champaign, Urbana, Illinois 61801, USA

²Department of Physics, Yale University, New Haven, Connecticut 06520, USA

³Institute for Advanced Study, Tsinghua University, Beijing 100084, China

⁴Institute of Physics, Chinese Academy of Sciences/Beijing National Laboratory for Condensed Matter Physics, Beijing 100190, China

⁵School of Physical Sciences, University of Chinese Academy of Sciences, Beijing 100049, China

⁶Songshan Lake Materials Laboratory, Dongguan, Guangdong 523808, China

one would postulate trial Wannier functions with a certain symmetry representation and Wyckoff position, then compute the overlap of these trial Wannier functions with the Bloch functions [40–46]. Unfortunately, the possible symmetry representations and Wyckoff positions are numerous in complicated space groups; even if they are correctly chosen for a given BR, it is still possible that a trial Wannier function has zero overlap with a given Bloch function on the k mesh. (It is worth interjecting that several groups have claimed to prove band-representability based on k-space symmetry representations and/or k-space holonomy [47–49]; we will explain why these alleged proofs are merely suggestive, and offer a theorem that makes some of these proofs rigorous.)

With the goal of determining band representability without trial Wannier functions, we propose to reformulate BRs from a topological perspective. This perspective emphasizes the notion of continuity that is fundamental to the topological classification of vector bundles. Applied to band theory, a rank-N vector bundle over the Brillouin torus is simply a band comprising N linearly independent Bloch functions at each k, and if such Bloch functions can be made continuous and periodic over the torus, the band is said to be topologically trivial. In two spatial dimensions, being topologically nontrivial is in one-to-one correspondence with a nontrivial first Chern class [50], which leads to a quantized Hall conductance for band insulators [51].

Our topological formulation of BRs can be formalized by the following *crystallographic splitting theorem*: being a rank-N BR is equivalent to being splittable into a sum of N unit-rank bands (indexed by $\{1, 2, ..., N\}$) which are each topologically trivial, such that any symmetry in the space-group symmetry acts by permuting $\{1, 2, ..., N\}$. Alternatively stated, being a rank-N BR is equivalent to being splittable into N independent sets of exponentially localized Wannier functions, such that each set is obtained by Bravaislattice translations of a single Wannier function, and any space-group symmetry acts by permuting these sets.

Our splitting theorem applies to any BR (of crystallographic space groups) whose Wannier functions transform in the integer-spin representation. For half-integer-spin BRs, the equivalence applies for any space group in two spatial dimensions; exceptions to this equivalence exist only for three-spatial-dimensional space groups with cubic point groups. All the above statements generalize to time-reversal-invariant BRs (in Wigner-Dyson [52] symmetry classes AI and AII), with the semantic replacement of space group by magnetic space group.

In comparing our topological formulation with Zak's real-space formulation, specifying the space group action on a finite set of topologically trivial, unit-rank bands is simpler than specifying the group action on an infinite set of Wannier functions. A considerable volume of the paper is spent on unpacking the conceptual simplifications and physical implications of the crystallographic splitting theorem, which we summarize in the following section. This summary will also serve as a guide to the structure of the paper.

To nip a possible confusion in the bud, we remark that our use of topological triviality (as defined above) is based on the standard definition in the theory of complex vector bundles [53] and coincides with the notion of triviality for Wigner-Dyson class A in the tenfold way [54]. We maintain the same definition of triviality even in the context of time-reversal symmetry: While a time-reversal-symmetric, rank-*N* band (in class AI or AII) is always topologically trivial by our definition, the same band may be decomposed into *N* unit-rank bands which need not individually be trivial. A final word of caution: Many other authors (e.g., in topological quantum chemistry [10] and the method of symmetry-based indicators [11]) have adopted a different definition of triviality, namely, that a trivial band is a BR.

II. SUMMARY AND OUTLINE

Our main technical accomplishment is a topological formulation of BRs, which is formalized by the crystallographic splitting theorem in Sec. IV.

In comparison with the real-space formulation of BRs, the topological formulation is conceptually closer to recent developments in the band-theoretic description of topological insulators. Indeed, the converse of the topological formulation says that a topologically trivial, rank-N band that is *not* band representable is spanned by N sets of exponentially localized Wannier functions which cannot all be permuted by spacegroup symmetry. (Being *band representable* is a convenient shorthand for being a BR.) For this reason, we call a spacegroup-symmetric band—that is *not* band-representabl—an *obstructed representation*. The full implications of this obstruction are explored in Sec. VI. In particular, we will derive three types of constraints on the Wannier functions of topological insulators:

- (i) Wannier functions cannot be localized to a single tightbinding lattice site.
- (ii) Wannier functions in Wigner-Dyson symmetry class AII cannot be fully spin-polarized (analogously, Wannier functions in class AI cannot be fully pseudospinpolarized).
- (iii) Wannier functions cannot form a representation of certain symmetries in the stabilizer of their Wyckoff position.
- (i)–(iii) are readily observable in numerical constructions of Wannier functions for topological insulators, as will be exemplified by topological insulators old and new.

Our topological formulation may be applied to determine if a given energy band is band representable. Our proposed method involves diagonalizing a projected symmetry operator that is a k-dependent Hermitian matrix; if the eigenbands of the projected symmetry operator are eigenvalue nondegenerate and have trivial first Chern class, then the given energy band is guaranteed to be band representable, in accordance with our crystallographic splitting theorem. The advantage of our method is that it can be carried out without having to deal with Wannier functions at all.

For demonstration, we prove in Sec. III that the filled band—of rotation-invariant topological crystalline insulators [36,55] (TCIs) in Wigner-Dyson symmetry class AI—is a *fragile obstructed representation* (FOR). By fragile obstructed, we mean that the filled band has an obstruction to symmetric Wannier functions, but this obstruction is removable by addition of a BR to the filled-band subspace. Once removed, the filled-band subspace is symmetrically deformable to a tight-binding (or "atomic") limit, which is

incompatible with boundary states that robustly cover the bulk energy gap; this statement is separately proven as the *symmetric tight-binding limit theorem* and the *boundary stability criterion* in Sec. IX. This means that if a FOR is accompanied by boundary states that robustly cover the bulk gap in finite-rank, tight-binding models (as exemplified by the above rotation-invariant TCIs), then these boundary states can be destabilized if the Hilbert space is expanded to include all symmetry-allowed representations—we refer to this as a *representation-dependent stability* of boundary states. It is worth remarking that the filled band of this TCI is identical to a BR with regard to its *k*-space symmetry representations, which cautions against generally inferring fragile obstructions or band representability from *k*-space representations alone [56].

While the above rotation-invariant TCIs have thus far not been realized in solid-state materials, we prove in Sec. VIII that their photonic analogs exist in a three-spatial-dimensional tetragonal photonic crystal designed by Tetsuki Ochiai [57] and in an existing hexagonal photonic crystal built by Yihao Yang et al. [58]. While previous theoretical works [58,59] have identified the hexagonal photonic crystal as an analog of the *nonfragile* \mathbb{Z}_2 topological insulator in Wigner-Dyson class AII, our group-theoretic analysis identifies it properly as an analog of the fragile \mathbb{Z} TCI [36] in class AI. The hexagonal photonic crystal is then a materialization of fragile topology with removable boundary states. These three-spatial-dimensional tetragonal and hexagonal crystals complement two recently designed, two-spatial-dimensional photonic crystals [49,60] which have been claimed to be fragile based on different crystallographic symmetries that we specify below.

While we have advertised that band representability can be proven without constructing Wannier functions, sometimes these functions are intrinsically desirable for other practical reasons, e.g., to analyze the formation of chemical bonds [41] to investigate the electronic polarization of disordered/distorted insulators [41] or to construct a lowerrank, tight-binding model which possibly includes many-body interactions. Thus motivated, we present in Sec. VII a numerical algorithm to construct symmetric Wannier functions—for any BR that satisfies the crystallographic splitting theorem.

The advantage of our method is that it is ansatz-free, that is, it does not require the user to guess a set of trial Wannier functions, unlike many existing methods [40–45,61].

As a final application of the topological formulation of BRs, we prove in Sec. V an equivalence between the obstruction of symmetric Wannier functions and nontrivial k-space holonomy; the latter is a geometric property of Bloch functions that is encoded in the Zak phase. This equivalence holds for point groups which are generated by time reversal and/or spatial inversion. As cases in point, a fragile obstruction against spatial-inversion-symmetric Wannier functions was explored theoretically in Refs. [20,21,31,62-64] and may even have a photonic analog [49,60]; a stable obstruction against time-reversal-symmetric Wannier functions characterizes bands with \mathbb{Z}_2 Kane-Mele topological order [10,43]; a fragile obstruction against spacetime-inversion-symmetric Wannier functions [31,47,65] is possibly realized by the nearly flat bands of twisted bilayer graphene [66,67]. While these examples having been studied extensively from the dual perspectives of k-space holonomy and symmetric Wannier obstructions, the equivalence of both perspectives is established here.

We have chosen to discuss the fragility of TCIs [cf. Sec. III] before the formal statement of the crystallographic splitting theorem [cf. Sec. IV]. This order of consumption is recommended for physically motivated readers who are versed in the theory of topological band insulators. However, a mathematically oriented reader who is less interested in our idiosyncratic application may skip to the splitting theorem in Sec. IV, which is written to be self-contained. Almost every other section should be consumed after having read Sec. IV. One possible exception is our case study of fragile topological photonic crystals in Sec. VIII, which is the recommended starting point for members in the photonics community.

This completes the summary of our results. For the reader's convenience, we have drawn in Fig. 1 a concept map for the various sections of this paper. The main results are recapitulated in the final Discussion section of Sec. X, where we also provide an outlook. Included in Appendix A is a review of basic notions in band theory, space groups, and bundle theory; this review may also be used as a glossary of specialized terms, which the reader may refer to when needed.

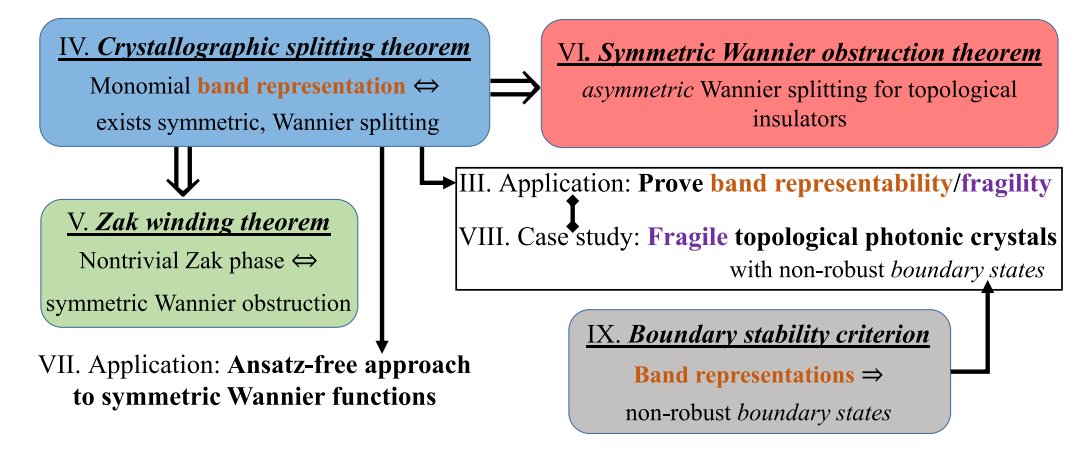


FIG. 1. Concept map of the sections in this paper, with Secs. III–IX indicated.

III. CASE STUDY: FRAGILE TOPOLOGICAL CRYSTALLINE INSULATORS IN CLASS AI

In Sec. III A, we will first give a pedagogical introduction to three-dimensional, rotation-invariant TCIs in Wigner-Dyson symmetry class AI, focusing on aspects that identify them as obstructed representations. One particular aspect—having boundary states with a representation-dependent stability—will be a recurrent theme in the subsequent Secs. VIII and IX.

Underlying the proof of fragility for this TCI is the crystal-lographic splitting theorem, which we will introduce casually in Sec. III B with a simple example. After these preliminaries, the proof begins properly in Sec. III C.

A. Topological crystalline insulators as obstructed representations of space groups

As theoretically proposed by Liang Fu in Ref. [55], the first-known TCI has space group $G_4 = \mathcal{T}_3 \rtimes C_{4v} \times \mathbb{Z}_2^T$, which is also the symmetry of the tetragonal photonic crystal. In general, \mathcal{T}_d denotes a translational group of a d-dimensional crystal, C_{nv} (n=2,3,4,6) denotes a point group generated by an n-fold rotation and a mirror plane that contains the rotational axis, and \mathbb{Z}_2^T is the order-two group generated by time reversal T; T^2 equaling the identity means we are in Wigner-Dyson class AI. The semidirect product \rtimes structure of G_4 reflects that G_4 is a symmorphic space group, as briefly reviewed in Appendix A 2.

We will focus on known qualities of the TCI that identify its filled band as an *obstructed representation of* G_4 . By obstructed representation, we mean that the projector (denoted $P_{\rm OR}$) to the filled band is invariant under all elements of G_4 , but the filled band is *not* a BR of G_4 .

A tight-binding model for the G_4 -symmetric TCI was first proposed by Liang Fu on a tetragonal lattice [55]. The tight-binding vector space consists of Wannier functions defined over two sublattices indexed by $\alpha = 1, 2$. On each sublattice, the Wannier functions transform as a rank-two BR of G_4 . By Zak's standard definition, a BR is an induced representation of a space group, as briefly reviewed in Appendix A 3 a. Here we will describe what induction (in our case study) entails:

- (a) Begin with a pair of Wannier functions $\{W_{+,\alpha,0}, W_{-,\alpha,0}\}$ centered at the C_{4v} -invariant Wyckoff position $\boldsymbol{\varpi}_a$, with $W_{\pm,\alpha,0}$ having the symmetry of a $p_{\pm} := (p_x \pm ip_y)$ orbital; these orbitals transform in the irreducible two-dimensional "vector" representation E of C_{4v} , the site stabilizer of $\boldsymbol{\varpi}_a$; the site stabilizer of a Wyckoff position is the group consisting of all elements of a space group (here, G_4) that preserve the Wyckoff position. Here and henceforth, it should be understood that any Wannier function is exponentially localized, i.e., decaying at least as fast as an exponential function.
- (b) We then generate an infinite set of Wannier functions $\{W_{+,\alpha,R},W_{-,\alpha,R}\}_{R\in BL}$ by Bravais-lattice translations. Throughout this paper, we use R to denote a vector in the Bravais lattice.

With regard to its symmetry properties, a BR $(G, \boldsymbol{\varpi}, D)$ is fully specified by a space group G, Wyckoff position $\boldsymbol{\varpi}$, and a representation D of the corresponding site stabilizer. Our illustrative BRs are denoted as $(G_4, \boldsymbol{\varpi}_a, E; \alpha)$, with $\alpha = 1, 2$

an additional sublattice index. The rank of a BR is the number of independent Wannier functions in one unit cell—two for each of $(G_4, \boldsymbol{\omega}_a, E; \alpha)$.

Suppose we began with a tight-binding Hamiltonian having zero matrix elements between tight-binding Wannier functions centered on distinct lattice sites. We introduce an on-site potential that distinguishes between $(G_4, \boldsymbol{\varpi}_a, E; 1)$ and $(G_4, \boldsymbol{\varpi}_a, E; 2)$, so they are separated by an energy gap throughout the Brillouin zone.

By cleverly tuning the hopping parameters (cf. Eq. (1) in Ref. [55]), Fu induced a momentary touching between low-and high-energy bands, after which the energy gap (at all k) is reestablished. A representative Hamiltonian in this phase is given by

$$H(\mathbf{k}) = \begin{pmatrix} H^{1} & H^{12} \\ H^{12\dagger} & H^{1} \end{pmatrix},$$

$$H^{\alpha}(\mathbf{k}) = 2t_{n}^{\alpha} \begin{pmatrix} \cos k_{x} & 0 \\ 0 & \cos k_{y} \end{pmatrix}$$

$$+ 2t_{nn}^{\alpha} \begin{pmatrix} \cos k_{x} \cos k_{y} & \sin k_{x} \sin k_{y} \\ \sin k_{x} \sin k_{y} & \cos k_{x} \cos k_{y} \end{pmatrix},$$

$$H^{12}(\mathbf{k}) = [t_{n}' + 2t_{nn}' (\cos k_{x} + \cos k_{y}) + t_{2}' e^{ik_{z}}]I, \qquad (1)$$

with H^{α} the Hamiltonian restricted to sublattice $\alpha \in \{1, 2\}$, H^{12} a matrix of intersublattice hoppings, and parameters $t_n^1 = -t_n^2 = 1$, $t_{nn}^1 = -t_{nn}^2 = 0.5$, $t_n' = 2.5$, $t_{nn}' = 0.5$, $t_2' = 2$. The basis chosen in Eqs. (1) is such that $2t_n^1 \cos k_x$ represents the nearest-neighbor hopping of a p_x orbital in sublattice 1.

Let P_{OR} be the projector to the resultant low-energy band. In terms of the symmetry representations of the little group of wave vectors [5], P_{OR} is identical to both $(G_4, \boldsymbol{\varpi}_a, E; \alpha)$ [68]. Nevertheless, there are indications that P_{OR} is *not* band representable: (i) if the tight-binding Hamiltonian is diagonalized with Dirichlet (open boundary) conditions that model a $\mathcal{T}_2 \times C_{4v} \times \mathbb{Z}_2^T$ -symmetric surface, eigensolutions exist which are localized to the surface and whose eigenenergies robustly cover the bulk gap, e.g., see Fig. 10 in Ref. [55]. (ii) P_{OR} also manifests nontrivial holonomy [69], which is incompatible [70] with a BR.

One aspect of the boundary states distinguishes the TCI phase from the well-known \mathbb{Z}_2 Kane-Mele topological insulator. While the TCI boundary states cannot be removed from the bulk gap by continuous deformations of the given tight-binding Hamiltonian (that maintain both symmetry and the bulk gap), the TCI boundary states can be removed from the bulk gap if the given tight-binding Hilbert space is enlarged—by inclusion of a boundary-localized band transforming as a unit-rank BR of $\mathcal{T}_2 \rtimes C_{4v} \rtimes \mathbb{Z}_2^T$ (the symmetry *in the presence of the boundary*) [55]. There are four such unit-rank BRs, corresponding to the four one-dimensional, real representations of $C_{4v} \rtimes \mathbb{Z}_2^T$. In contrast, the TCI boundary states would be robust against the addition of BRs corresponding to the two-dimensional vector representation of $C_{4v} \rtimes \mathbb{Z}_2^T$.

We see that an obstructed representation can be accompanied by boundary states which robustly cover the bulk gap of a finite-rank tight-binding model with a restricted set of symmetry representations, however, such boundary states can be destabilized by expanding the Hilbert space to include all symmetry-allowed representations. This notion of a

representation-dependent stability for boundary states is reminiscent of (but *not* equivalent to) the defining property [62] of a fragile obstructed representation (FORFOR. Namely, a FOR of G_4 is an obstructed representation of G_4 with the property that a BR of G_4 exists, such that the direct sum of this BR with FOR is a higher-rank BR. Schematically, FOR \oplus BR=BR'. We emphasize that all objects in this equality are representations of $G_4 = \mathcal{T}_3 \times C_{4v} \times \mathbb{Z}_2^T$, the space group of a three-dimensional crystal without boundaries; moreover, the projector to each of {FOR,BR,BR'}, if restricted to a wave vector k, is an analytic function (of k) throughout the Brillouin zone [71]. In contrast, the TCI boundary states have the reduced symmetry $\mathcal{T}_2 \times C_{4v} \times \mathbb{Z}_2^T$, and if we insist on distinguishing filled and unfilled boundary states, then the filled states cannot continuously be defined in the boundary Brillouin zone [72].

Proving that P_{OR} is a FOR will occupySecs. III C-III F. The proof might have been simple, if hypothetically the unfilled band (of Liang Fu's tight-binding model) transforms as a BR of G_4 —this would imply FOR \oplus BR=BR', with BR' corresponding to the tight-binding vector space. In fact, the unfilled band is also an obstructed representation [36] which motivates a more general methodology to proving fragility.

Before we begin the proof, we remark that both a non-trivial k-space holonomy and a representation-dependent stability of boundary states also characterize the $\mathcal{T}_3 \rtimes C_{3v} \times \mathbb{Z}_2^T$ -symmetric TCI, which was theoretically proposed in Refs. [36,69]. $\mathcal{T}_3 \rtimes C_{3v} \times \mathbb{Z}_2^T$ is also the symmetry of the hexagonal photonic crystal discussed in Sec. VIII.

B. Casual introduction to the crystallographic splitting theorem

Underlying our proof is a mathematically equivalent reformulation of BRs that comprise Wannier functions with integer-valued spin: Being a rank-N BR is equivalent to being splittable into N independent sets of exponentially localized Wannier functions (denoted $\{P_1, \ldots, P_N\}$), such that (a) each set is derived by Bravais-lattice translations of a single Wannier function and (b) any symmetry in the space group acts to permute $\{P_1, \ldots, P_N\}$. We shall refer to a splitting satisfying (a) as a Wannier splitting, satisfying (b) as a symmetric splitting, and satisfying both (a) and (b) as a symmetric Wannier splitting.

This equivalence is formalized as the crystallographic splitting theorem in Sec. IV, and proven in Appendix C; also discussed therein is the partial generalization to Wannier functions with half-integer-valued spin. While not essential to our proof, we now offer a simple example of a symmetric Wannier splitting to develop intuition.

Example: Symmetric Wannier splitting of $BR(G_4, \varpi_a, E)$

Let $P_{a,E}$ be the rank-two projector of BR $(G_4, \boldsymbol{\varpi}_a, E)$; presently, we omit the sublattice index. As shown in Sec. III A, $P_{a,E} = \sum_{j=\pm} \sum_{\boldsymbol{R}} |W_{j\boldsymbol{R}}\rangle \langle W_{j\boldsymbol{R}}|$ is spanned by a set of Wannier functions transforming (on each site) in the $p_x \pm ip_y$ representation of C_{4v} .

Consider the Wannier splitting $P_{a,E} = P_+ + P_-$, with $P_{\pm} = \sum_{\mathbf{R}} |W_{\pm,\mathbf{R}}\rangle\langle W_{\pm,\mathbf{R}}|$ corresponding to $p_x \pm ip_y$ orbitals on each site [73]. By construction, each unit-rank projector consists of Wannier functions related by Bravais-lattice translations,

hence any translation $\in \mathcal{T}_3$ trivially permutes $\{P_+, P_-\}$. What remains is to determine the permutation actions for the generators of the point group $C_{4v} \times \mathbb{Z}_2^T$. In the $p_x \pm ip_y$ basis, the two-dimensional matrix representation of fourfold rotation (C_4) is diagonal, while that of time reversal (T) and reflection $(\mathfrak{r}_x : (x, y, z) \to (-x, y, z))$ are off-diagonal. It follows that all point-group symmetries act as permutations:

$$[\hat{C}_4, P_{\pm}] = 0, \quad \hat{T}P_+\hat{T}^{-1} = P_-, \quad \hat{\mathfrak{r}}_x P_+\hat{\mathfrak{r}}_x^{-1} = P_-,$$
 (2)

meaning that $P_{a,E} = P_+ + P_-$ is a symmetric Wannier splitting.

The permutation relations in Eq. (2) are deducible from a general observation: For any Wannier splitting of a rank-N representation of space group G, if there exists N representative Wannier functions which are permuted by $g \in G$ [up to a U(1) phase], then g would similarly permute the N unit-rank projectors corresponding to that Wannier splitting [74].

C. An outline for the proof of fragility

Taking the crystallographic splitting theorem as a given [cf. Sec. IV], we now begin the proof of fragility, which is split into three subsections:

- (i) In Sec. III D, we will introduce a systematic method to obtain a symmetric Wannier splitting. This method involves the diagonalization of a projected symmetry operator and will be used in the remainder of the proof.
- (ii) P_{OR} being an obstructed representation of G_4 [cf. Sec. III A] means an obstruction to a symmetric Wannier splitting must exist, which we illustrate in Sec. III E.
- (iii) Finally, in Sec. III F, we prove that a symmetric Wannier splitting exists for the sum of $P_{\rm OR}$ with a unit-rank BR—this would prove that $P_{\rm OR}$ is a FOR of G_4 .

D. Symmetric Wannier splitting via projected symmetry operators

In proving the fragility of $P_{\rm OR}$, we hypothesize the existence of a BR such that $P_{\rm OR} \oplus P_{\rm BR}$ is a band representation BR'. A priori, we would neither know what the Wyckoff position of BR' is nor know the representation of the site stabilizer—without this information, one would not know how $P_{\rm OR} \oplus P_{\rm BR}$ decomposes into a symmetric Wannier splitting. What is desirable is a systematic method to deduce the symmetric Wannier splitting for BRs in any space group. On this front, we have made partial progress that is reported in Appendix D; one of the techniques discussed therein will be applied to the present paper.

To summarize the technique, we propose to diagonalize a symmetry operator that is projected to a hypothesized BR. (Our approach may be viewed as a space-group generalization of the projected spin operator proposed by Prodan in Ref. [75].) The symmetry in our case study is the fourfold rotation C_4 . If a Hermitian matrix representation \tilde{C}_4 of this symmetry is chosen, then the *projected symmetry operator* is a k-dependent Hermitian operator distinct from the original tight-binding Hamiltonian. The projected symmetry operator can be chosen so its eigenbands (assumed nondegenerate in eigenvalue) are permuted by all elements of the space group. Thus, if each eigenband is determined to have trivial first

Chern class, there must exist a basis of exponentially localized Wannier functions for each eigenband, and the corresponding Wannier splitting is symmetric by construction.

E. Obstruction to symmetric Wannier splitting for the filled band of the TCI

While not strictly necessary for the proof of fragility, it is instructive to diagonalize the projected \tilde{C}_4 operator for the obstructed representation $P_{\rm OR}$, for which a symmetric Wannier splitting does *not* exist. How this obstruction manifests (as a nodal-line degeneracy in the projected symmetry spectrum) will help us identify which BR should be summed with $P_{\rm OR}$, such that their sum becomes band representable.

In more detail, the Hermitian representation of C_4 is given by $\tilde{C}_4 = (-i\pi/2) \ln \hat{C}_4$, with \hat{C}_4 the unitary matrix representation of C_4 in the tight-binding basis of Wannier functions. \tilde{C}_4 has two eigenvalues ± 1 which distinguish the $p_x \pm ip_y$ basis vectors; each eigenvalue is doubly degenerate due to the presence of two sublattices. The projected symmetry operator is $\tilde{C}_{4k} := p(k)\tilde{C}_4p(k)$, with $p(k) = \sum_{i=1}^2 |u_{ik}\rangle\langle u_{ik}|$ the rank-two projector the low-energy band of Fu's tight-binding Hamiltonian $h(k) = \sum_{n=1}^4 \varepsilon_{nk}|u_{nk}\rangle\langle u_{nk}|$ (cf. Eq. (2) of Ref. [55]). Like h(k), \tilde{C}_{4k} is periodic under reciprocal-lattice translations and has a fourfold symmetry:

$$\hat{C}_4 \tilde{C}_{4k} \hat{C}_4^{-1} = \tilde{C}_{4, C_4 \circ k}, \quad C_4 \circ k = (-k_y, k_x, k_z).$$
 (3)

However, time reversal and spatial reflection act unconventionally as antisymmetries,

$$\hat{\tau}_x \tilde{C}_{4k} \hat{\tau}_x^{-1} = -\tilde{C}_{4,\tau_x \circ k}, \quad \hat{T} \tilde{C}_{4k} \hat{T}^{-1} = -\tilde{C}_{4,-k},$$
 (4)

because both spacetime transformations nontrivially permute the $p_x \pm i p_y$ basis vectors. The action of \hat{T} is analogous to that of particle-hole conjugation in a Bogoliubov-de Gennes Hamiltonian.

It is vanishingly improbable for the spectrum of \tilde{C}_{4k} to be degenerate—except on a set of k with measure zero. If the spectrum were nondegenerate throughout the Brillouin zone, then the two eigenbands would be permuted trivially by C_4 [cf. Eqs. (3)] and permuted nontrivially by T and \mathfrak{r}_x [cf. Eqs. (4)]. Furthermore, if each nondegenerate eigenband were to have trivial first Chern class (that is, the first Chern number vanishes in any 2D cut of the 3D Brillouin zone), then each eigenband has a basis of exponentially localized Wannier functions [76,77]—the eigenbands would then give a symmetric Wannier splitting, in contradiction with P_{OR} projecting to an obstructed representation. This means one of our assumptions must break down: Either (i) the wave function is nonanalytic at a zero-measure set of k where the spectrum (of \tilde{C}_{4k}) is degenerate or (ii) if the spectrum were everywhere nondegenerate, the first Chern class must be nontrivial. Alternatively stated, for an obstructed representation, the projected symmetry operator must be the Hamiltonian of either a topological semimetal or a Chern insulator.

For this TCI, the obstruction (to a symmetric Wannier splitting) manifests as a nodal-line spectral degeneracy confined to the $k_z = \pi$ slice of the Brillouin torus, as illustrated in Fig. 2(a). To explain the robustness of this nodal line, the group of any wave vector in this slice contains C_2T symmetry—the composition of twofold rotation and time

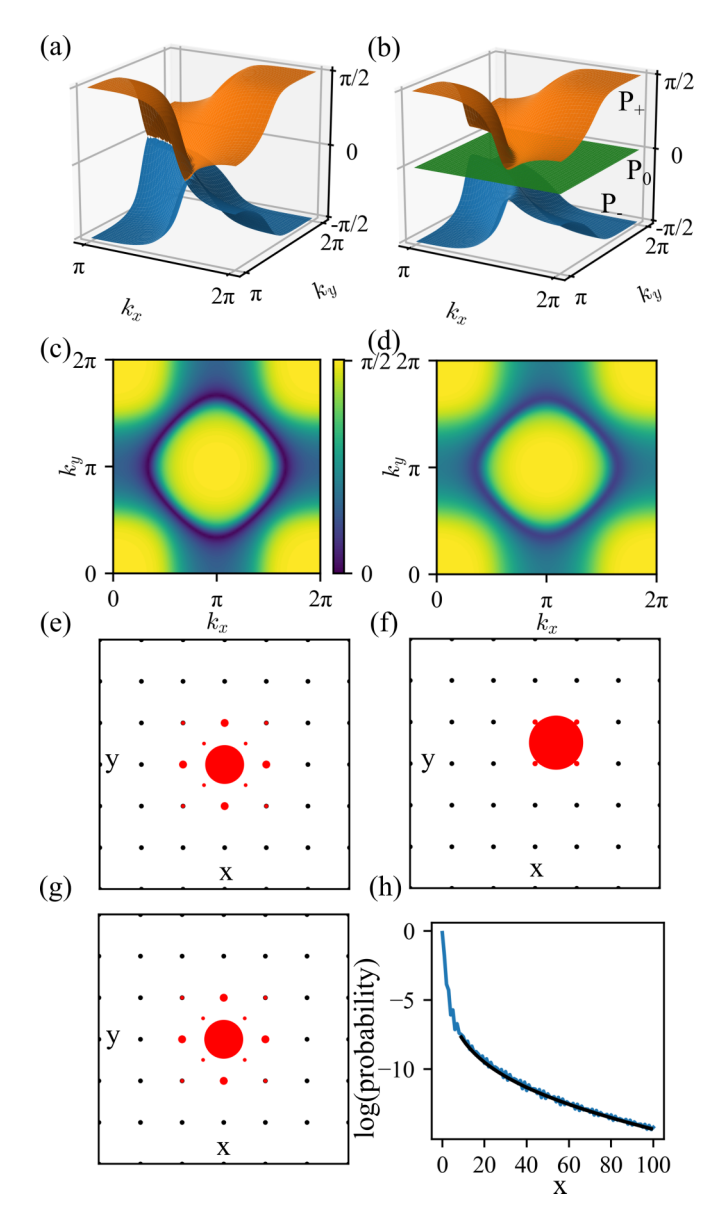


FIG. 2. Removing the symmetric Wannier obstruction for the obstructed representation P_{OR} of $\mathcal{T}_3 \rtimes C_{4v} \times \mathbb{Z}_2^T$. Focusing on the $k_z = \pi$ slice of the Brillouin zone, we illustrate the spectra of the projected rotation operator of P_{OR} [(a),(c)] and $P_{OR} + P_{BR}$ [(b),(d)], with $P_{\rm BR}$ a unit-rank BR. (a), (b) plot the band dispersions over a rotation-reduced quarter of the $k_z = \pi$ slice. (c) shows that the spectral gap (scaled by a factor of half) vanishes over a circular nodal line, while (d) shows the nonvanishing spectral gap between the lowest (P_{-}) and middle (P_{0}) band. The Wannier functions constructed for P_+ , P_0 , and P_- are shown in (e)–(g), respectively. The size of the red dots represents the probability of a representative Wannier function on each tight-binding lattice site (indicated by black dots). For a representative Wannier function in P_{-} , (h) is the plot of its probability distribution (blue curve) along a real-space line; this line is parametrized by x and begins from the Wannier center (x = 0). The tail of this curve is fitted to the exponential function $-2.45562 \exp(-0.0175546x)/x^{2.1928}$, which is plotted as a black curve.

reversal. Acting as an antitunitary antisymmetry, C_2T constrains \tilde{C}_{4k} to be skew symmetric under transpose; there being only one Pauli matrix that is skew symmetric, the

codimension of a twofold eigenvalue degeneracy (for \tilde{C}_{4k}) is unity. This means that the nodal-line degeneracy is at least stable (within the $k_z=\pi$ slice) against symmetric perturbations of \tilde{C}_{4k} . In fact, the nodal-line degeneracy is even stable against any continuous deformation of P_{OR} that preserves symmetry and analyticity (in k). This is because the nodal line is not contractible—it encircles a C_4 -invariant k line, where the spectrum is necessarily gapped due to Bloch states having distinct C_4 eigenvalues.

F. Breaking the obstruction by adding a band representation

The codimension argument for the stability of the nodalline degeneracy relied not just on C_2T symmetry, but also on P_{OR} having rank two. The codimension is generally greater for a threefold eigenvalue degeneracy than it is for a twofold degeneracy.

This suggests the following scenario that is illustrated in Fig. 2: We introduce an additional zero-eigenvalue band *without* interband hybridization, so as to enhance the degeneracy of the nodal line [cf. Fig. 2(a)]; this triple degeneracy is then unstable upon hybridization of bands [cf. Fig. 2(b)]. A zero-eigenvalue band of the projected rotation operator is simply a unit-rank BR induced from a trivial representation of $C_{4v} \times \mathbb{Z}_2^T$, e.g., an *s* orbital on a fourfold invariant Wyckoff position.

To outline the procedure: (i) we expand the tight-binding vector space to include this unit-rank, s-like BR. Initially the s band is introduced below the bulk energy gap (of the tight-binding Hamiltonian), with zero s-p hybridization. (ii) This hybridization is then introduced by way of additional tight-binding matrix elements (detailed in Appendix E), taking care that G_4 symmetry is preserved and the bulk energy gap never closes. (iii) We then rediagonalize the projected rotation operator \tilde{C}_{4k} , with $\tilde{C}_4 = (-i\pi/2) \ln \hat{C}_4$ now having an additional zero eigenvalue and p(k) now a rank-three projector. \tilde{C}_{4k} still satisfies the symmetry constraints of Eqs. (3) and (4), with an appropriate generalization of \hat{T} and $\hat{\tau}_x$.

The resultant spectrum shows three bands which we numerically verify to be nondegenerate (throughout the Brillouin zone) and to have trivial first Chern class [78]. The projectors to the top (P_+) and bottom bands (P_-) are still permuted as in Eq. (2), while the projector P_0 to the zero-eigenvalue band is invariant under all symmetries. In combination, all symmetries in G_4 act as a permutation on $\{P_+, P_0, P_-\}$. Thus $P_{OR} \oplus P_{BR} = P_+ \oplus P_0 \oplus P_-$ is a symmetric Wannier splitting, and must be a BR of G_4 according to the crystallographic splitting theorem in Sec. IV B.

To recapitulate, we have proven that the filled band of the Fu TCI, while transforming as a rank-two obstructed representation of $\mathcal{T}_3 \rtimes C_{4v} \times \mathbb{Z}_2^T$, becomes a rank-three BR upon addition of a unit-rank BR—this means that the Fu TCI phase is fragile obstructed. In an essentially identical fashion, we have proven that the TCI with $\mathcal{T}_3 \rtimes C_{3v} \times \mathbb{Z}_2^T$ symmetry is also fragile obstructed; the details are given in Appendix E 2. Our *rigorous* proofs of fragility are consistent with the topological classification by Zhida *et al.* [79] which has predicted that all obstructed representations in class AI are fragile, based on an *argument* of adiabatic continuity to a topological crystal.

We remark that the projected symmetry operator provides an alternative method to numerically construct symmetric Wannier function without need for trial Wannier functions. Given a symmetric Wannier splitting for a BR (e.g., $P_+ \oplus P_0 \oplus P_-$), half the work is already done. What remains is to numerically construct a basis of Wannier functions for each of $\{P_+, P_0, P_-\}$, such that each Wannier function transforms in a definite representation of $C_{4v} \times \mathbb{Z}_2^T$ on each lattice site. This is accomplished by a numerical algorithm that is described in Sec. VII, and we present the final result for our case study in Figs. 10(e)–2(h).

IV. TOPOLOGICAL FORMULATION OF BAND REPRESENTATIONS

Our topological formulation applies to a class of BRs that are monomial. The notion of *monomial band representations*—which will be introduced in Sec. IV A—naturally generalizes the standard notion of monomial representations in finite-order groups to representations of infinite-order space groups. As we will prove in Sec. IV C, all BRs of space groups in two spatial dimensions (d=2) are monomial; the only exceptions in d=3 exist for double cubic point groups.

A. From monomial representations of point groups to monomial band representations of space groups

Let us briefly review some basic notions in the representation theory of finite groups. We shall primarily be concerned with point groups whose elements are discrete isometries of two- or three-dimensional space; also of interest are magnetic point groups, whose elements are either spatial isometries, or combinations of spatial isometries with time reversal.

A complex, linear representation of a finite group H maps every $h \in H$ to a finite-dimensional, invertible matrix U(h), which may be taken to be unitary without any loss of generality [5]. A monomial representation of a finite group H is defined to be a representation of H induced from a one-dimensional representation of a subgroup of H. (We review the notion of induction in Appendix B; a subgroup H' of H is denoted as H' < H.) A direct sum of monomial representations will also be referred to as a monomial representation. Equivalently, a representation of H is monomial if and only if there exists a basis (for the representation space) where every element of H is mapped to a complex permutation matrix (a permutation matrix whose nonzero matrix elements are generalized to unimodular complex numbers). The proof of this equivalence is provided in Appendix B.

If all irreducible representations (irreps) of H are monomial, then H is referred to as a *monomial group*. As we will see in Sec. IV \mathbb{C} , the great majority of point groups are monomial.

Example of monomial representation of the point group $C_{4v} \times \mathbb{Z}_2^T$. Let E be a two-dimensional representation spanned by $p_x \pm ip_y$ orbitals. The generators of $C_{4v} \times \mathbb{Z}_2^T$ are represented as

$$C_4 \to \begin{pmatrix} +i & 0 \\ 0 & -i \end{pmatrix}; \quad \mathfrak{r}_y, T \to \begin{pmatrix} 0 & 1 \\ 1 & 0 \end{pmatrix}.$$
 (5)

 C_4 is mapped to a complex generalization of the trivial permutation matrix, while \mathfrak{r}_y and T are mapped to the same transposition matrix.

A monomial band representation of a space group G is a BR $(G, \boldsymbol{\varpi}, D)$ for which D is a monomial representation of the site stabilizer $G_{\boldsymbol{\varpi}}$.

Example of monomial band representation. Consider $BR(G=\mathcal{T}_3 \rtimes C_{4v} \times \mathbb{Z}_2^T, \boldsymbol{\varpi}_a, E)$, which make up the tight-binding basis in a model considered in Sec. III A. As described in the previous example, E is a two-dimensional monomial representation of the site stabilizer $G_{\varpi a} = C_{4v} \times \mathbb{Z}_2^T$, and therefore the corresponding BR is monomial.

B. The crystallographic splitting theorem

We propose an equivalent formulation of a monomial BR that emphasizes the topological perspective.

Crystallographic splitting theorem. Let P be a rank-N representation of G. P is a monomial BR of G if and only if there exists a splitting $P = \bigoplus_{i=1}^{N} P_i$ satisfying

- (A) each P_j is analytic (throughout the Brillouin torus) and has trivial first Chern class, and
- (B) G acts as a permutation on $\{P_j\}_{j=1}^N$, i.e., for all $g \in G$, $g: P_j \to P_{\sigma_g(j)}$ with σ_g a permutation on $\{1, \ldots, N\}$.

Having trivial first Chern class means being topologically trivial as a complex vector bundle, as reviewed in Appendix A 1. Being analytic throughout the Brillouin torus means that the restriction of P_j to k is an analytic function of k (for all k in the Brillouin zone), and is periodic in reciprocal-lattice translations. All g in the translational subgroup of G always acts as the trivial permutation on the indices $\{1, \ldots, N\}$. This theorem is proven in Appendix \mathbb{C} .

C. Which band representations are monomial?

The applicability of the crystallographic splitting theorem depends on the generality of monomial BRs, which we summarize in Fig. 3 and explain in the following three remarks:

- (i) All unit-rank BRs are monomial BRs. The reason is that a one-dimensional representation (of a site stabilizer) is automatically a monomial representation. Thus, if P has unit rank, then the splitting theorem simplifies to: P is a BR of G if and only if P is analytic with trivial first Chern class. Condition (B) is trivially satisfied. This unit-rank statement was previously proved by two of us in Ref. [80].
- (ii) All BRs of crystallographic space groups (and grey magnetic space groups) are monomial. By *crystallographic space group* (denoted G), we mean a group of spatial isometries for ($d \leq 3$)-dimensional crystals. A *grey magnetic space group*, denoted G_T , is a direct product of any crystallographic space group G with \mathbb{Z}_2^T , the order-two group generated by time reversal T in Wigner-Dyson class AI. By a BR of G or G_T , we restrict ourselves to linear (i.e., integer-spin) representations of the corresponding site stabilizer. That all BRs of G (and G_T) are monomial follows from a result that we prove in Appendix F: the 32 crystallographic point groups (\mathcal{P}), as well as the 32 grey magnetic point groups ($\mathcal{P} \times \mathbb{Z}_2^T$), are monomial groups. Indeed for any G or G_T , any site stabilizer must be one of the 32 (magnetic) point groups, which are all

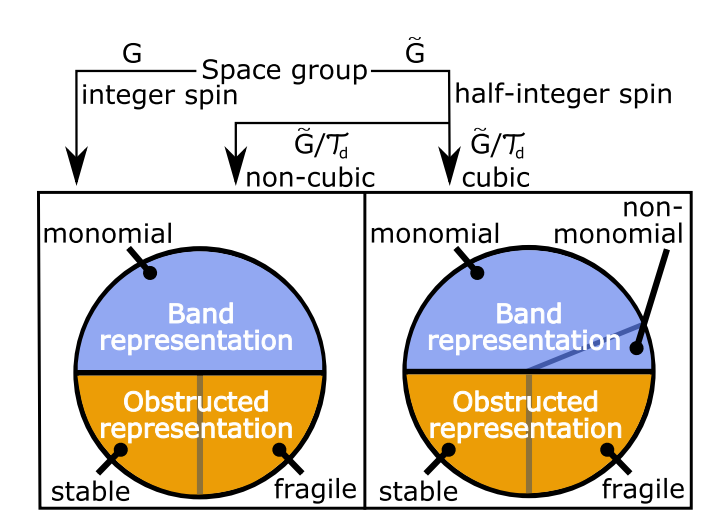


FIG. 3. Flow chart for the categorization of rank-N bands with analytic projector and space-group symmetry, in spatial dimension d=1,2, and 3. Included in this chart are the crystallographic space groups, the grey magnetic space groups, as well as their double covers (which apply to particles with half-integer spin). The translational subgroup of double space group \tilde{G} is denoted as \mathcal{T}_d . For d=3, the point group $(\tilde{G}/\mathcal{T}_d)$ of \tilde{G} is subdivided as cubic versus noncubic; for $d\leqslant 2$, all point groups are noncubic. Rank-N bands with nontrivial first Chern class fall under the category of stable obstructed representations; for rank N=1, having trivial first Chern class is equivalent to being a BR [80].

monomial groups; thus for any BR(G or G_T , $\boldsymbol{\varpi}$, D), D must be a monomial representation.

(iii) In spatial dimension d=2, all BRs of double space groups \tilde{G} , as well as type-1 magnetic double space groups \tilde{G}_T (class AII), are monomial BRs. (The double groups \tilde{G} and \tilde{G}_T are the double covers of G and G_T , respectively, as reviewed in Sec. A 2. We shall only concern ourselves with the half-integer-spin representations of the double groups.) In d=3, there exists BRs (of \tilde{G} or \tilde{G}_T) which are not monomial BRs, owing to the existence of nonmonomial irreducible representations of the *cubic* double point groups (comprising the three tetrahedral groups and the two octahedral groups); we prove in Appendix F that all other double point groups (numbering 32-5=27) are monomial groups. Note the noncubic double point groups of three-dimensional crystals include all double point groups of two-dimensional crystals. Further discussion of the nonmonomial BRs is postponed to Sec. X.

Example of nonmonomial band representation of the double space group G = P23. The point group of this space group is the double cover \tilde{T} of the tetrahedral group, which is isomorphic to the alternating group of four elements—a standard example of a nonmonomial group. A BR of G = P23 that is induced from the two-dimensional representation \bar{E} of the site stabilizer $\tilde{G}_{1a} \approx \tilde{T}$ is nonmonomial, as we show in Appendix F 6 [81].

D. Applications of the crystallographic splitting theorem

(a) The splitting theorem may be applied to prove that a given band P is a (monomial) BR. One approach would be to first decompose $P = \bigoplus_{j=1}^{N} P_j$ into unit-rank projectors

satisfying the symmetry condition (B), namely, that for all $g \in G$, $g: P_j \to P_{\sigma_g(j)}$ with σ_g a permutation on $\{1, \ldots, N\}$. We define this as a *symmetric splitting of P with respect to G*. Having a symmetric splitting, we would then verify (A), e.g., by numerical computation of the winding number of the Zak phase. We have illustrated this approach for fragile obstructed insulators in Sec. III; a systematic methodology for symmetric splitting will be described in Appendix D 1.

- (a') In complementarity with (a), an alternative approach (to proving P is a monomial BR) is to first decompose $P = \bigoplus_{j=1}^N P_j$ into unit-rank projectors satisfying condition (A), namely, that each P_j is analytic (throughout the Brillouin torus) and has trivial first Chern class. Such a splitting will be referred to as a *Wannier splitting of P with respect to G*, because condition (A) guarantees [82] that each P_j has a basis of exponentially localized Wannier functions. Given this Wannier splitting, we would then verify (B). While this alternative approach is possible in principle, we do not know if it is practical. Given the above definitions, $P = \bigoplus_{j=1}^N P_j$ [which satisfies both (A) and (B)] shall also be called a *symmetric Wannier splitting of P with respect to G*.
- (b) The crystallographic splitting theorem implies that any representation of a space group that is not a monomial BR cannot simultaneously satisfy conditions (A) and (B). In particular, (A) and B) cannot simultaneously hold for *obstructed representations* defined as representations of a space group which are not band representable.
- (b) (i) Suppose (A) holds, giving a set of Wannier functions that span P, then [not (B)] manifests as an obstruction to symmetry conditions of the Wannier functions, as we elaborate in Sec. VI.
- (b) (ii) If instead (B) holds, with $P = \bigoplus_{j=1}^{N} P_j$ a symmetric splitting, then [not (A)] manifests as an obstruction to an exponentially localized Wannier basis for P_j . This obstruction may manifest as a nonanalyticity of P_j , as exemplified by the nodal-line semimetal in the case study of Sec. III F. Alternatively, P_j may be analytic but has nontrivial first Chern class—this has nontrivial implications for the Zak phase of P_j that is elaborated in Sec. V.

V. ZAK PHASE OF MONOMIAL BAND REPRESENTATIONS AND OBSTRUCTED REPRESENTATIONS

The crystalline generalization of Berry's phase [83] is known as the Zak phase [24]—it encodes the holonomy of Bloch functions around loops in the Brillouin torus. A rank-N band, which consists of N-independent Bloch functions at each k, may then be characterized by N Zak phases for each cycle. The Zak phase has increasingly been used as a diagnostic of obstructed representations—bands which are not band representable.

A priori, there is no direct relation between k-space holonomy (a geometric property of Bloch functions) and band representability (a symmetry condition on exponentially localized Wannier functions). For a band whose projector is analytic throughout the Brillouin zone, it is known that the nonexistence of exponentially localized Wannier functions is a necessary and sufficient condition for the nontriviality of the first Chern class [76,77]; this nontriviality also manifests

as a nontrivial Zak phase [20]. The goal of this section is to prove an analogous relation for obstructed representations with a trivial first Chern class; our proof will rely on the crystallographic splitting theorem of Sec. IV B.

Generally, if the Zak phase is nontrivial (in a manner that will be made precise), it is guaranteed that the band is not band representable; this point of view has been advocated by topological quantum chemistry [10,31,63]. However, the converse statement, namely, that an obstructed representation must have a nontrivial Zak phase, has not been proven. This will be proven in Sec. VB for certain space groups to be specified. Before this result is presented, we review basic properties of the Zak phase in Sec. VA, and also clarify the distinction between trivial versus nontrivial Zak phases.

A. Preliminaries on the Zak phase

Let C denote a loop (in the Brillouin torus) with base point k, end point k + G, and G a reciprocal vector. Two k loops which are continuously deformable into each other are said to be equivalent under homotopy. A homotopy class [C] of k loops is specified by the reciprocal lattice vector G that connects the base and end points—for any representative of [C].

Given a rank-N P that is analytic throughout the Brillouin torus, it is always possible [84] to choose a basis for the Bloch functions $\{\psi_{nk}\}_{n=1...N}$ that is (i) analytic for all k in the Brillouin zone, and (ii) periodic under translation by the reciprocal vector G specifying [C].

Defining $u_{n,k}(\mathbf{r}) = e^{-i\mathbf{k}\cdot\mathbf{r}}\psi_{nk}(\mathbf{r})$ as the cell-periodic component of the Bloch function, the non-Abelian Berry connection is given by

$$[A(k)]_{j'j} = \langle u_{j'k} | i \nabla_k u_{jk} \rangle_{\text{cell}}, \tag{6}$$

where in $\langle \cdot | \cdot \rangle_{\text{cell}}$, we integrate (or sum) over the coordinates in one unit cell. The Wilson loop of the Berry gauge field is given by path-ordered integration of A over C:

$$W(C) = \mathcal{P}\exp\left[i\oint_{C} A(\mathbf{k}) \cdot d\mathbf{k}\right]. \tag{7}$$

The spectrum of the Wilson loop is given by

$$\operatorname{spec} \mathcal{W}(\mathcal{C}) = \{e^{i2\pi x_j(\mathcal{C})}\}_{j=1}^N, \tag{8}$$

with $2\pi x_j$ defined as the *Zak phase*. In general, x_j depends on \mathcal{C} and not just on $[\mathcal{C}]$.

Given P of rank N, and a homotopy class of loops (specified by G), we say that the Zak phase of (P, G) is trivial if $x_j(C)$ is independent of the representative choice for [C], for all j = 1 ... N.

Example of trivial Zak phase. For a category of BRs that has been termed strong BRs [21], their projected position operators $\{PxP, PyP, PzP\}$ mutually commute in the symmetric tight-binding limit, which would imply that the Zak phase of (P, G) is trivial in this limit, for $G = 2\pi e_x$, $2\pi e_y$, and $2\pi e_z$; e_a here denotes the unit vector in the a direction. Strong BRs include all BRs having only a single Wannier function on each Wannier center.

If P can be continuously deformed (while preserving analyticity and symmetry) such that x_j is representative-independent, we say that the Zak phase of (P, G) is

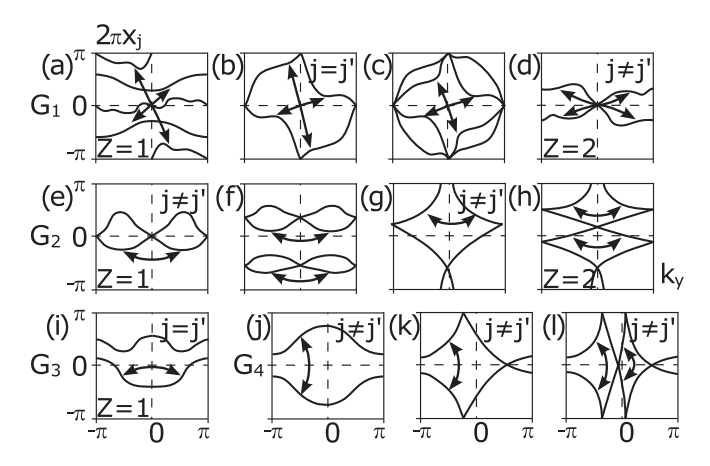


FIG. 4. Representative examples of the Zak phase for the family of k loops $\{\mathcal{C}(k_y)\}_{k_y}$, and with the space-group symmetry $G_{1,2,3,4}$, as defined in the main text. The first row has G_1 symmetry, the second row has G_2 , while in the last row the leftmost panel is G_3 symmetric, while the right three panels are G_4 symmetric. In each panel, the vertical axis is $2\pi x_j$ (Zak phase) and horizontal axis is k_y . The nontrivial point-group symmetry in G_j constrains $g_{\parallel} \circ x_j(k_y) = x_{j'}(s_g\check{g}_{yy}k_y)$, which is indicated by double-headed arrows. For panels describing rank-two bands, $j,j'\in\{1,2\}$, and we distinguish j=j' vs $j\neq j'$. We also indicate the Zak permutation order $Z\in\{1,2\}$; each panel without an indicated Z has the same value (for Z) as the panel to its left.

trivializable; in particular, a trivial Zak phase is trivializable. A *nontrivial Zak phase* is not trivializable.

For simplicity of presentation, we henceforth assume a rectangular real-space lattice and set all lattice periods to unity. (All results in Sec. V also hold for nonorthogonal lattices, if one replaces (k_x, k_y) with $(\mathbf{k} \cdot \mathbf{R}_1, \mathbf{k} \cdot \mathbf{R}_2)$, \mathbf{R}_i being a primitive Bravais-lattice vector.) To diagnose a nontrivial Zak phase for P of rank N, we introduce the notion of winding numbers for the Zak phase. Let [C] be specified by G = $2\pi e_x$; a set of representatives for [C] is given by $\{C(k_v)\}_{k_v}$; for the straight k-loop $C(k_y)$, k_x is varied while fixing k_y . From Eq. (8), we obtain N Zak phases parametrized by k_y : $\{2\pi x_j(k_y)\}_{j=1}^N$. Since $P(k) := \sum_{n=1}^N |\psi_{nk}\rangle\langle\psi_{nk}|$ is analytic and periodic over the Brillouin torus, each $e^{i2\pi x_j(k_y)}$ is a smooth function in k_y , and when k_y is advanced by 2π there is generally a permutation Σ_G in the Zak-phase index: $e^{i2\pi x_j(k_y+2\pi)}$ $e^{i2\pi x_{\Sigma_G(j)}(k_y)}$. Let us define the smallest positive integer Z_G such that $\Sigma_G^{Z_G}$ = identity as the Zak permutation order; examples of which are illustrated in Fig. 4. Generally, the phase $2\pi x_i$ may wind as k_v is advanced by Z_G periods; focusing on $Z_G = 1$, we define the Zak winding number $W_{i,G}$ through

$$x_j(k_y + 2\pi) - x_j(k_y) = W_{j,2\pi e_x} \in \mathbb{Z}.$$
 (9)

If N=2, we say that the Zak phase has a *relative winding* if $W_{1,G}=-W_{2,G}\neq 0$. If in addition, $W_{1,G}=-W_{2,G}$ is not reducible to zero by an analytic, G-symmetric deformation of P, then we say that the relative winding is *robust*. If $W_{1,G}$ is odd, the Zak phase has an *odd relative winding*.

Since every BR of G has a symmetric tight-binding (or atomic) limit (as proven in Sec. IXB), then P being a BR implies that W_j must either be zero, or reducible to zero by

an analytic, *G*-symmetric deformation of *P*. This follows from the following lemma that we prove in Appendix H:

Lemma for Zak phases of tightly-bound band representations. In the tight-binding limit of any BR, $x_j(k_y)$ becomes independent of k_y , for all j.

Conversely, if $W_{j,G}$ is neither zero nor reducible to zero, then the Zak phase is not trivializable and P cannot be a BR of G. This fact is used throughout this paper for proving that certain P are obstructed representations.

Finally, we review the spectral equivalence between the Wilson loop and the projected position operator:

$$(PxP - x_j(k_y) - R)|h_{j,k_y,R}\rangle = 0, \quad j = 1...N, \ R \in \mathbb{Z}.$$
(10)

The eigenfunctions of PxP are hybrid functions that are extended in y as a Bloch wave (with crystal wave number k_y), and exponentially localized in x as a Wannier function (with unit cell coordinate R) [85]. Modulo lattice translations in x (with unit lattice period), the eigenvalues of PxP are in one-to-one correspondence [20] with the Zak phases; cf. Eq. (8). If $x_j(k_y)$ is nondegenerate, one can uniquely define a unit-rank projector

$$P_j^x := \sum_{R \in \mathbb{Z}} \int \frac{dk_y}{2\pi} |h_{j,k_y,R}\rangle \langle h_{j,k_y,R}|, \tag{11}$$

which gives a splitting of $P = \bigoplus_{j=1}^{N} P_{j}^{x}$. Even if a degeneracy $x_{j}(k_{y}) = x_{j'}(k_{y})$ exists at isolated k_{y} , the assumed condition $Z_{2\pi e_{x}} = 1$ means that we can still uniquely define P_{j}^{x} by imposing that $|h_{j,k_{y},R}\rangle\langle h_{j,k_{y},R}|$ is smooth in k_{y} . We will refer to P_{j}^{x} as the projector to a *band of the projected position operator* PxP, and $x_{j}(k_{y})$ as the corresponding *dispersion* (assumed smooth in k_{y}).

Analogous to the above discussion, we may also consider a family of k loops represented by $\{C'(k_x)\}_{k_x}$, and the corresponding Zak phases $\{2\pi y_j(k_x)\}_{j=1}^N$. If the Zak permutation order $Z_{2\pi e_y} = 1$, then the winding numbers $W_{j,2\pi e_y}$ are well-defined by Eq. (9) with $x \leftrightarrow y$, and a splitting $P = \bigoplus_{j=1}^N P_j^y$ is given by Eqs. (10) and (11) also with $x \leftrightarrow y$.

B. Relating the winding of the Zak phase to the crystallographic splitting theorem

Here we will show how the crystallographic splitting theorem constrains the winding numbers of the Zak phases, as defined in –Eqs. (6)-(9); in turn, the Zak-phase winding is related to a winding in the dispersion of the projected position operator [cf.Eqs. (10) and (11).

To recapitulate, the splitting theorem states a necessary and sufficient condition for a monomial BR, namely, that there must exist a symmetric Wannier splitting. (We remind the reader that all BRs of two-spatial-dimensional space groups are monomial; cf. Sec. IV C.) We will find that a symmetric (but not necessarily Wannier) splitting is given by the bands of the projected position operator, for certain space groups that are identified by the following lemma.

Symmetric splitting lemma. Let G be a space group such that all $g \in G$ satisfy two conditions:

- (i) The action of g on r decomposes as $g \circ (x, y) = (g_{\parallel} \circ x, g_{\perp} \circ y)$, such that both g_{\parallel} and g_{\perp} are one-dimensional isometries.
- (ii) g does not enforce a degeneracy $x_j(k_y) = x_{j'}(k_y)$ for $j \neq j'$, except possibly at isolated k_y .

Then $P = \bigoplus_{j=1}^{N} P_j^x$, with P_j^x defined through Eqs. (9)–(11) is a symmetric splitting with respect to G. Moreover, each P_j^x is analytic in k over the Brillouin torus.

The above lemma also holds with $x \leftrightarrow y$.

To clarify condition (i), any symmetry of a two-spatial-dimensional space group acts on spacetime as $g \circ r = \check{g}r + t_g$ and $t \to s_g t$, with \check{g} a two-by-two orthogonal matrix acting on a two-component vector (x, y), and $s_g = -1$ if g reverses time; for a general review of space groups, we refer the reader to Appendix A 2. If \check{g} is a diagonal matrix with on-diagonal elements $(\check{g}_{xx}, \check{g}_{yy})$ being either of ± 1 , then $g_{\parallel} \circ x = \check{g}_{xx}x + t_{g,x}$ and $g_{\perp} \circ y = \check{g}_{yy}y + t_{g,y}$ indeed act as one-dimensional isometries. The corresponding action on k would also decompose into one-dimensional isometries: $k_x \to s_g \check{g}_{xx} k_x$ and $k_y \to s_g \check{g}_{yy} k_y$. We list a few representative examples of space groups satisfying conditions(i) and (ii):

Example 1. $G_1 = \mathcal{T}_2 \rtimes \mathbb{Z}_2^i$, with \mathbb{Z}_2^i an order two-group generated by the spatial inversion i [which maps $(x, k_y) \to (-x, -k_y)$], and \mathcal{T}_2 the translational subgroup of a two-dimensional crystal.

Example 2. $G_2 = \mathcal{T}_2 \times \mathbb{Z}_4^T$, with \mathbb{Z}_4^T an order-four group generated by T symmetry $[(x, k_y) \to (x, -k_y)]$. T squares to a 2π rotation which is distinct from the identity element; this corresponds to Wigner-Dyson class AII.

Example 3. $G_3 = \mathcal{T}_2 \rtimes \mathbb{Z}_2^T$, with \mathbb{Z}_2^T generated by T symmetry; this corresponds to Wigner-Dyson class AI.

Example 4. $G_4 = \mathcal{T}_2 \rtimes \mathbb{Z}_2^{C2T}$, with \mathbb{Z}_2^{C2T} generated by the composition of twofold rotation C_2 with time reversal $[(x, k_y) \to (-x, k_y)]$.

Proof of symmetric splitting lemma. Condition (ii) allows for P_i^x to be uniquely defined, as shown in Sec. VA. Conditions (i) and (ii) imply that $P = \bigoplus_{i=1}^{N} P_i^x$ is a symmetric splitting; this follows from an elementary argument, which is simple to write for rank N = 2: for any $g \in G$, we have assumed that $x \mapsto g_{\parallel} \circ x$ and $k_y \mapsto s_g \check{g}_{yy} k_y$ are isometries. This implies that $P(g_{\parallel} \circ x)P|_{k_{\nu}}$ is unitarily equivalent to $PxP|_{s_{\varrho}\check{g}_{\nu\nu}k_{\nu}}$, thus its eigenvalues satisfy $g_{\parallel} \circ x_j(k_y) \equiv x_{j'}(s_g \check{g}_{yy} k_y)$ (modulo integer) with $j, j' \in \{1, 2\}$. If j = j', then g trivially permutes $\{P_1^x, P_2^x\}$ (the bands of PxP); if $j \neq j'$, then the permutation is nontrivial. Both cases are illustrated in Fig. 4 for the space groups $G_{1,2,3,4}$. It follows that any $g \in G$ acts as a permutation, hence $P = \bigoplus_{j=1}^{N=2} P_j^x$ is a symmetric splitting. (The generalization of the above argument for rank N > 2 is straightforward, and illustrated for a few examples in Fig. 4.) The analyticity of P_i^x , is proven in Appendix D 2.

 $\vec{Z}ak$ winding theorem. Assume P is a rank-N representation of the space group G, with G satisfying conditions (i) and (ii) in the symmetric splitting lemma, and $Z_G = 1$ for either $G = 2\pi e_x$ or $2\pi e_y$. Then P is a BR of G if and only if all Zak winding numbers $W_{j,G} = 0$, or are reducible to zero by an analytic, G-symmetric deformation of P.

Proof. If each $W_{j,G} = 0$, then each P_x^j has a trivial Chern class. The *symmetric splitting lemma* implies that $P = \bigoplus_{j=1}^N P_j^x$ is a symmetric Wannier splitting; consequently, all conditions

in the splitting theorem are met for *P* to be a monomial BR. To prove the converse statement, we apply the symmetric tight-binding limit theorem (cf. Sec. IX B) and the *Lemma for Zak phases of tightly-bound BRs* (cf. Sec. V A); together they imply that all Zak winding numbers (for BRs) are zero or reducible to zero.

A useful corollary of the Zak winding theorem states:

Relative winding corollary. Let P with trivial first Chern class be a rank-two representation of space group G, with G satisfying conditions (i) and (ii) in the symmetric splitting lemma and $Z_G = 1$ for either $G = 2\pi e_x$ or $2\pi e_y$. Then P is an obstructed representation of G if and only if there is a robust relative winding for the Zak phase of (P, G).

Indeed, if P is obstructed with $Z_G = 1$, then $\{W_{1,G}, W_{2,G}\}$ cannot both vanish according to the Zak winding theorem. Since P has trivial first Chern class, $W_{1,G} = -W_{2,G} \neq 0$, implying a relative winding of the Zak phase.

The Zak winding theorem does not say that an obstructed representation of G [satisfying (i) and (ii) and with $Z_G = 1$] always exists. If it does exist, the theorem does not say what winding numbers $W_{j,G}$ are allowable or robust—these numbers can only be determined by further symmetry analysis of the Wilson loop matrix [20,39,86,87] as will be exemplified by several applications in the subsequent Sec. V C.

C. Applications of the Zak winding theorem

We briefly outline the remainder of this Sec. V:

- (i) In Sec. V C 1, we will apply the Zak winding theorem to prove that no obstructed representations (fragile or stable) exist for $G_3 = \mathcal{T}_2 \times \mathbb{Z}_2^T$ (Wigner-Dyson class AI).
- (ii) For class AII, we will prove in Sec. V C 2 that having Z_2 Kane-Mele topological order is equivalent to being an obstructed representation of $G_2 = \mathcal{T}_2 \times \mathbb{Z}_4^T$.
- (iii) The obstructed representations of $G_1 = \mathcal{T}_2 \rtimes \mathbb{Z}_2^i$ and $G_4 = \mathcal{T}_2 \rtimes \mathbb{Z}_2^{c2T}$ are discussed subsequently in Secs. V C 3 and V C 4, with emphasis on the possible Zak winding numbers. In Sec. V C 3, we will also exemplify how the Zak winding theorem may be used as an alternative method to prove band representability or to prove fragility for an obstructed representation.
- (iv) We end this section by discussing the limitations of the Zak winding theorem in Sec. V D with an outlook toward possible generalizations.

1. Wigner-Dyson class AI

The Zak winding theorem can be used to prove that there exists no obstructed representations of certain space groups. Indeed, for a *subset* of space groups satisfying conditions (i) and (ii) in the *symmetric splitting lemma*, it is guaranteed that Z_G is reducible to unity by an analytic, symmetric deformation, and $W_{i,G}$ is also reducible to zero.

In general, $Z_G > 1$ being robust requires at least one symmetry-protected degeneracy for the Zak phase, as illustrated in Fig. 4(d). If the first Chern class is trivial, $W_{j,G} \neq 0$ being robust also requires symmetry-protected degeneracies, because the net winding number must vanish. Whether such degeneracies exist can be determined by a symmetry analysis of the Wilson loop matrix [20,21,39,86,87].

Applying this analysis to $G_3 = \mathbb{Z}_2^T \times \mathcal{T}_2$, we find that there is no symmetry-enforced degeneracy of the Zak phase, hence the Zak permutation order is always reducible to unity. Moreover, G_3 ensures that the first Chern class is trivial, hence if any $W_{j,G}$ is nonzero, there must be other nontrivial windings such that the net sum vanishes. If two winding numbers have opposite sign, their corresponding Zak-phase functions must necessarily be degenerate at isolated wave vectors. But we have just claimed that such degeneracies are never protected by G_3 alone, hence all $W_{j,G}$ are eventually reducible to zero. We are led to the following no-go theorem:

No-go theorem for Wigner-Dyson class AI. In spatial dimension d=2, there exists no obstructed representation of $G_3 = \mathbb{Z}_2^T \times \mathcal{T}_2$.

While it is known that there is no stable obstructed representation of G_3 from K-theoretic approaches [54], our no-go theorem goes further to say there is no FOR of G_3 . Our no-go theorem is consistent with the absence of nonstable topological insulators in class AI that has been derived from the equivariant homotopy properties of Real vector bundles [88].

2. Wigner-Dyson class AII

One special feature in Wigner-Dyson class AII is that the Zak permutation order Z_G ($G = 2\pi e_x$, $2\pi e_y$) is always reducible to unity for any BR of $G_2 = \mathcal{T}_2 \times \mathbb{Z}_4^T$, but not necessarily for any obstructed representation of G_2 .

This follows from a symmetry analysis of the Wilson-loop matrix [20,26] which shows that all Zak phases are pair-wise degenerate at time-reversal-invariant wave vectors ($k_v = 0, \pi$ for $G = 2\pi e_x$, and $k_x = 0$, π for $G = 2\pi e_y$); there are no G_2 -protected degeneracies at generic k_x and k_y . This implies that $x_i(k_v)$ can always be reduced to two classes of graphs illustrated in Figs. 4(e)-4(h). One class of graphs corresponds to a splitting into a direct sum of rank-two projectors with unit Zak permutation order; the trivial Zak winding then implies that P is a BR of G_2 , according to the Zak winding theorem. The second class of graphs has a robust zigzag connectivity that has been described as a "switching of Kramers partners" [55]—such a nontrivial Zak phase implies that P is an obstructed representation of G_2 , according to the symmetric tight-binding limit theorem [cf. Sec. IX B] and the Lemma for Zak phases of tightly bound BRs [cf. Sec. VA]. Combining these results leads to the following theorem:

Zak winding theorem for Wigner-Dyson class AII. P is a BR of $G_2 = \mathcal{T}_2 \times \mathbb{Z}_4^T$ if and only if all Zak winding numbers are reducible to zero by an analytic, G_2 -symmetric deformation of P.

It has been established that the two classes of Wilson-loop graphs are in one-to-one correspondence with the \mathbb{Z}_2 Kane-Mele topological invariant [26,89]. Combining this correspondence with the above Zak winding theorem, we derive that having \mathbb{Z}_2 Kane-Mele topological order is equivalent to being an obstructed representation of G_2 .

3. With spatial inversion symmetry

For the space group $G_1 = \mathcal{T}_2 \rtimes \mathbb{Z}_2^i$, it is possible for the Zak phase to be symmetry-fixed to an integer multiple of π at inversion-invariant wave vectors $(k_y = 0, \pi)$ for

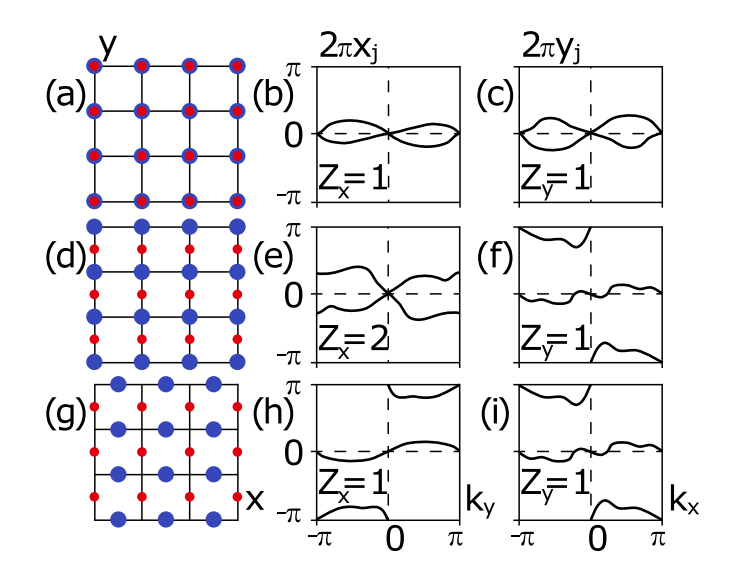


FIG. 5. For three BRs of space group G_1 , we illustrate their real-space distribution of Wannier centers (left column), and their corresponding Zak phases $2\pi x_j(k_y)$ and $2\pi y_j(k_x)$ (middle and right columns). All Zak phases equaling 0 or π are rigidly fixed to those values by spatial inversion symmetry, implying, e.g., that panel (b) cannot be continuously deformed to (h). Red and blue dots in the first column indicate Wannier centers for linearly independent Wannier functions with even parity. All Wannier centers lie on inversion-invariant Wyckoff positions on a rectangular lattice.

 $G = 2\pi e_x$, and $k_x = 0$, π for $G = 2\pi e_y$); the multiplicity of the symmetry-fixed eigenvalue depends on the symmetry representation of P at i-invariant wave vectors in the Brillouin torus [20,21]. There are no G_1 -protected degeneracies of the Zak phase at generic k_x and k_y . Figures 5(a)-5(f) illustrate the Zak phases of two BRs of G_2 , one with Zak permutation order $Z_{2\pi e_x} = Z_{2\pi e_y} = 1$ and the other with $Z_{2\pi e_x} = 2$, $Z_{2\pi e_y} = 1$.

Obstructed representations of G_1 exist for any even rank [20,60,63,64,90] and are characterized by the Zak windings illustrated in Figs. 4(a)–4(d) for rank N=2 and 4, respectively.

Focusing on the case N=2 with an odd relative winding (cf. relative winding corollary), we now show the corresponding rank-two P is fragile obstructed. Fragility is proven by adding a rank-two BR to P and recomputing the Zak phase for the resultant rank-four subspace. The required rank-two BR is given by the Wannier representation and Zak phases in Figs. 5(g)–5(i). Applying a theorem for symmetry-protected Zak phases [20,21], which takes as input the i-symmetry eigenvalues in Table I, we derive that the four Zak-phase functions are reducible to a graph with unit permutation order

TABLE I. For the obstructed representation of G_1 , we give the i eigenvalues (of Bloch functions at i-invariant k-points Γ , X, Y, M) in the upper row. The symmetry obstruction can be removed by adding a BR with i eigenvalues that are given in the lower row.

$\mathfrak{i}(\Gamma)$	$\mathfrak{i}(X)=\mathfrak{i}(Y)$	$\mathfrak{i}(M)$	
-1, -1	1, 1	1, 1	
1, 1	-1, 1	-1, -1	

and trivial winding, as illustrated in Fig. 4(a). This means that the rank-four band is a BR of G_1 , according to the Zak winding theorem.

4. With spacetime inversion symmetry

For a rank-two obstructed representation of the space group $G_4 = \mathcal{T}_2 \times \mathbb{Z}_2^{C2T}$ (and also its double cover \tilde{G}_4), it is possible that the Zak winding number robustly takes on any integer value; the case of $W_{1,2\pi e_x} = -W_{2,2\pi e_x} = 2$ is illustrated in Fig. 4(1). This robust winding follows from irremovable degeneracies (of the Zak phase) that are movable along the k_x (or k_y) axis [31,47,87]. The integer winding number has also been related to the Euler class of rank-two bundles with C_2T symmetry [65].

D. Generalizations and limitations of the Zak winding theorem

As stated, the Zak winding theorem applies directly to space groups which satisfy conditions (i) and(ii) in the *symmetric splitting lemma*. What of space groups (denoted G') not satisfying conditions (i) and (ii) but containing a space subgroup G < G' that does? Our theorem may then be used, in combination with a Zak-phase calculation, to determine whether a representation P' of G' subduces to a BR of G. However, it would not be possible to deduce if P' is a BR of G' from a Zak-phase calculation, contrary to the illogical procedures in Refs. [47,49]. This is because the splitting given by the projected position operator is symmetric under G but not under G'.

In all cases of robust Zak winding [20,21,26,47,48,63,65] that we know of (some of which have been discussed in the previous Sec. V C), space group G of the obstructed representation either satisfies (i) and (ii) or contains a space subgroup that satisfies (i) and (ii) and is also bigger than the translational subgroup $\mathcal{T}_2 < G$. This suggests that robust Zak windings can always be rationalized by the existence of a symmetric splitting by the projected position operator.

Our Zak winding theorem is agnostic of obstructed representations (P'') of G'', if the only space subgroup of G'' that satisfies (i) and (ii) is the translational subgroup $\mathcal{T}_2 < G''$. We are not aware of any robust winding of the Zak phase of (P'', \mathbf{G}) , for any G''. In spite of this, it is possible that Zak windings for other families of \mathbf{k} loops may diagnose the obstruction in P''. As a case in point, a family of contractible, hexagonal \mathbf{k} loops can be used to diagnose an obstructed representation of $G'' = \mathcal{T}_2 \times \mathbb{Z}_3^{C_3} = P3$ [91], which was previously studied in Ref. [31] with an additional reflection symmetry.

VI. WANNIER FUNCTIONS OF OBSTRUCTED REPRESENTATIONS

The topological triviality of an analytic band projector P is equivalent to the existence of a *Wannier basis*, i.e., an infinite set of exponentially-localized Wannier functions which span P. (In spatial dimension d=2 or 3, having trivial first Chern class is a necessary and sufficient condition for topological triviality in the category of complex vector bundles. This condition is assumed henceforth in this section.) P being a representation of a space group G means that the *complete* set

of Wannier functions is invariant under any element of G. (In this section, we will not use the previously developed notation which distinguishes the different categories of space groups: crystallographic versus magnetic, integer- versus half-integer spin. Unless otherwise specified, space group G includes all said categories.)

By definition, an obstructed representation of G is not a BR of G, that is to say, it is not induced from a finite set of Wannier functions centered on a Wyckoff position ϖ and transforming in a representation of the site stabilizer G_ϖ . Our goal is to unpack the physical implications of this definition by utilizing the new perspective afforded by the crystallographic splitting theorem. Though there is no obstruction to the existence of Wannier functions that are G invariant as a complete set spanning P, there is a subtler obstruction to G permuting translation-invariant subsets of Wannier functions, as encapsulated by the following theorem.

Symmetric Wannier obstruction theorem. Let P be a rank-N, obstructed representation of a space group G. Suppose $P = \bigoplus_{j=1}^{N} P_j$ is a Wannier splitting. Then the following cannot hold true, namely, for all $g \in G$, $g : P_j \to P_{\sigma_g(j)}$ with σ_g a permutation on $\{1, \ldots, N\}$.

The symmetric Wannier obstruction theorem follows directly from the splitting theorem of Sec. IV B.

Application to Wigner-Dyson class AII: Suppose $P = P_1 \oplus P_2$ were a rank-two BR of $\mathcal{T}_2 \times \mathbb{Z}_4^T$. Owing to our splitting theorem, time reversal T must permute $\{P_1, P_2\}$. This permutation must be nontrivial owing to the Kramers degeneracy at time-reversal-invariant wavevectors. If instead $P = \sum_{j=1}^2 \sum_R |W_{jR}\rangle \langle W_{jR}|$ were an obstructed representation of $\mathcal{T}_2 \times \mathbb{Z}_4^T$, then one must relax the nontrivial permutation condition and allow for $TP_1T^{-1}P_1 \neq 0$. This relation, in combination with the Kramers orthogonality of $\hat{T}|W_{10}\rangle$ and $|W_{10}\rangle$ [92] implies that time reversal has a nonlocal action on the unit-cell coordinate R of Wannier functions: $\langle W_{1R\neq 0}|\hat{T}W_{10}\rangle \neq 0$; in contrast, time reversal has a local action on the continuous spatial coordinate.

For a rank-N obstructed representation of G, our symmetric Wannier obstruction theorem establishes that the entirety of G cannot permute $\{P_j\}_{j=1}^N$. However, it would be possible that a proper subgroup H < G permutes $\{P_j\}_{j=1}^N$, if P subduces to a BR of H. (Alternatively said, if P becomes band representable when the group G is relaxed to H, then H may permute $\{P_j\}_{j=1}^N$.) Such H would determine the symmetry properties of Wannier functions for an obstructed representation. Depending on G, the choice of H may not be unique and becomes a matter of preference.

Example of symmetry-distinct Wannier bases for the same obstructed representation. The nonuniqueness of H applies to our case study of rotation-invariant TCIs in class AI [cf. Sec. III]. The obstructed representation (P_{OR}) of $\mathcal{T}_3 \rtimes C_4 \vee \mathbb{Z}_2^T$ subduces either to a BR of $\mathcal{T}_3 \rtimes C_4$ or to a BR of $\mathcal{T}_3 \rtimes \mathbb{Z}_2^T$. The two possible subductions correspond to two symmetry-distinct Wannier bases for the same obstructed representation of $\mathcal{T}_3 \rtimes C_4 \vee \mathbb{Z}_2^T$, as we illustrate in Fig. 6. Figures 6(a) and 6(b) show our numerical simulation for the former type of Wannier splitting $P_{OR} = P_+ \oplus P_-$, where $P_+ = \sum_R |W_{+,R}\rangle \langle W_{+,R}|$ projects to Wannier functions transforming in the vector representation of C_4 : $\hat{C}_4W_{+,0} = \pm iW_{+,0}$. While

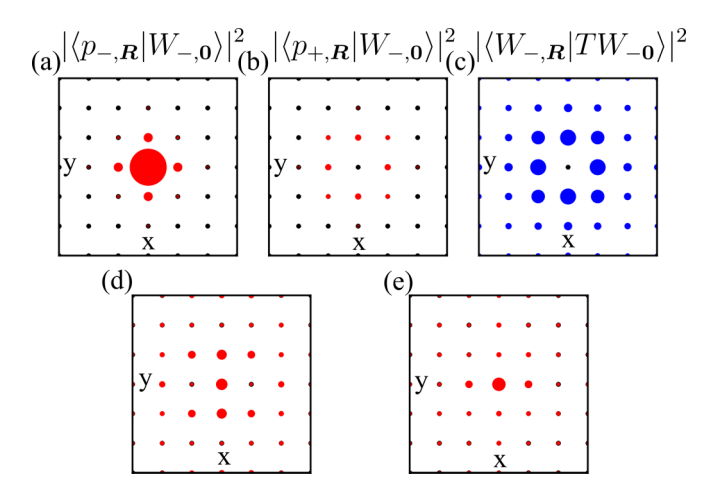


FIG. 6. (a), (b) Illustrate the fourfold symmetric Wannier function $W_{-R=0}$ constructed for the P_- band of the projected symmetry operator. To illustrate the lack of pseudospin polarization [cf. Sec. VIB], the overlap of $W_{-,0}$ with the $p_-=p_x-ip_y$ orbital [respectively, $p_+=p_x+ip_y$] on each lattice site is indicated by the radii of red dots in (a) [respectively, (b)]. To illustrate the nonlocal action of time reversal (T) symmetry on the unit-cell coordinate, the overlap between $TW_{-,0}$ and $W_{-,R}$ (R being the unit-cell coordinate) is indicated by the radii by blue dots in panel (c). Alternatively, real-valued Wannier functions ($\{W_{x,R}\}_R$ and $\{W_{y,R}\}_R$) can be constructed for the same obstructed representation; the probability distributions of $W_{y,0}$ and $W_{x,0}$ are illustrated with red dots in (d) and (e), respectively. By inspection, the two distributions are neither individually four-fold invariant, nor mutually related by a fourfold rotation.

the fourfold rotation acts as the trivial permutation: $[\hat{C}_4, P_\pm] = 0$, time reversal does *not* act as a nontrivial permutation; note, if both symmetries were to act as permutations, the splitting theorem would be violated. One implication is that T has a nonlocal action on the unit-cell coordinate [cf. Fig. 6(c)], which rules out Wannier functions that are localized to a single lattice site; the theme of localization is explored more generally in Sec. VI A. In comparison, Figs. 6(d) and 6(e) illustrate the real-valued Wannier functions $(W_{x,0} \text{ and } W_{y,0})$ of a symmetry-distinct Wannier splitting for $P_{\text{OR}} = P_x \oplus P_y$, where time reversal acts as a trivial permutation $([\hat{T}, P_{x,y}] = 0)$ but fourfold symmetry fails to act as any permutation.

Additionally, we describe how the symmetric Wannier obstruction theorem is applied to constrain three properties of Wannier functions—namely, their real-space localization [cf. Sec. VIA], their spin (or pseudospin) polarization [cf. Sec. VIB], and their symmetry representations of the site stabilizers [cf. Sec. VIC]. We hope these constraints serve to guide the numerical construction of Wannier functions for topological insulators in any space group, as pioneered for the Kane-Mele topological insulator by Soluyanov and Vanderbilt [43–45].

A. Localization obstruction

The tension of localizing Wannier functions in topologically nontrivial bundles is a recurrent theme in topological band theory [93–98]. It is well known that the exponential localization of Wannier functions is in one-to-one correspon-

dence with topological triviality as a complex vector bundle [76,77,99].

For tight-binding Wannier functions which are defined in a tight-binding lattice model, one may consider a stricter form of localization, namely, that the functions vanish everywhere except on a finite number of points. Such Wannier functions will be said to have compact support. In recent works on the tenfold classification of topological insulators and superconductors [98,100], it was found that the only nontrivial bands that can be spanned by compactly supported Wannier functions are those with a nontrivial winding that occurs in the same symmetry class in one spatial dimension. Their result was derived assuming discrete translational symmetry, but not assuming any other crystallographic spatial symmetry.

Our symmetric Wannier obstruction theorem allows us to formulate an analogous obstruction—to localization—that applies to bands with crystallographic symmetry. We consider an even stricter form of localization for tight-binding Wannier functions, namely, *one-site localized* Wannier functions that have support only on a single tight-binding lattice site (cf. Sec. IX).

Localization obstruction lemma. Suppose an obstructed representation of a space group has a basis of exponentially localized Wannier functions. Then it is not possible for all Wannier functions to be one-site localized.

Postponing a general proof of the lemma to Appendix I, we offer here an elementary version of the proof—for a specific space group—to develop intuition.

Example: \mathbb{Z}_2 Kane-Mele topological insulator. Let P be an obstructed representation of $\mathcal{T}_2 \times \mathbb{Z}_4^T$. Suppose on the contrary that $P = \sum_{j=1}^2 \sum_R |W_{jR}\rangle\langle W_{jR}|$ has a Wannier basis in which all Wannier functions are one-site localized. Since the representation \hat{T} of time reversal squares to minus identity, $\hat{T}W_{1R}$ must be orthogonal to W_{1R} . Since all Wannier functions are one-site localized, and time reversal is a spatially local operation, $\hat{T}W_{1R}$ must have zero overlap with any Wannier function $W_{1R'\neq R}$ —hence $\hat{T}W_{1R}$ must equal W_{2R} up to a phase. This being true for all R implies that T nontrivial permutes P_1 and P_2 , hence $P = P_1 \oplus P_2$ is a symmetric Wannier splitting—in contradiction with P being an obstructed representation.

A few remarks are in order.

- (i) The impossibility of one-size localization (for all Wannier functions of obstructed representations) allows for the possibility of spectrally robust boundary/domain-wall states [cf. Sec. IX], as exemplified by the Kane-Mele topological insulator.
- (ii) One may relax the one-site localization condition to a less stringent condition that all Wannier functions have compact support, with no two Wannier functions (centered on different positions) having intersecting support. In fact the localization obstruction lemma also holds with this generalized localization condition, as can be proven by following essentially the same steps in the proof of Appendix I.

B. Spin and pseudospin frustration

1. Wigner-Dyson class AII

Let \mathbb{Z}_4^T be the order-four group generated by time reversal (Wigner-Dyson class AII), and \mathcal{T}_d the translational subgroup of a d-dimensional crystal (d = 2, 3).

Spin frustration corollary. Let P be a rank-two, obstructed representation of $\mathcal{T}_d \times \mathbb{Z}_4^T$. Then for any Wannier basis of P, it is not possible that a Wannier function is fully spin polarized (along any spin quantization axis).

Proof of spin frustration corollary. Let $P = \sum_{j=1,2} P_j = \sum_{j=1,2} \sum_{R} |W_{jR}\rangle\langle W_{jR}|$ satisfy all premises stated in the corollary. Suppose W_{10} were fully spin polarized, then by translational symmetry any Wannier function W_{1R} in P_1 is likewise fully spin polarized. Since time reversal T inverts spin (whichever the quantization axis), TP_1T^{-1} must be orthogonal to P_1 . Since P is a representation of $\mathcal{T}_d \times \mathbb{Z}_4^T$ (which includes T symmetry), TP_1T^{-1} must belong in P. Given that P is rank two, we may identify $P_2 = TP_1T^{-1}$, hence T symmetry acts as a nontrivial permutation on $\{P_1, P_2\}$. Our splitting theorem then states that P must be a BR of $\mathcal{T}_d \times \mathbb{Z}_4^T$, which contradicts the premise in the corollary.

One implication of the spin frustration corollary may be deduced from an elementary argument if one assumes that $\mathcal{T}_{d=2} \times \mathbb{Z}_{4}^{T}$ -symmetric P has additionally a U(1) symmetry for the conservation of the spin component S_z . We present this argument to develop intuition, as well as to establish a relation with the spin Chern number, as formulated for an infinite sample without boundaries [75]. As proven in Sec. VC, an obstructed representation of $\mathcal{T}_2 \times \mathbb{Z}_4^T$ must have \mathbb{Z}_2 Kane-Mele topological order. With the addition of S_z symmetry, the Kane-Mele phase can be split into two unit-rank bands with opposite S_7 and opposite Chern numbers (which are necessarily odd); the latter are known as spin Chern numbers [75]. Due to the topological nontriviality of each unit-rank band in the S_7 basis, a Wannier basis can only be constructed from linearly combining Bloch functions with different S_7 . We emphasize that our spin frustration corollary makes a stronger statement in three regards: (i) if only one spin component (e.g., S_7) is conserved, the Wannier function cannot be polarized along any spin quantization axis, and not just S_7 . This spin frustration (ii) holds even if not one spin component is conserved, and (iii) applies also to the three-spatial-dimensional \mathbb{Z}_2 topological insulators.

We offer a physical interpretation for spin frustration. It is often said that the \mathbb{Z}_2 Kane-Mele obstructed representation requires spin-orbit coupling. (Indeed, if such coupling were absent, spin SU(2) and time-reversal symmetries enforce that the spin Chern number vanishes, which implies the trivial phase in the \mathbb{Z}_2 classification.) In solids, spin-orbit coupling is predominantly described in the k-space perspective [101] with reference to how the spin of a Bloch state is locked to its momentum [102]. In complementarity, we may view spin frustration as a manifestation of the topology-enforced spin-orbit coupling—in the real-space, Wannier perspective.

There is a second interpretation of the spin frustration corollary that emphasizes a relation with the mirror Chern insulator [103]. We consider the mirror operation \mathfrak{r} that maps the spatial coordinate $(x, y, z) \to (x, y, -z)$ and rotates spin by a π angle about z. If restricted to the z=0 plane, $\mathfrak{r}=e^{-i\pi S_z/\hbar}=-iS_z$ becomes a spatially local operation in x and y. This means that the spin frustration corollary can, in spatial dimension d=2, be viewed as the impossibility for a Wannier function to transform in a definite representation of \mathfrak{r} . Such an obstruction is already known in case \mathfrak{r} is a symmetry of P, i.e., if P is the filled band of a mirror Chern insulator [80]. The

implication of our corollary is that this obstruction persists even where \mathfrak{r} is not a symmetry.

2. Wigner-Dyson class AI

We present an analog of the spin frustration corollary that applies to integer-spin representations of time reversal (Wigner-Dyson class AI), as well as to grey magnetic space groups with a nontrivial crystallographic point group. We remind the reader that a grey magnetic space group is expressible as $G \times \mathbb{Z}_2^T$, with G a crystallographic space group (without time-reveral symmetry) and \mathbb{Z}_2^T an order-two group generated by time reversal.

To formulate an analog of spin polarization in class AI, we utilize Wigner's seminal classification [5,104,105] of crystallographic point-group representations as real, complex and quaternionic; this classification is briefly reviewed in Appendix F5. A one-dimensional representation is real or complex; if real, it is T invariant; if complex, it is not T invariant, and must be paired up with its complex-conjugate representation in the presence of T symmetry, i.e., the pair forms a two-dimensional (pseudospin) representation.

Example of pseudospin. As we have encountered in Sec. III A, the two-dimensional irreducible representation of the point group $C_4 \times \mathbb{Z}_2^T$ is the direct sum of two complex representations, which transform like $p_x \pm ip_y$ orbitals.

Let us formulate a notion of pseudospin polarization for Wannier functions in a tight-binding model. The tight-binding vector space is generally spanned by one-site localized Wannier functions transforming as a BR of $G \times \mathbb{Z}_2^T$; for simplicity, we consider all basis Wannier functions (in one unit cell) to be one-site localized on a single position $\boldsymbol{\varpi}$, with associated site stabilizer G_{ϖ} ; by applying the translational subgroup $\mathcal{T}_d < G$ on $\boldsymbol{\varpi}$ (the Wyckoff position), we generate the *tight-binding lattice*. Let D be a one-dimensional complex representation of the site stabilizer G_{ϖ} of a crystallographic space group G. We say that a tight-binding Wannier function W is *polarized with respect to* $(G, \boldsymbol{\varpi}, D)$, if for all sites $\{g \circ \boldsymbol{\varpi} | g \in \mathcal{T}_d\}$ related to $\boldsymbol{\varpi}$ by Bravais-lattice translations, the restriction of W to $g \circ \boldsymbol{\varpi}$ transforms in a representation of $G_{g \circ \boldsymbol{\varpi}}$ that is isomorphic to D; note $G_{g \circ \boldsymbol{\varpi}} \cong G_{\boldsymbol{\varpi}}$ are isomorphic as groups.

Pseudospin frustration corollary. Let $P_{\mathcal{H}}$ project to a tight-binding vector space, which transforms as a BR of $G \times \mathbb{Z}_2^T$ with the Wyckoff position $\boldsymbol{\varpi}$. Let $P \subset P_{\mathcal{H}}$ be a rank-two obstructed representation of $G \times \mathbb{Z}_2^T$, with the Wannier splitting $P = P_1 \oplus P_2$. Then it is not possible that $P_1 = \sum_{\boldsymbol{R}} |W_{1\boldsymbol{R}}\rangle\langle W_{1\boldsymbol{R}}|$ represents G with W_{10} that is polarized with respect to $(G, \boldsymbol{\varpi}, D)$, for any D that is a one-dimensional complex representation of $G_{\boldsymbol{\varpi}}$.

Proof of corollary. If W_{10} were polarized with respect to $(G, \boldsymbol{\varpi}, D)$, then any Wannier function W_{1R} (in P_1) is likewise polarized, owing to the translational symmetry of P_1 . Since time reversal maps each D representation to its complex conjugate \bar{D} , each Wannier function in TP_1T^{-1} must be polarized with respect to $(G, \boldsymbol{\varpi}, \bar{D})$. Therefore, TP_1T^{-1} must be orthogonal to P_1 , further implying that T acts as a nontrivial permutation on $\{P_1, P_2\}$. Given that both P_1 and P_2 represent P_2 , hence any P_2 acts as the trivial permutation on P_1 , P_2 . In combination, all $P_2 \in G \times \mathbb{Z}_2^T$ acts

as a permutation on $\{P_1, P_2\}$, which implies P is a BR of $G \times \mathbb{Z}_2^T$ – in contradiction with our premise.

Application to fragile obstructed crystalline insulator. Let P_{OR} be an obstructed representation of $\mathcal{T}_3 \rtimes C_4 \rtimes \mathbb{Z}_2^T$. A tight-binding model with a C_4 -invariant Wykcoff position $\boldsymbol{\varpi}$ was proposed by Fu [55] and is reviewed in Sec. III A. Applying the pseudospin frustration corollary, we find there does not exist a Wannier splitting $P_{\text{OR}} = P_+ \oplus P_-$ with $P_\pm = \sum_R |W_{\pm R}\rangle\langle W_{\pm R}|$ representing $\mathcal{T}_3 \rtimes C_4$, and W_{j0} being polarized with respect to $(\mathcal{T}_3 \rtimes C_4, \boldsymbol{\varpi}, D)$, where D is the complex representation (e.g., $p_x + ip_y$) of the site stabilizer C_4 . For illustration, we decomposed the Wannier function of P_- into $p_x - ip_y$ and $p_x + ip_y$ orbitals, in Figs. 6(a) and 6(b), respectively.

C. Symmetry frustration

Certain symmetry representations of site stabilizers are impossible for the Wannier functions of obstructed representations—we refer to this as a *symmetry frustration* for Wannier functions.

Example 1: Inversion-symmetric fragile obstructed insulator. As a case in point, consider the space group $G_1 = \mathcal{T}_2 \rtimes \mathbb{Z}_2^i$, with \mathbb{Z}_2^i being the order-two group generated by spatial inversion i symmetry, and \mathcal{T}_2 the translational subgroup of a 2D lattice. A rank-two obstructed representation (P'_{OR}) of G_1 was proven in Sec. V C to have odd relative winding of the Zak phase. The symmetry frustration manifests in the following way: for any Wannier basis of P'_{OR} , it is not possible for any single Wannier function to represent a site stabilizer that is isomorphic to \mathbb{Z}_2^i . This result is an application of the following corollary.

Symmetry frustration corollary. Let P be a rank-N, obstructed representation of a space group G. Assume P has a tight-binding Wannier basis where the N linearly-independent Wannier functions in one unit cell are centered at $\{r_j\}_{j=1}^N$, with each site stabilizer G_{rj} being isomorphic to the point group of G. Then the following cannot hold for any order-(N-1) subset of $\{1...N\}$, namely, that the Wannier function centered at r_j transforms in a one-dimensional representation of G_{rj} .

Proof of corollary. Given $P = \sum_{j=1}^{N} \sum_{\mathbf{R}} |W_{j\mathbf{R}}\rangle \langle W_{j\mathbf{R}}|$ and J that is an order-(N-1) subset of $\{1\dots N\}$, suppose on the contrary that for $j \in J$, W_{j0} that is centered at \mathbf{r}_j transforms in a one-dimensional representation of G_{rj} . Since G_{rj} is isomorphic to the point group of G, the extension of G_{rj} by the translational subgroup $\mathcal{T}_d < G$ simply gives $G = \mathcal{T}_d \rtimes G_{rj}$ [106]. It follows that for $j \in J$, $P_j = \sum_{\mathbf{R}} |W_{j\mathbf{R}}\rangle \langle W_{j\mathbf{R}}|$ is invariant under all elements of G [107]. Since by assumption this invariance holds also for P, it must be that G acts as the trivial permutation on $\{P_1, \dots, P_N\}$, implying $P = \bigoplus_{j=1}^N P_j$ is BR of G, and contradicting our premise.

Example 2: Rotation-symmetric fragile obstructed insulators. In d=2, twofold rotation C_2 and spatial inversion i act identically on integer-spin representations, hence the conclusions in Example 1 carry forward with i replaced by C_2 . (However, the conclusions of Example 1 are more generally applicable to half-integer-spin representations.) A rank-two, obstructed representation of $\tilde{P}3 = \mathcal{T}_2 \rtimes \tilde{C}_3$ exists, with the symmetry-frustration property that its Wannier functions cannot represent a site stabilizer isomorphic to \tilde{C}_3 . This obstructed representation has been realized by tight-binding

models with symmetry that is higher than $\tilde{P}3$, namely, $\tilde{P}6mm$ [62], $\tilde{P}31'$ [47], and $\tilde{P}3m1$ [31]. However, the additional symmetries are superfluous to the C_3 symmetry obstruction for Wannier functions, as proven through a holonomy argument in Sec. V D. It can further be shown that the obstructed representation of \tilde{P}_3 is fragile, by the numerical procedure used in Ref. [62].

VII. ANSATZ-FREE APPROACH TO SYMMETRIC WANNIER FUNCTIONS

Given P that is a monomial BR of a space group G, we would like to construct a locally symmetric Wannier basis for P, without having to postulate trial Wannier functions. (What it means for a Wannier basis to be locally symmetric is reviewed in Appendix 3 b.)

We first obtain a symmetric Wannier splitting $P = \bigoplus_{i=1}^{N} P_j$, which is guaranteed to exist by the crystallographic splitting theorem. Depending on G, such a splitting may be obtained from bands of the projected symmetry or position operator, as described in Secs. III D and VB and Appendix D. The symmetries of each P_j form a group that we denote as $G_j := \{g \in G | [\hat{g}, P_i] = 0\}$.

The next step is to find a Bloch function ψ_{jk} that spans P_j at each k, with the property that ψ_{jk} is periodic over and analytic throughout the Brillouin torus. Such a Bloch function is guaranteed to exist because each P_j (of a Wannier splitting) is analytic and has trivial first Chern class. Such a Bloch function can be obtained by the parallel-transport procedure described in Ref. [44], where it is described as a smooth gauge.

The last step is to perform a U(1) phase transformation $\psi_{jk} \to \psi_{jk} e^{i\varphi_j(k)} := \tilde{\psi}_{jk}$, with $e^{i\varphi_j(k)}$ that is periodic and analytic in k, such that $\tilde{\psi}_{jk}$ becomes *canonically symmetric*. By this, we mean that every element $g = (t_g | \tilde{g})$ in the site stabilizer $G_{j, \overline{w}_j} := \{g \in G_j | g \circ \overline{w}_j = \overline{w}_j\}$ acts on the Bloch function as [108]

$$\hat{g}\tilde{\psi}_{jk} = \rho_{g,j}\,\tilde{\psi}_{js_g\check{g}k},\tag{12}$$

where $s_g = -1$ if g inverts time and otherwise $s_g = +1$. $\boldsymbol{\varpi}$ can be determined, modulo Bravais-lattice translations, by computing the Brillouin-zone average of the Berry connection in accordance with the geometric theory of polarization [109]. $\rho_{g,j}$ is a U(1) phase factor determined by the action of g on the Wannier function obtained by Fourier transform of $\tilde{\psi}_{jk}$,

$$\tilde{W}_{jR} := \int_{BZ} d\mathbf{k} \frac{e^{-i\mathbf{k}\cdot\mathbf{R}}}{\sqrt{|BZ|}} \tilde{\psi}_{jk}, \quad \hat{g}\tilde{W}_{j0} = \rho_{g,j}\tilde{W}_{j0}, \quad (13)$$

with |BZ| the volume of the Brillouin zone. The advantage of canonically symmetric Bloch functions is that the Wannier functions $\{\tilde{W}_{jR}\}_{R\in BL}$ form a locally symmetric Wannier basis for a BR of G_j [17,80] thus $\{\tilde{W}_{jR}\}_{j\in\{1...N\},R\in BL}$ gives the desired locally symmetric Wannier basis for P, a monomial BR of G.

The existence of a canonically symmetric Bloch function [cf. Eq. (12)] has been rigorously proven in Ref. [80] for any unit-rank band with analytic projector, trivial first Chern class, and the symmetry of a symmorphic space group. (A symmorphic space group is a semidirect product of its translational subgroup and its point group, as reviewed in Appenidx A 2.)

We are not aware that any nonsymmorphic space group allows for unit-rank bands [15,110–112], so we assume henceforth that G_j is symmorphic; it is not necessary, however, to assume G is symmorphic. While Eq. (12) exists in principle, we now present an algorithm that inputs an analytic, periodic Bloch function ψ_{jk} , and outputs a Bloch function $\tilde{\psi}_{jk}$ that is analytic, periodic and canonically symmetric.

Symmetrization algorithm. For any $g \in G_{j,\varpi_j}$, we define

$$\tilde{\psi}_{jk} = \frac{1}{|G_{j,\varpi_j}|} \sum_{g \in G_{j,\varpi_j}} \rho_{g,j}^{-1} \, \hat{g} \psi_{js_g \check{g}^{-1} k}, \tag{14}$$

with |H| denoting the order of a finite group H. One may verify that Eq. (14) indeed satisfies Eq. (12) for all $g \in G_{i, \varpi_i}$.

Applying the symmetrization algorithm to the three bands of the projected rotation operator (cf. Sec. III F), we obtain a locally symmetric Wannier basis for the rank-three BR of $\mathcal{T}_3 \times C_{4v} \times \mathbb{Z}_2^T$, which is illustrated in Fig. 2.

VIII. FRAGILE TOPOLOGICAL PHOTONIC CRYSTALS

Time-reversal-invariant topological photonic and phononic crystals (with a full energy gap) have recently emerged that emulates the spin-orbit-coupled Kane-Mele \mathbb{Z}_2 topological insulator [49,59,113–116]. By exploiting an analogy between the electronic spin and a photonic pseudospins, much progress has been made in the design and construction of fully gapped topological photonic crystals. The practical success of this analogy has obscured the correct topological classification of these photonic crystals, which relies on a precise group-theoretic treatment of photonic band structure.

Photons transform in the integer-spin representation of crystallographic spacetime symmetries. Therefore, timereversal-invariant photonic crystals lie in Wigner-Dyson symmetry class AI and not AII. This distinction is crucial: In class AII, there exists electronic topological insulators whose filled bands transform as obstructed representations (of space group G), regardless of the addition of any BR (of G) to the filled-band subspace. More generally stated, these are obstructed representations which are not fragile obstructed; they will be referred to as stable obstructed. (A stable obstructed representation is nontrivial in the stably-equivalent classification of G-equivariant K-theory [9,54,117,118]). A paradigmatic example is the Kane-Mele \mathbb{Z}_2 topological insulator. In contrast, all known topological insulators in class AI are fragile obstructed. Moreover, it has been argued that every topological insulator is adiabatically deformable to a topological crystal [79], which would imply that all topological insulators in class AI are fragile obstructed.

The distinction between fragile versus stable is not just academic. If a FOR is accompanied by in-gap boundary states, the possibility of FOR \oplus BR=BR' makes the in-gap boundary states less robust than might naively be expected—from tight-binding or $k \cdot p$ methods. (We shall be concerned with the possibility of *spectrally robust* boundary states, that are irremovable from the energy gap by any continuous deformation that preserves both gap and symmetry [119]). In practice, this means that a great majority of topological insulators and gapped photonic crystals (in class AI) do not have spectrally

robust boundary states—a perspective that we explore generally in Sec. IX and more specifically in Sec. IX C.

While Sec. IX contains general arguments for the non-robustness of boundary states, more specific arguments have been given for FORs of space group $\mathcal{T}_3 \rtimes C_{nv} \times \mathbb{Z}_2^T$ (n=3,4), whose accompanying boundary states manifest a representation-dependent stability (cf. Sec. III A). In the present section, we prove that (a) a tetragonal photonic crystal designed by Ochiai realizes the FOR of $\mathcal{T}_3 \rtimes C_{4v} \times \mathbb{Z}_2^T$ (cf. Sec. VIII A), and (b) a hexagonal photonic crystal built by Yihao *et al.* realizes the FOR of $\mathcal{T}_3 \rtimes C_{3v} \times \mathbb{Z}_2^T$ (cf. Sec. VIII B). Finally, in Sec. VIII C, we prove the spectral nonrobustness of the observed domain-wall states [58] of the hexagonal photonic crystal.

A. Topological classification of tetragonal photonic crystal

The 3D tetragonal photonic crystal designed by Tetsuyuki Ochiai is composed of an array of circular pillars with high refractive index. A geometrical anisotropy of the pillar breaks spatial inversion symmetry (i) and reduces the space group to $\mathcal{T}_3 \rtimes C_{4v} \times \mathbb{Z}_2^T$ [57]. A secondary effect of the anisotropy is to introduce an energy gap between the lowest rank-three band and an energetically isolated rank-two band (Q_{phc}) illustrated in the middle of Fig. 7(a).

If the photonic crystal is terminated by a $\mathcal{T}_2 \times C_{4v} \times \mathbb{Z}_2^T$ -symmetric surface with the boundary condition of a perfect electric conductor (zero surface-parallel electric field), Ochiai found evanescent eigensolutions to Maxwell's equations which are localized to the surface. For the specific termination chosen by Ochiai, the eigenenergies of these surface states cover the bulk energy gap below Q_{phc} , and their energy-momentum dispersion is qualitatively equivalent to Liang Fu's prediction for the rotation-invariant TCI, as was reviewed in Sec. III A.

However, the stability of these surface states are representation dependent, which raises some doubt as to the analogy with the TCI. For a conclusive proof it is desirable to have a bulk diagnostic that is insensitive to the choice of surface termination. One approach is to calculate the \mathbb{Z}_2 bulk topological

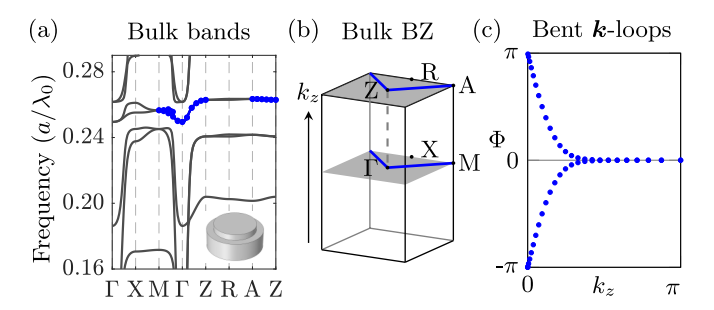


FIG. 7. (a) Bulk band structure of the tetragonal photonic crystal, in which a is the lattice constant, λ_0 is the vacuum wavelength, and a/λ_0 is the dimensionless normalized frequency. The middle rank-two band, indicated by blue dots, is denoted Q_{phc} . The inset in panel (a) illustrates the high-refractive-index pillar in one real-space unit cell of the photonic crystal. (b) The bulk Brillouin zone of the tetragonal photonic crystal. The bent k loops $\mathcal{C}(k_z)$, for $k_z=0$ and π , are illustrated as blue lines. (c) Zak phases (Φ) of Q_{phc} for the family of bent k loops.

invariant originally formulated by Fu [55] and equivalently reformulated (by one of the present authors) in terms of Zak phases [69]; the latter formulation is simpler for numerical computation. For a general review of Zak phases, we refer the reader to Sec. V A.

Summary of Zak-phase diagnostic of \mathbb{Z}_2 *invariant.* Suppose P is a rank-two energy band that is energetically isolated, and carries the same symmetry representations (in k space) as a BR of $\mathcal{T}_3 \rtimes C_{4v} \times \mathbb{Z}_2^T$, induced from the two-dimensional irreducible representation of $C_{4v} \times \mathbb{Z}_2^T$. To diagnose if P is nontrivial in the \mathbb{Z}_2 classification, we would numerically diagonalize the Wilson loop of the non-Abelian Berry gauge field [cf. Eq. (7)] for a family of bent k-loops [$C(k_z)$] illustrated in Fig. 7(b). For each loop $C(k_z)$, k_z is fixed and (k_x, k_y) varied along a path with an orthogonal kink at each C_4 -invariant wave vector. Since P has rank two, the Wilson loop matrix has two eigenvalues $\{e^{i\Phi_1(k_z)}, e^{i\Phi_2(k_z)}\}$, with Φ_i the Zak phase. Due to the fourfold symmetry, $\Phi_1(k_z) \equiv -\Phi_2(k_z) \pmod{2\pi}$ and it suffices to consider just Φ_1 . At $k_z = 0$ (and also $k_z = \pi$), the symmetries of time reversal and fourfold rotation result in the Zak phase being fixed either to $\Phi_1 = 0$ or π . Then $\Phi_1(0) \equiv$ $\Phi_1(\pi)$ versus $\Phi_1(0) \not\equiv \Phi_1(k_z)$ correspond, respectively, to the trivial verus nontrivial \mathbb{Z}_2 class.

The above diagnostic cannot be applied to the rank-three subspace below the gap [69] but can be applied to the rank-two subspace Q_{phc} just above the gap. We plot how the Zak phase of Q_{phc} disperses with respect to k_z in Fig. 7(c), thus confirming its nontriviality in the \mathbb{Z}_2 classification.

We remark that the same obstructed representation of $\mathcal{T}_3 \times C_{4v} \times \mathbb{Z}_2^T$ can in principle be realized by a 3D tetragonal lattice of dielectric cavities embedded in an artificial metallic plasma [120]. Based on a tight-binding Hamiltonian description of weakly coupled plasmons (associated to the surfaces of dielectric cavities), Yannopapas proposed to realize Liang Fu's tight-binding model of the TCI; however, this remains a hypothesis in the absence of a concrete design. If ever such a design is conceived, it would be interesting to explore the implications of fragility in a setting that differs from Ochiai's.

B. Topological classification of hexagonal photonic crystal

The photonic crystal by Yang *et al.* consists of metallic split-ring resonators arranged in a 3D hexagonal array with symmetry of $\mathcal{T}_3 \rtimes C_{3v} \times \mathbb{Z}_2^T \equiv P31m$ and has been claimed to be the first experimental realization of a topological band gap in three spatial dimensions [58].

The design principle for this hexagonal photonic crystal (and related crystals [114,115]) has been to emulate the spin-orbit-coupled \mathbb{Z}_2 Kane-Mele topological insulator. That is, by fine-tuning the crystalline structure, Yinghao *et al.* have designed a photonic band touching at the K point, which is described by the following $k \cdot p$ Hamiltonian:

$$H = v_{\parallel} \tau_0 \otimes (k_x \sigma_x + k_y \sigma_y) + m \tau_x \otimes \sigma_z + v_z k_z \tau_y \otimes \sigma_z.$$
 (15)

This Hamiltonian is identical (as a k-dependent matrix) with that of the critical point of the spin-orbit-coupled Kane-Mele model. (Above, $\sigma_{i=0,x,y,z}$ and $\tau_{i=0,x,y,z}$ are distinct sets of Pauli matrices. For concreteness, we have shown the form of the Hamiltonian, but postpone its technical description.)

Despite being identical as matrices, the bases of the two $k \cdot p$ Hamiltonians differ—the photonic basis forms an integer-spin representation of crystallographic point-group symmetries, while the electronic basis forms a half-integer-spin representation. The difference in bases will not matter to the *existence* of Jackiw-Rebbi soliton eigen-solutions [121] of Eq. (15), which are localized to a mass domain wall—this is how Yinghao *et al.* (and related works) justify their experimentally observed domain-wall states that disperse as a Dirac cone. However, the difference in bases will matter to the *robustness* of these domain-wall states—unlike time-reversal-invariant topological insulators, the domain-wall states of the time-reversal-invariant hexagonal photonic crystal is not spectrally robust, as we prove in Sec. VIII C.

There is yet another motivation for a proper group-theoretic analysis of the Hamiltonian in Eq. (15). Ultimately, photonic bands cannot realize the Kane-Mele \mathbb{Z}_2 topological invariant; the appropriate topological invariant for threefold-invariant photonic crystals in Wigner-Dyson class AI has been identified (by one of the present authors) as the *halved-mirror chirality* χ [69] so named because it is an *integer* topological

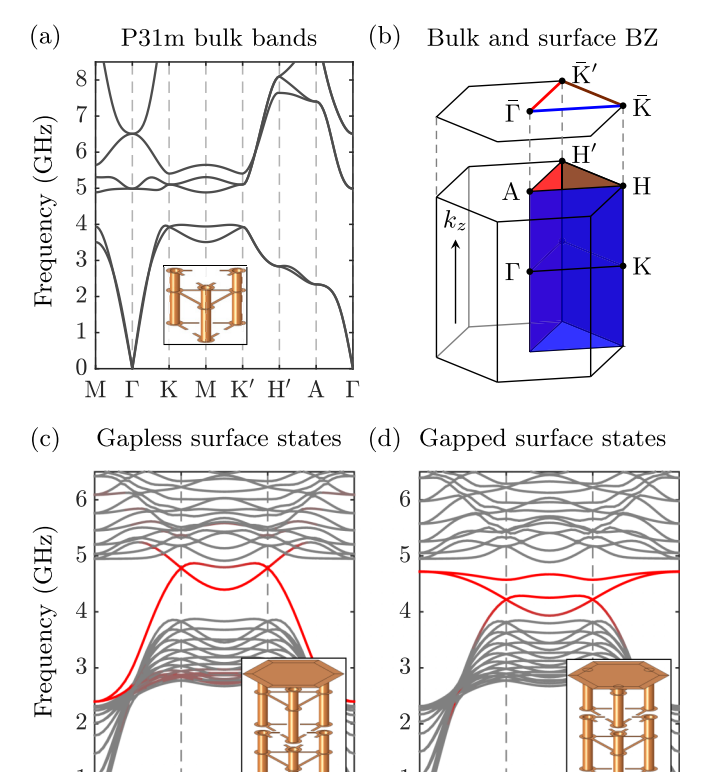


FIG. 8. (a) Bulk band structure of the hexagonal photonic crystal, with the split-ring resonator illustrated in the inset. Our simulated crystal is deformed from the experimental system of Yihao Yang et al., so the crystal is closer to the critical point of the topological phase transition. This deformation preserves both symmetry and the relevant bulk gap. Bottom of (b) panel: Bulk Brillouin zone of hexagonal photonic crystal; the halved mirror plane is colored blue. Top: 001 surface Brillouin zone. (c), (d) illustrate the spectrum of Maxwell's equation with perfect-electric-conductor boundary condition imposed on the 001 surface, for two different surface terminations; surface-localized states are colored red.

 \bar{K}

 \bar{K}'

K

 $\bar{\mathrm{K}}'$

invariant defined over a halved mirror-invariant plane (illustrated by the blue rectangle in Fig. 8). We will prove below that the Hamiltonian in Eq. (15), when interpreted with the correct photonic basis, describes a topological phase transition where χ changes by unity. $\chi = 1$ indicates a FOR, as we have proven in Appendix E 2.

Accompanying this change from $\chi = 0$ to $\chi = 1$ is the development of in-gap, surface-localized states that are illustrated in Fig. 8(c); for this figure, we have terminated the crystal with a $\mathcal{T}_2 \rtimes C_{3v} \times \mathbb{Z}_2^T$ -symmetric 001 surface, on which is imposed the perfect-electric-conductor boundary condition. The nontrivial connectivity of surface states (colored red) over the high-symmetry line $\bar{\Gamma}\bar{K}\bar{K}'\bar{\Gamma}$ was initially predicted by one of us in Ref. [69]. However, in principle, these surface states are removable from the bulk gap while preserving both gap and symmetry, owing to hybridization with conventional surface states (transforming as a unit-rank BR of $\mathcal{T}_2 \rtimes C_{3v} \times \mathbb{Z}_2^T$). Figure 8(d) illustrates how such conventional gapped surface states may emerge from the continuum of high-energy bands above the bulk gap, owing to a slightly different surface termination that maintains $\mathcal{T}_2 \rtimes C_{3v} \times \mathbb{Z}_2^T$ symmetry. This is another manifestation of the representation-dependent stability of surface states [cf. Sec. III A].

Proof that Eq. (15) (with m = 0) is a critical point for χ

The Hamiltonian in Eq. (15) is a small-k expansion around the K point of the hexagonal Brillouin zone; the little group of K is the point group C_{3v} , which is generated by the three-fold

$$U^{\dagger}HU = \begin{pmatrix} m & v_{\parallel}k_x + iv_zk_z & 0 & 0 \\ v_{\parallel}k_x - iv_zk_z & -m & 0 & 0 \\ 0 & 0 & m & v_{\parallel}k_x - iv_zk_z \\ 0 & 0 & v_{\parallel}k_x + iv_zk_z & -m \end{pmatrix}, \quad U = \frac{1}{2}\begin{pmatrix} 1 & 1 & 1 & -1 \\ 1 & 1 & -1 & 1 \\ 1 & -1 & 1 & 1 \\ -1 & 1 & 1 & 1 \end{pmatrix}.$$

On inspection, Eq. (17) is a massive Dirac Hamiltonian with opposite chiralities in the different mirror eigenspaces. When the Dirac mass m changes sign, the integrated Berry curvature $(\int_{k_{\nu}=0} F_{\eta})$ in the η subspace changes by $\eta \in \{+1, -1\}$ [124]. It follows that $\chi = \int_{HMP} (F_{\eta=+1} - F_{\eta=-1})$, being an integral (over the halved mirror plane) of the differential Berry curvature [69] changes by unity. This completes the proof.

C. Instability of domain-wall states of tetragonal and hexagonal photonic crystals

Here we investigate the robustness of domain-wall states of fragile topological photonic crystals. A simple example of a two-dimensional domain wall separates two threedimensional crystals, which differ only in that one crystal is geometrically reflected relative to the other. A domainwall configuration of the tetragonal [respectively, hexagonal] photonic crystal is illustrated in Fig. 9(a) here (respectively, Fig. 2(a) of [58]). A domain-wall configuration generally has the symmetry of a crystallographic layer group, and we will find that certain layer groups allow for the existence of rotation C_3 (about z) and a reflection \mathfrak{r}_{v} that inverts $y \to -y$. These symmetries are represented as

$$\hat{C}_3 = \tau_0 \otimes e^{i2\pi\sigma_z/3}, \quad \hat{\mathfrak{r}}_y = \tau_z \otimes \sigma_x.$$
 (16)

Two of four basis vectors transform under C_{3v} as $x \pm iy$, corresponding to circularly-polarized transverse electric modes $E_x \pm iE_y$; the other two basis vectors transform as $\mp iz(x \pm iE_y)$ iy), corresponding to circularly polarized transverse magnetic modes $H_x \pm iH_y$. $\sigma_z = \pm 1$ distinguishes the two circular polarizations, which are inverted under reflection [cf. Eq. (16)].

While not crucial to our proof, it is worth clarifying the physical origin of these transverse modes. The design principle of the hexagonal photonic crystal relies on first constructing a D_{3h} -symmetric crystal, and then reducing the symmetry to $C_{3\nu}$ with a structural bi-anisotropy [122] that breaks $\mathfrak{r}_z: z \to -z$ reflection symmetry [58]; \mathfrak{r}_z is mapped to $\tau_z \otimes \sigma_0$ in the representation space of Eq. (15), and the bianisotropy is reflected by the mass term in Eq. (15). The transverse electric and magnetic modes transform, respectively, in the E' and E'' representations of D_{3h} [123] but in the same E representation of C_{3v} ; therefore, the bianisotropy allows to couple electric and magnetic modes.

Focusing on the r_v -invariant plane ($k_v = 0$), we perform a unitary transformation U (specified below) such that $U^{\dagger} \hat{\mathfrak{r}}_{\nu} U$ is diagonal with on-diagonal elements: 1, 1, -1, -1. The first two (respectively, last two) basis vectors will be said to belong in the $(\eta = +1)$ -eigenspace [respectively, $(\eta = -1)$ eigenspace] of reflection. The Hamiltonian then becomes block diagonal with respect to η :

$$\begin{pmatrix} 0 \\ 0 \\ v_{\parallel} k_x - i v_z k_z \end{pmatrix}, \quad U = \frac{1}{2} \begin{pmatrix} 1 & 1 & 1 & -1 \\ 1 & 1 & -1 & 1 \\ 1 & -1 & 1 & 1 \\ -1 & 1 & 1 & 1 \end{pmatrix}.$$
 (17)

Dirac-type domain-wall states. However, we will prove that such domain-wall states are removable from the bulk energy gap by a continuous deformation that preserves both gap and the layer-group symmetry. Though not spectrally robust, we will explain that these domain-wall states have a weaker type of robustness that is analogous to topological Dirac-Weyl (semi)metals [36,125–130].

In fact, Dirac-type domain-wall states have been experimentally observed for the hexagonal case [58] and numerically simulated for the tetragonal case in Fig. 9(c) for a specific domain-wall thickness. To explain the existence of Dirac points, the crucial observation is that both domain-wall configurations (of the tetragonal and hexagonal photonic crystals) have in common a screw symmetry, which is the composition of a twofold rotation axis (lying parallel to the domain wall), and a half Bravais-lattice translation along this axis. (We see that the layer group can be nonsymmorphic, even though the three-spatial-dimensional space group of either crystal is symmorphic.) Each Dirac point is then a crossing between two distinct screw representations, of the type first theoretically predicted by one of us for gapless photonic crystals [130]. As illustrated schematically

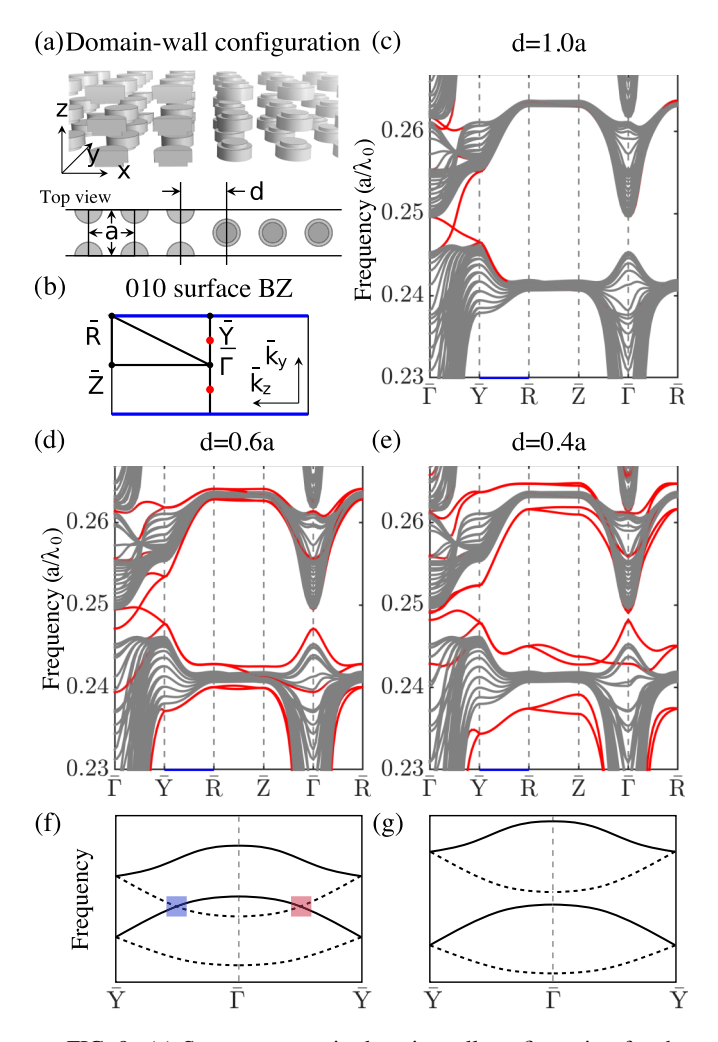


FIG. 9. (a) Screw-symmetric domain-wall configuration for the tetragonal photonic crystal. The bulk lattice period a and domain-wall thickness d are indicated in the bottom panel. (b) Two-dimensional BZ of the domain-wall configuration. (c)–(e) illustrate band structure calculations for d/a=1.0, d/a=0.6, and d/a=0.4, respectively. States localized to the domain wall are colored red. The k positions of the Dirac points (for d/a=1.0) are indicated by red dots in (b). Note that the two fold degeneracy of domain-wall states along the high-symmetry k-line $\bar{Y}\bar{R}$ is due to a combination of screw and time-reversal symmetry. A pair of screw-symmetric Dirac points is schematically illustrated in (f); after mutual annihilation, the band structure is illustrated in (g).

in Fig. 9(f), a pair of Dirac points with opposite chirality originate from a band inversion between two rank-two bands, with solid and dashed lines corresponding to the two screw representations.

If the screw symmetry of the domain-wall configuration is broken, then the two screw representations are allowed to hybridize, and the Dirac-point degeneracy would generically lift.

One may, however, ask if the Dirac points are robust in the presence of screw symmetry. Here, a nuanced notion of robustness is advantageous. On one hand, the Dirac-type domain-wall states are *not spectrally robust*. Indeed, since the Dirac points result from a band inversion of domain-wall states rather than bulk states, it is possible to reverse the inversion while preserving both the bulk gap and screw symmetry. Through this reversal, a pair of Dirac points with opposite chirality [89] would eventually meet (at a time-reversal-invariant k point) and mutually annihilate. The result is that the domainwall states no longer cover the bulk gap—this proves the spectral nonrobustness of domain-wall states for both tetragonal and hexagonal photonic crystals. This reversal of the band inversion is numerically simulated for the tetragonal crystal—by screw-symmetrically decreasing the domain-wall thickness, as illustrated in Figs. 9(d)-9(e). Schematically, the Dirac points in Fig. 9(f) meet and annihilate at $\bar{\Gamma}$, leading to Fig. 9(g).

On the flip side, one may say that the screw-protected Dirac crossings persist so long as two crossings of opposite chirality do not meet and annihilate; such persistence may be rationalized by a nontrivial Berry-Zak phase of π , for any screw-symmetric k-loop that encircles an odd number of Dirac points [130]. This weaker notion of robustness is closely analogous to a class of nonsymmorphic topological semimetals without spin-orbit-coupling, as was proposed in Ref. [130].

We will describe three more examples of domainwall states in the literature of photonic crystals. In all cases mentioned here, the role of crystallographic symmetry, as well as the spectral nonrobustness, has not been appreciated.

- (i) A different realization of screw-symmetric domain-wall states can be found for the all-dielectric metamaterial crystal of Ref. [59]; see, in particular, their Fig. 3.
- (ii) Not just screw symmetry can protect Dirac-type domain-wall states. For example, the domain-wall configuration in Fig. 7 of Ref. [131] has a twofold rotational axis *parallel* to the domain wall, and their simulated Dirac point is a crossing between distinct representations of rotation.
- (iii) Our last example is the domain-wall configuration in Fig. S6 of Ref. [59], which has a twofold rotational axis *perpendicular* to the domain wall; their simulated Dirac points exist because of the composition of rotation and time reversal, which reduces the codimension of an eigenvalue degeneracy to two, according to the well-known Wigner-von Neumann non-crossing rule [132]. This case is closely analogous to the Dirac points of graphene.

IX. BAND REPRESENTATIONS ARE INCOMPATIBLE WITH ROBUST BOUNDARY AND DOMAIN-WALL STATES

Throughout this paper, we have employed the crystallographic splitting theorem in various guises to determine if a given band is a BR or an obstructed representation. Here we argue for one utility of such a determination, namely, that BRs are incompatible with spectrally robust in-gap states—localized either to a boundary interface between crystal and vacuum, or to a domain-wall interface between two crystals which are relatively inverted. After elaborating on the distinction between a boundary and domain wall in Sec. IX A, we will formalize the above-mentioned incompatibility by proving a necessary condition for spectrally robust boundary and domain-wall states in Sec. IX B (the precise meaning of spectrally robust will also be given there). Finally, we will

apply these results to the in-gap states of fragile topological insulators and photonic crystals in Sec. IX C.

In proving the absence of spectrally robust in-gap states for BRs, we will apply that every BR has a symmetric deformation to an tight-binding (or atomic) limit. In fact, the converse is also true: If a tight-binding limit exists for a band, then it must be band representable. The equivalence between the existence of a symmetric tight-binding limit and band representability is formalized in a theorem in Sec. IX B.

A. Distinguishing boundary from domain wall

Here we precisely define a boundary versus a domain wall, and give a casual introduction to the tight-binding method; this preliminary discussion is to prepare us for a subsequent proof of the boundary/domain-wall stability criterion in Sec. IX B.

Suppose we are given a d-spatial-dimensional crystalline insulator (or a photonic crystal) with space group G, and an energy gap separating the low-energy subspace and the complementary, high-energy subspace. Any continuum description of crystals formally involves an infinite number of bands; however, one is typically interested in physics within a finite energy window, and it is common practice to truncate the continuum Hilbert space and model the truncated subspace by a finite-rank tight-binding lattice model. In this manner, we obtain a tight-binding Hamiltonian with an energy gap separating a low- and high-energy subspace, with corresponding finite-rank projectors that are assumed to be analytic throughout the Brillouin zone.

Let us enclose the crystal by a (d-1)-spatial-dimensional hypersurface and ask if there are evanescent eigenstates that are exponentially-localized to the hypersurface, with energies lying within the energy gap (defined by the translation-invariant crystal). The answer depends on what lies on both sides of the hypersurface; two scenarios are commonly encountered:

Definition of boundary. For any crystal with an energy gap, it is convenient to define a crystalline vacuum that satisfies two properties: its symmetry group contains the space group (of the crystal) as a subgroup, and energy eigenstates below a threshold energy E_v are forbidden; the minimal bound for E_v is given by the maximal energy of the gap (of the translationinvariant crystal). We define a boundary as a hypersurface that separates the "bulk" crystal from its vacuum. Moving away from the hypersurface and into the crystalline bulk, we assume that the Hamiltonian (or classical mode equation) asymptotically approaches a form that is locally identical to a translation-invariant crystal; concretely, we insist that the deviation (from the translation-invariant form) decays at least as fast as an exponential function. Moving away from the hypersurface into the crystalline vacuum, we also assume that the Hamiltonian exponentially approaches a form locally identical to a translation-invariant vacuum.

In practice, E_v is determined by the specific physical realization of the crystalline vacuum. For example, a metal acts as a vacuum for photons owing to the screening ability of metallic electrons, and E_v is then given by the plasma frequency of the metal. In cases where the energy window of interest lies far below E_v , one may reasonably take E_v to infinity and impose

idealized boundary conditions, such as the Dirichlet (open) boundary condition sometimes used to model finite-size, solid-state crystals, or the perfect-electric-conductor boundary condition [57,133] often used for photonic crystals. We will not need to assume that the boundary is smooth—evanescent eigenstates which are localized to (d-2)-spatial-dimensional boundary kinks (or hinges) have been explored in higher-order topological insulators [134–137] and form a subclass of what we call boundary states.

Definition of domain wall. A domain wall is a hypersurface separating two crystals with the same space group and the same bulk energy gap; the two crystals differ only in that bulk states (in the relevant energy window) are inverted with respect to the center of the bulk energy gap. Such a spatially inhomogeneous band inversion can be engineered in photonic crystals [57,58]. Our notion of a domain wall is conceptually similar but not identical to a massive domain wall of the Dirac equation [121] whose chiral zero modes are anomalous [138].

B. Necessary criteria for spectrally robust boundary and domain-wall states

The sense in which robust boundary states are incompatible with BRs is stated in the following criterion.

Boundary stability criterion. Given a crystal with space group G and a bulk energy gap, a necessary condition for spectrally robust, in-gap boundary states is that the low-energy subspace is an obstructed representation of G.

By spectrally robust, we mean that the eigenenergies of the boundary states form a band that covers the bulk energy gap, and this covering is insensitive to continuous and (G_{int}, G) -symmetric deformations that preserve the energy gap. Here, $G_{\text{int}} < G$ is the symmetry of the interface; if the interface has discrete translational symmetry in two independent directions, G_{int} is generally a layer group. By a (G_{int}, G) -symmetric deformation, we mean that the deformation is everywhere G_{int} -symmetric; moving away from the interface, the G-asymmetric component of the deformation is assumed to decay exponentially. While specifying G_{int} is necessary to uniquely define spectral robustness, actually the boundary stability criterion holds regardless of the choice for G_{int} . The following criterion for domain walls also holds regardless of the symmetry of the domain-wall interface.

Domain-wall stability criterion. Given a crystal with space group G and a bulk energy gap, a necessary condition for spectrally robust, in-gap domain-wall states is that either the low-energy subspace or the high-energy subspace is an obstructed representation of G.

The proof of the above criteria is based on two physically intuitive claims: (i) every BR has a symmetric tight-binding limit and (ii) the boundary (or domain wall) of a crystal does not have to intersect any tight-binding lattice site.

Statement (i) is widely believed folklore, and our contribution is a restatement of (i) that is amenable to a rigorous, bundle-theoretic derivation. We define a *tightly bound BR* of *G* as a BR of *G* with the property that each Wannier function only has support on a single lattice site. (In the tight-binding formalism, each Wannier function is defined over a real-space lattice with a finite-dimensional complex vector space on each

lattice site.) Each Wannier function in a tightly-bound BR is said to be *one-site localized*.

Symmetric tight-binding limit theorem. For a G-symmetric band, being a BR of G is equivalent to the existence of a G-symmetric homotopy to a G-symmetric band spanned by one-site localized Wannier functions.

To qualify this statement, for P a BR of G, the just-stated G-symmetric homotopy always exists for a tight-binding model that contains P as the complete, low-energy subspace, and also contains a high-energy subspace with sufficiently large rank—this will shortly be clarified in Sec. IX B 1.

The forward arrow of the above theorem is proven by showing that a $BR(G, \varpi, D)$ and a tightly bound $BR(G, \varpi, D)$ are isomorphic as G-vector bundles (cf. Appendix G], and then applying the universal G-bundle theorem [139] to prove existence of the G-symmetric homotopy [140]. Such a homotopy will be referred to as a *deformation to the symmetric tight-binding limit*, and is exemplified numerically by the adiabatic deformation in Ref. [62]. The backward arrow is proven in Sec. VI A, where we also discuss its implications for the Wannier functions of topological insulators.

The remaining argument will separately treat boundaries and domain walls.

1. Proof of boundary stability criterion

We will argue for the contrapositive restatement of the boundary stability criterion. Our strategy is to exclude boundary states for a model tight-binding Hamiltonian H_b (to be specified below) whose low-energy subspace is bandrepresentable. This would imply the absence of spectrally robust boundary states for any Hamiltonian that is continuously deformable to H_b , while preserving the bulk energy gap and (G_{int}, G) symmetry, for any $G_{\text{int}} < G$.

Our model Hamiltonian is

$$H_b = PB_bP + Q + 2Q',$$
 (18)

where P (respectively, Q) is the analytic, finite-rank projector to the low-energy (respectively, high-energy) band of the crystal [141]. While P and Q lie within the energy window of interest, a formal proof will additionally require Q' which projects to energy bands lying above Q on the energy axis; such bands always exist because we are approximating a continuum description of crystals. Q' has the following properties: (a) Q' has finite rank and is orthogonal to both P and Q; I = P + Q + Q', (b) Q' is analytic over the Brillouin torus, and (c) Q' transforms as a BR of G. While P, Q, and Q' have the symmetry of the space group G, G is not a symmetry of H_b owing to the leftmost term involving B_b —a spatial-bipartition operator that equals -1 within the crystalline bulk and +1without. Since matrix elements of P have exponential decay in real space, H_b exponentially approaches the form 2Q' + Q -P within the crystalline bulk; this form models a crystalline Hamiltonian with spectrally flattened bulk bands, and with the relevant bulk energy gap in the interval (-1, +1); outside of the bulk region, H_b exponentially approaches Q' + I, which models a crystalline vacuum with threshold energy $E_v = +1$.

If P is a BR, then by the symmetric tight-binding limit theorem, P is continuously deformable to a tightly bound

BR by a G-symmetric homotopy. The corresponding onesite-localized Wannier functions are all eigenstates of H_b , assuming that the G_{int} -symmetric boundary hypersurface does not intersect any tight-binding lattice site. (No matter G_{int} , it is always possible to symmetrically deform the hypersurface to satisfy this zero-intersection condition.) Since any state in the orthogonal subspace Q (respectively, Q') is an eigenstate of H_b with eigenvalue +1 (respectively, eigenvalue +2), the spectrum of H_b is just $\{-1, +1, +2\}$, with no eigenenergies in the bulk energy gap.

We now address a subtlety in the above argument that formally justifies the presence of Q' in H_b . Supposing Q' = 0, it is possible that the G-symmetric homotopy (between P and a tightly bound BR) does not exist.

Given a *G*-symmetric tight-binding lattice model with a band subspace *P* that forms a BR of *G*, we say that *P* has a *symmetric tight-binding obstruction* if it cannot be deformed to a symmetric tight-binding limit.

A symmetric tight-binding obstruction is an artifact of the tight-binding formalism and reflects that a subset of the Wannier centers of P are rigidly displaced from any tightbinding lattice site (a lattice site is the positional center of a localized, tight-binding basis vector). Such an obstruction has some conceptual similarities with the "obstructed atomic limit" formulated by Refs. [10,60]; one important distinction is that the tight-binding obstruction does not apply to continuum crystals. In the proof of the symmetric tight-binding limit theorem, the universal G-bundle theorem guarantees the existence of the G-symmetric homotopy if P is a subspace of a tight-binding vector space with sufficiently large rank, as explained in Appendix G3. A continuum description of crystals might be viewed heuristically as a tight-binding lattice model with an infinitely fine real-space mesh—in this case the symmetric tight-binding obstruction should not exist. In the tight-binding formalism, one removes the obstruction by enlarging the tight-binding lattice model to include the higher-energy bands in Q_c —this justifies the presence of Q'in H_h .

We know of two mechanisms for a symmetric tight-binding obstruction for fixed-rank, tight-binding Hamiltonians:

- (i) Both the tight-binding lattice sites and the Wannier centers of *P* are rigidly fixed to *distinct* positions, owing to nontranslational symmetries of the tight-binding model. This type of obstruction is exemplified by the nontrivially polarized filled band of the Su-Schrieffer-Heeger model [80] and also by a BR in a modified Kane-Mele honeycomb model [62].
- (ii) The second mechanism exists even if the point group of space group G is trivial, implying that the Wannier centers of P lie at generic Wyckoff positions. Naively, these Wannier centers would always be continuously tunable to lie on the tight-binding lattice sites. However, there exists finiterank tight-binding Hamiltonians without any nontranslational symmetry, but having a low-energy BR that is topologically obstructed from a tight-binding limit—such is the case for the Hopf insulator [142] as clarified in Ref. [143].

2. Proof of domain-wall stability criterion

Let us argue for the contrapositive restatement of the domain-wall stability criterion. Our strategy is to exclude

domain-wall states for a model Hamiltonian $H_{\rm dw}$ (specified below) whose low- and high-energy subspaces are both band-representable; this would rule out spectrally robust domain-wall states for any Hamiltonian that is deformable to $H_{\rm dw}$ while preserving both bulk gap and $(G_{\rm int}, G)$ symmetry.

Our model Hamiltonian for a domain wall is

$$H_{\text{dw}} = (Q - P)B_{\text{dw}}(Q - P) + 2Q',$$
 (19)

with $B_{\rm dw}$ a real-space bipartition operator that equals +1 on one side of the domain wall, and -1 on the other side. Moving away from the domain wall, $H_{\rm dw}$ asymptotically approaches 2Q' + (Q - P) on one side of the wall and 2Q' - (Q - P) on the other side; the difference is that P and Q are inverted with respect to the center of the bulk gap.

If both P and Q are BRs, then they are both deformable to tightly bound BRs. Once again, the presence of Q' nullifies any possible symmetric tight-binding obstruction for P and Q. Since (Q-P) and Q' act in orthogonal subspaces, the spectrum of $H_{\rm dw}$ is obtained by independently diagonalizing the two terms on the right-hand side of Eq. (19). Any one-site localized Wannier function of P is an eigenstate of $(Q-P)B_{\rm dw}(Q-P)$ with eigenvalue +1 on side of the domain wall, and eigenvalue -1 on the other side. The same can be said for the one-site localized Wannier functions of Q, except that the eigenvalues ± 1 are inverted. We thus obtain that the spectrum of $H_{\rm dw}$ is $\{-1, +1, +2\}$, with no eigenvalues in the relevant energy gap (-1, +1), and hence no domain-wall states. This completes the proof.

The above two proofs can easily be generalized to include energy bands (P') lying lower than P on the energy axis, and transforming as a BR of G. (In the domain wall case, we will not assume P' is inverted across the domain wall.) Generalizing $H_{b,\text{dw}} \to H_{b,\text{dw}} - 2P'$, the above steps in excluding boundary/domain-wall states would essentially be unchanged.

As a final remark, we have assumed throughout this paper that a band has only the symmetry of a crystallographic space group; it is possible that other types of symmetries (e.g., particle-hole symmetry) may protect spectrally robust boundary states, even in the case of BRs.

C. Application to fragile topological insulators and photonic crystals

Boundary states whose eigenenergies cover the bulk gap are a well-known feature of many stable obstructed representations [33,35,37–39,89,144–154]. Less well known is that such boundary states also manifest in tight-binding models of some FORs [55,69,155]. There is, however, a danger in naively extrapolating the predictions of an idealized tight-binding model to a real material. As mentioned in Sec. IX B, a tight-binding model always involves truncating the infinite-rank Hilbert space of a continuum crystal. Thus even if the low-energy band of a tight-binding model is fragile obstructed with accompanying boundary states, it is possible that the complete, continuum low-energy subspace is actually band representable—this would imply that boundary states are *not* spectrally robust, according to the boundary stability criterion.

In the just-described hypothetical scenario, we may say that a BR in the continuum low-energy subspace "breaks" the fragile obstruction of the tight-binding model in the sense that $BR \oplus FOR = BR'$. Not just any BR can break a given fragile obstruction; to determine the appropriate BR, one can use the projected symmetry method (cf. Sec. III) or the projected position method (cf. Sec. V C 3). Now if FOR has boundary states covering the bulk gap, while BR' is deformable to a symmetric tight-binding limit without boundary states, the combined implication is that the hybridization of FOR with BR allows for the removal of all in-gap boundary states. This removal may be envisioned in the following thought experiment: Suppose BR

FOR were placed on a finite sample with boundaries, but with zero hybridization between BR and FOR. In addition to the boundary states (of FOR) which cover the bulk gap, it is also possible to have conventional boundary states (of BR) which do not cover the gap. Once the two types of boundary states hybridize, they must be adiabatically removable from the bulk gap; this has been described in Sec. III A (our case study of Fu's TCI) as a representation-dependent stability of boundary states. To recapitulate, we have argued that if boundary states (of a FOR) covers the energy gap, they must have a representation-dependent stability.

In practice, we believe that our boundary stability criterion rules out spectrally robust boundary states for a great majority of electronic insulators and photonic crystals. To support our claim, a recent study of 26 938 stoichiometric electronic materials claimed that none of them has a low-energy occupied subspace that is fragile obstructed [156]; this was rationalized in Ref. [157] as there being "usually enough occupied elementary band representations" to break any FOR below the Fermi level. However, we caution that their claim is based on identifying band/obstructed representations from their symmetry representations in *k*-space—such an identification method is not generally exhaustive (cf. Sec. III A).

A fragile obstruction of a finite-rank, high-energy band is even more likely to be breakable. This is because the continuum high-energy subspace formally has infinite rank, while there are only a finite number of elementary BRs which all have finite rank [18,19]—the existence of a BR that can break any given fragile obstruction is overwhelmingly probable. Such considerations become relevant when evaluating the spectral robustness of domain-wall states (cf. domain-wall stability criterion).

On the other hand, the continuum low-energy subspace has finite rank, and this rank can be of order one if the bulk gap lies close to the bottom of the energy spectrum. The closer to the bottom, the likelier to find unbreakable fragile obstructions. In this regard, photonic crystals have an advantage over electronic crystals; the latter have a fixed Fermi level, but photonic crystals can be experimentally probed at any frequency.

Application to electronic insulators and gapped photonic crystals in class AI. Let us assume that the topological classification by the method of topological crystals is complete [79] with the implication that any G-symmetric band in class AI is either a BR or a FOR of G. Given a crystal with an energy gap, the high-energy band is overwhelmingly likely to be band representable, hence spectrally robust in-gap states are only possible if the low-energy subspace is fragile obstructed. Presently, this possibility remains an unproven principle, and

is not realizable by any FOR that we know. [The reader may wonder if the rotation-invariant TCIs described in Sec. III satisfy the bill. Unfortunately, its unconventional boundary states can be destabilized by conventional boundary states emerging from *above* the energy gap, as illustrated in Fig. 8(d).]

X. DISCUSSION AND OUTLOOK

In vector bundle theory, the splitting principle has been used to reduce difficult questions on multirank bundles to simpler questions on sums of unit-rank bundles [158,159]; this reductionist approach is known to simplify the derivation of relations between Chern classes [53]. One may ask if an analogous splitting principle exists in band theory, where crystallographic space-group symmetry must be incorporated into the band/bundle.

In this paper. we have reduced the difficult question—of whether a given rank-N band is a BR—to simpler questions on a splitting into N unit-rank bands. For a majority of space groups (specified below), the necessary and sufficient condition for band representability is the existence of a splitting satisfying (A) that each unit-rank band has an analytic projector and a trivial first Chern class, and (B) the set of unit-rank bands are permuted by all crystallographic symmetries.

This statement is formalized by the crystallographic splitting theorem of Sec. IV B. As shorthand, a splitting that satisfies condition (A) [respectively, (B)] is said to be a Wannier splitting [respectively, a symmetric splitting]; if both conditions are satisfied, it is a symmetric Wannier splitting.

To apply this theorem to prove band representability, it is desirable to have a systematic method to symmetrically split a band, and then to verify if condition (A) is satisfied; once (A) is verified, the corresponding symmetric Wannier functions can be constructed via an algorithm detailed in Sec. VII. We have proposed two methods for symmetric splitting: the first involves diagonalizing a projected position operator, applies to a limited set of space groups (specified in the symmetric splitting lemma of Sec. VB), but has the advantage that all unit-rank bands automatically have analytic projectors (proven in Appendix D2). The second method involves diagonalizing a projected symmetry operator, applies to a wider set of space groups (specified in Appendix D1), but does not guarantee that each unit-rank band has an analytic projector (cf. Sec. III E). Of the two methods, only the projected symmetry method can be used for space groups with a three- (or fourfold) rotational symmetry, and this is how we proved in Sec. III that the hexagonal (or tetragonal) topological insulator in Wigner-Dyson class AI is fragile; the implications of fragility for the analogous photonic crystals are discussed in Sec. VIII. A general methodology that would apply to any space group is still lacking, and in our opinion would be a significant advance.

It should be clarified that P being band representable implies the existence of a symmetric Wannier splitting but does not imply that *all* Wannier splittings of P are symmetric or that *all* symmetric splittings of P are Wannier. To exemplify a symmetric, non-Wannier splitting, some *elementary* BRs [18,160–162] are each splittable into unit-rank bands which are *trivially* permuted by the space group and have analytic

projectors, and it is guaranteed that at least two of the unit-rank bands must have *nontrivial* first Chern class [80].

One implication of our splitting theorem is that obstructed representations—defined as non-BRs—cannot have a splitting that is simultaneously Wannier and symmetric. This has varied implications for topological insulators whose filled bands are obstructed representations: if (A) is satisfied, then [not (B)] can be interpreted as a symmetry obstruction for exponentially localized Wannier functions (cf. Sec. VI). If (B) is satisfied, then [not (A)] can be interpreted as the absence of exponential localization, or as a holonomy obstruction for Bloch functions. The holonomy interpretation is encapsulated by the Zak winding theorem in Sec. VB, provides a rigorous justification for the concept of "individual Chern numbers" [20,44,75,163], and may be useful as a design principle for model Hamiltonians of topological insulators. In future work, it will be interesting to generalize the Zak winding theorem to three spatial dimensions, where notions such as the "nested Wilson loop" [135] might come into play.

Our splitting theorem provides an equivalent description of BRs for nearly all crystallographic space groups and grey magnetic space groups. The only exceptional BRs have been referred to as nonmonomial, and they occur for three-spatial-dimensional double space groups having cubic point groups. These exceptions reflect that some half-integer-spin representations of cubic point groups are fundamentally two-dimensional, that is to say, they cannot be induced from a one-dimensional representation of a subgroup of the cubic point group (cf. Sec. IV C). It is interesting to speculate on a generalization of our splitting theorem that equivalently describes nonmonomial BRs—perhaps the splitting of a rank-*N* band must allow for sums of rank-two bands as well.

Condition (A) in our theorem involves the triviality of the first Chern class, which guarantees that each unit-rank band is topologically trivial as a *complex* vector bundle. Topological notions in *real* vector bundle theory have been fruitfully applied [48,65,80,88,164] to bands with spacetime inversion symmetry [165]. Being topologically nontrivial as a unit-rank, real vector bundle is equivalent to a nontrivial first Stiefel-Whitney class; this by itself does not imply an obstruction to symmetric Wannier functions [166], however, it does imply that the Wannier center cannot lie on a prespecified spatial origin [80,164]. It may be that a real analog of our splitting theorem exists for BRs whose Wyckoff positions are fixed to the origin.

ACKNOWLEDGMENTS

We are grateful to Barry Bradlyn and Nicholas Read, who independently encouraged us to generalize our theorem to bundles of arbitrary rank; Barry Bradlyn first pointed us to an example of a nonmonomial point group. Zhida Song provided expert advice on fragile topological insulators. L.L. thanks Hao Lin and Thomas Christensen for comparing numerical results. We are also indebted to Simon Altmann for clarifying his semidirect product decomposition of space groups, and for mailing his book, *Induced Representations in Crystals and Molecules*. A.A. was supported initially by

the Yale Postdoctoral Prize Fellowship and subsequently by the Gordon and Betty Moore Foundation EPiQS Initiative through Grant No. GBMF4305 at the University of Illinois. A.A. is grateful to the hospitality of Brewlab at Champaign-Urbana, where most of this paper was written. J.H. obtained financial support from NSF Grant No. 1724923. L.L. was supported by the National key R&D Program of China under Grants No. 2017YFA0303800, No. 2016YFA0302400, by NSFC under Project No. 11721404, and by the Strategic Priority Research Program of Chinese Academy of Sciences, Grant No. XDB33000000. C.W. acknowledge support from Ministry of Science and Technology of China, Grant No. 2016YFA0301001, the National Natural Science Foundation of China, Grants No. 11674188 and No. 51788104.

APPENDIX A: REVIEW OF BANDS, BUNDLES, AND SPACE GROUPS

1. Bands, vector bundles, and topological triviality

A rank-*N* band is given by *N* orthogonal Bloch functions at each wave vector k in the Brillouin torus. The Bloch functions span an *N*-dimensional vector space at each k and the union of all such vector spaces (over the base space of the Brillouin torus) defines a rank-*N* vector bundle. We typically use P(k) to denote the rank-*N* projector to the vector space at k and $P = \sum_{k} P(k)$ as the projector to the full band; \sum_{k} is our shorthand for a direct integral splitting [167] over the Brillouin torus and P(k) is periodic in reciprocal-lattice translations.

To minimize notation, we sometimes use P to denote the band itself, and not just the projector to the band. As a case in point, suppose P is an energy band (of a tight-binding or Schrödinger-type Hamiltonian) that is energetically isolated, that is, having an energy gap separating P from higher- and lower-energy bands, at each k. If the tight-binding Hamiltonian has matrix elements that decay exponentially in real space, then P(k) is an analytic function of k throughout the Brillouin zone [93]. As shorthand, we will just say that P is analytic throughout the Brillouin zone. This analyticity condition also holds given a physically reasonable condition on the Schrödinger-type Hamiltonian ($p^2/2m + V(r)$), namely, that the potential term V is square integrable over the unit cell [168].

Given a rank-N band/bundle, if there exist N Bloch functions which span the N-dimensional vector space at each k and are both continuous and periodic over the Brillouin torus, then the band is said to be $topologically\ trivial$ as a complex vector bundle. The distinct notion of topological triviality for real vector bundles is only mentioned briefly in Sec. X. Everywhere else, topologically trivial should always be understood as in the category of complex vector bundles.

In spatial dimension $d \le 3$ (which is assumed throughout), a band is topologically trivial if and only if it has trivial first Chern class [76,77]; for d = 3, this means that the first Chern number vanishes over any two-dimensional submanifold of the Brillouin three-torus; for d = 1 the first Chern class is always trivial.

In this paper, all bands are assumed topologically trivial, unless otherwise specified. Applying the Oka-Grauert

theorem [169,170] topological triviality implies that the N Bloch functions can also be chosen analytic in k, which further implies that their Fourier transforms—known as Wannier functions—are exponentially localized in real space [76]. Therefore, a topologically trivial rank-N band is equivalent to N orthogonal Wannier functions in each unit cell, with other Wannier functions related by discrete Bravais lattice translations. The specification of such Wannier functions which equivalently span a band shall be called a *Wannier basis*.

2. Space groups, point groups, and Wigner-Dyson symmetry classes

Let g denote an isometry in d spatial dimensions, possibly combined with the reversal of time. $g = (t_g | \check{g})$ may be decomposed into point-preserving and translational components, with \check{g} a $d \times d$ orthogonal matrix and $t_g \in \mathbb{R}^d$. g has the following action on spacetime: $r \to g \circ r = \check{g}r + t_g$ and $t \to s_g t$; $\check{g}r$ should be understood as a matrix multiplying a d-component vector (x, y, \ldots) , and $s_g = -1$ for g that reverses time.

Not including time reversal, all spatial isometries that preserve a crystal form a *crystallographic space group G*; there are 230 such groups in spatial dimension d=3, and 17 such groups in d=2; the latter are also known as wallpaper groups. \mathcal{T}_d denotes the translational subgroup of G, where the subscript d equals the number of linearly independent translation vectors. The *crystallographic point group* of G is defined as the quotient group $\mathcal{P}=G/\mathcal{T}_d$. There are 32 crystallographic point groups in d=3, which are further categorized into six crystal families. For example, the cubic crystal family consists of the three tetrahedral and two octahedral point groups, which are therefore also referred to as the five *cubic* point groups.

A grey magnetic space group, denoted G_T , is a direct product of any crystallographic space group G with \mathbb{Z}_2^T , the order-two group generated by time reversal T. (In general, \mathbb{Z}_n^g will denote a cyclic group of order n and generated by g, i.e., $g^n = e$ with e the identity element.) $T^2 = e$ corresponds to Wigner-Dyson symmetry class AI. The point group of G_T will be referred to as a grey magnetic point group.

Throughout this paper, we are concerned only with linear representations of groups and not their projective representations. In particular, linear representations of a crystallographic point group transform with integer spin. We shall also only concern ourselves with the half-integer-spin, linear representations of *double crystallographic group* \tilde{G} and the *double grey magnetic space group* \tilde{G}_T ; these groups are, respectively, the double covers of G and G_T . In a double cover, we introduce an additional element \tilde{e} that squares to the identity and physically corresponds to a 2π rotation. For double grey magnetic groups, $T^2 = \tilde{e}$ corresponds to Wigner-Dyson class AII; in particular, the double cover of \mathbb{Z}_2^T is \mathbb{Z}_4^T .

Except in Sec. VI A, all of our results (including the splitting theorem of Sec. IV) hold for both symmorphic and nonsymmorphic space groups. A symmorphic space group is a semidirect product of a point group with a translational subgroup, which shall be denoted $\mathcal{T}_d \rtimes \mathcal{P}$; a nonsymmorphic space group is a space group that is not symmorphic.

Example of symmorphic space group $\mathcal{T}_3 \rtimes C_{4v} \times \mathbb{Z}_2^T$, a grey magnetic space group, is the symmetry of the tetragonal photonic crystal in Sec. VIII A. The crystallographic point group C_{4v} is generated by a fourfold rotation C_4 and a mirror reflection \mathfrak{r}_x with mirror plane containing the rotational axis. It is convenient to adopt Cartesian coordinates with C_4 : $(x, y, z) \to (-y, x, z)$ and \mathfrak{r}_x : $(x, y, z) \to (-x, y, z)$. $\mathcal{T}_3 \rtimes C_{4v}$ can only be the crystallographic space group P4mm (No. 99).

Implicit in the semidirect notation is an action of \mathcal{P} on \mathcal{T}_d , and inequivalent actions may result in inequivalent space groups, as we next illustrate.

Example $\mathcal{T}_3 \rtimes C_{3v} \times \mathbb{Z}_2^T$ is the symmetry of the hexagonal photonic crystal in Sec. VIII B. C_{3v} is generated by a threefold rotation C_3 and a mirror plane \mathfrak{r}_d containing the rotational axis. There are two symmorphic crystallographic space groups (P31m and P3m1) with the point group C_{3v} , and we will use $\mathcal{T}_3 \rtimes C_{3v}$ as a synonym for P31m. P31m is distinguished by having \mathfrak{r}_d relate two of three rotation-invariant Wyckoff positions, the third position being reflection invariant.

If space group is used in a sentence without any of the above qualifiers, it is safe to assume that the sentence applies to all categories of space groups. As a case in point, to any space group G we may associate a *Wyckoff position* $\boldsymbol{\varpi} \in \mathbb{R}^d$ and a *site stabilizer* $G_{\boldsymbol{\varpi}} = \{g \in G | g \circ \boldsymbol{\varpi} = \boldsymbol{\varpi}\}$. The site stabilizer consists of all elements in G that preserve the Wyckoff position.

3. Representations of space groups

A spacetime isometry $g \in G$ may be represented by an operator \hat{g} , which acts on functions of real space as $\hat{g}f(r) = \overline{f(g^{-1} \circ r)}^{s_p}$, where $\bar{a}^1 := a$ and $\bar{a}^{-1} := \bar{a}$ (the complex conjugate).

The symmetry representation of g on Bloch functions $\{|\psi_{j,k}\rangle\}_{j=1}^N$ is defined by a unitary $N\times N$ "sewing" matrix $U_{\varrho}(k)$:

$$\hat{g}|\psi_{j,k}\rangle = U_g(k)_{j'j} |\psi_{j',-s_g\check{g}k}\rangle. \tag{A1}$$

 $U_g(\mathbf{k})$ can be explicitly expressed in terms of the normalized cell-periodic component of Bloch functions, $u_{j,k}(\mathbf{r}) = e^{-i\mathbf{k}\cdot\mathbf{r}}\psi_{j,k}(\mathbf{r})$, as

$$U_{g}(\mathbf{k})_{j'j} = \langle u_{j',s_{\sigma}\check{g}\mathbf{k}} | \hat{g}(\mathbf{k}) | u_{j,\mathbf{k}} \rangle_{\text{cell}}, \tag{A2}$$

with $\hat{g}(\mathbf{k}) := e^{-is_g \check{g}\mathbf{k} \cdot t_g} \hat{g}$ and $\langle .|. \rangle_{\text{cell}}$ denoting an integral over \mathbf{r} in one unit cell (possibly with a summation over spin).

We say that a band (with projector P) transforms as a representation of the space group G, if $[\hat{g}, P] = 0$ for all $g \in G$. In short, P is referred to as a representation of G.

Let P_0 and P_1 be two representations of G with equal rank and being both analytic throughout the Brillouin zone. P_0 and P_1 are said to be *equivalent* if there exists a continuous interpolation $\{P_t\}_{t\in[0,1]}$ that preserves analyticity (throughout the Brillouin zone) and the symmetry condition $[\hat{g}, P_t] = 0$, for all $g \in G$ and all $t \in [0, 1]$. In bundle language, this means that P_0 and P_1 are isomorphic as G-vector bundles, as elaborated in Appendix G.

Space-group representations fall into two categories: BRs (cf. Appendixes A 3 a and A 3 b) and obstructed representations (cf. Appendix A 3 c).

a. Zak's definition of band representations

In the standard definition by Zak, a band representation of a space group G, denoted BR (G, ϖ, D) , is a representation of G that is induced from a representation (D) of a site stabilizer G_{ϖ} .

We briefly review this *induction process*: Begin with a set of exponentially localized Wannier functions centered on the Wyckoff position $\boldsymbol{\varpi}$, and transform in a representation D of the site stabilizer G_{ϖ} . By application of G on these Wannier functions, we generate an infinite set of Wannier functions which form a representation of G. Such Wannier functions that are obtained by induction will be said to form a *locally symmetric Wannier basis* for the BR; we elaborate on this point of view next.

b. Equivalent formulation of band representations by the locally-symmetric Wannier basis

In various proofs throughout this paper, it is useful to have an equivalent definition of BRs that emphasizes the symmetry properties of Wannier functions: *P* is a BR of *G* if and only if *P* is a (finite) direct sum of (infinite-dimensional) subspaces, each of which is spanned by a *locally-symmetric Wannier basis*. This equivalent definition of BRs has been proven in Appendix A of Ref. [80].

A locally-symmetric Wannier basis $\{|w_{n,R}^{\alpha}\rangle\}_{n,\alpha,R\in\mathcal{T}_d}$ with Wyckoff position $\boldsymbol{\varpi}_1$ is an orthonormal basis of an infinite-dimensional representation of G, which satisfies the following properties for all $n=1,...,M, \alpha=1,...,A, (\boldsymbol{R}|e)\in\mathcal{T}_d$:

- (1) $|w_{n,\mathbf{R}}^{\alpha}\rangle = \widehat{(\mathbf{R}|e)}|w_{n,\mathbf{0}}^{\alpha}\rangle$,
- (2) $|w_{n,0}^{\alpha}\rangle$ is exponentially localized,
- (3) $\{|w_{10}^{\alpha}\rangle\}_{\alpha=1}^{A}$ spans an A-dimensional representation of G_{∞} .
- (4) $\{|w_{n,\mathbf{0}}^{\alpha}\rangle\}_{\alpha}$ and $\hat{g}_n\{|w_{1,\mathbf{0}}^{\alpha}\rangle\}_{\alpha}$ span the same A-dimensional representation of $G_{\varpi_n}=g_nG_{\varpi_1}g_n^{-1}$,

where $G/(\mathcal{T} \rtimes G_{\varpi_1}) = \{[g_1 = (\mathbf{0}|e)], [g_2], ..., [g_M]\}$ is a coset decomposition of G.

It is worth clarifying that property 4 was not stated explicitly in Definition 4 in Appendix A of Ref. [80], however, the property was implicitly assumed.

c. Fragile versus stable obstructed representations

An obstructed representation of a space group G is a representation of G that is not a BR of G (in Zak's definition). The filled, low-energy band of a G-symmetric topological insulator is an obstructed representation of G.

If G has a trivial point group, then an obstructed representation of G is equivalent to [76] the topological nontriviality of the corresponding complex vector bundle. This is not generally true if the point group of G is nontrivial, e.g., for $G = \mathcal{T}_2 \times \mathbb{Z}_4^T$ (Wigner-Dyson class AII), all its representations necessarily constitute a topologically trivial complex vector bundle, owing to the time-reversal symmetry. In particular, the filled band of the \mathbb{Z}_2 Kane-Mele topological insulator is both topologically trivial (as a complex vector bundle) and an obstructed representation (of G); a proof of the latter statement is given in Sec. V.

Obstructed representations of a space group G may be further subdivided into fragile obstructed and stable obstructed.

A FOR of G is an obstructed representation of G, with the property that a BR of G exists, such that the direct sum of this BR with the FOR is a higher-rank BR. A *stable obstructed representation* of G is an obstructed representation of G that is not fragile obstructed.

APPENDIX B: MONOMIAL REPRESENTATIONS OF FINITE GROUPS

In the main text, we have amply used the notion of monomial representations of point groups. Monomial representations can equivalently be viewed as induced representations (from one-dimensional representations of subgroups) (cf. Appendix B 1) or as complex permutation representations (cf. Appendix B 2). Both views are elaborated pedagogically in this Appendix, and their equivalence established in Appendix B 3. Lastly, we prove a useful lemma for monomial direct-product groups in Appendix B 4.

Throughout this Appendix, we let H denote a finite group; a representation (U,V) of H on an n-dimensional representation space V is given by a map $h \to U(h)$, with U(h) generally an n-dimensional unitary matrix. If H is a point group (consisting of discrete spatial isometries that preserve a point in space), then $h_1h_2 \to U(h_1)U(h_2)$. If H is a magnetic point group,

$$h_1 h_2 \to U(h_1) \overline{U(h_2)}^{s(h_1)},$$
 (B1)

where $\bar{a}^{s(h)}$ equals the complex conjugate of a if h involves time reversal, and otherwise $\bar{a}^{s(h)} = a$. Equation (B1) is the multiplication rule for corepresentations [105,171].

1. Induced representations

Let H be a finite group with subgroup A, and (Π, V) be a representation of A, with V an n-dimensional representation space. For every $a \in A$ and basis vector $v_{\alpha} \in V$, a acts on v_{α} as $a \circ v_{\alpha} = \sum_{\beta=1}^{n} \Pi(a)_{\alpha\beta}v_{\beta}$, with $\Pi(a)$ an n-dimensional matrix. We define D as the index of A in H, and $\{h_1 = e, h_2 \dots, h_D\}$ as a full set of representatives of the left cosets H/A, such that H can be decomposed as $H = \bigcup_{i=1}^{D} h_i A$. For any $g \in H$ and representative h_i , $gh_i \in H$, and therefore by the coset decomposition there exists $h_{\sigma_g(i)}$ [with $\sigma_g(i) \in \{1, \dots, D\}$] and $a_i \in A$ such that $gh_i = h_{\sigma_g(i)}a_i$. It will be useful to show that σ_g is a permutation of $\{1, \dots, D\}$.

Proof of permutation. Let us first prove that σ_g is injective. Suppose it were not, i.e., $\sigma_g(i) = \sigma_g(i')$ for $i \neq i'$. It would follow that $h_i a_i^{-1} = h_{i'} a_{i'}^{-1}$. Since $a_i, a_{i'} \in A, h_i a_i^{-1} \in h_i A$ and $h_{i'} a_{i'}^{-1} \in h_{i'} A$ must belong in distinct cosets of H/A, which contradicts the just-stated equality. An injective map from $\{1, \ldots, D\}$ to itself must also be surjective, hence σ_g is a permutation.

Let $\operatorname{ind}_A^H(\Pi, V)$ denote the *induced representation* of (Π, V) . The representation space of $\operatorname{ind}_A^H(\Pi, V)$ is $W = \bigoplus_{i=1}^D h_i V$, with basis vectors $\{h_i v_\alpha | i = 1 \dots D, \alpha = 1 \dots n\}$; $g \in H$ is defined to act on the basis vector as

$$g \circ h_i v_{\alpha} = \sum_{\beta=1}^n [\Pi(a_i)]_{\alpha\beta} h_{\sigma_g(i)} v_{\beta}.$$
 (B2)

2. Complex permutation representations

A complex permutation representation is a representation of H where every element of $h \in H$ is mapped to a complex permutation matrix U(h), which satisfies the multiplication rule of Eq. (B1).

In what follows, we maintain a basis $\{v_1, \ldots, v_n\}$ for the representation space V such that each $h \in H$ is represented by a complex permutation matrix. It is useful to introduce the notion of a *transitive* complex permutation representation. By transitive, we mean that for every pair of basis vectors (v_i, v_j) , there exists $h \in H$ such that $[U(h)]_{ij}$ is nonzero.

Claim. A complex permutation representation is either transitive, or it is a direct sum of transitive complex permutation representations.

Proof. For every complex permutation representation U: $h \mapsto U(h)$ of H, there exists a (real) permutation representation U' of H obtained by replacing every nonzero matrix element in U(h) by 1. Then H has the following permutation group action, denoted \circ , on the set of basis indices $N := \{1, \ldots, n\}$: $h \circ i = j$ for the unique j for which $[U'(h)]_{ij} = 1$ – in this case, we say that i is in the orbit of j. (The orbit of j is the equivalence class of j.) The set of equivalence classes (or orbits) forms a partitioning of N. This partitioning then implies a splitting of V, where each summand is spanned by all basis vectors with indices in one orbit. By construction, the restriction of $\{U(h)\}_{h \in H}$ to one summand is transitive.

3. Complex permutation representations as induced representations

A transitive complex permutation representation of H is equivalently a representation of H induced from a one-dimensional representation of a subgroup of H. The proof of the forward direction (transitive complex permutation representation \Rightarrow induced representation) may be found in the proof of Theorem 2.6 in Ref. [172]. Here we provide an elementary proof of the backward direction, which we did not find in the standard literature.

Proof of equivalence. Consider $\operatorname{ind}_A^H(\Pi,V)$ with V a one-dimensional vector space. For every $h \in H$, $\Pi(h)$ is a unimodular phase factor. As a particular case of Eq. (B2), the action of g on a basis vector is $g \circ h_i V = \Pi(a_i)h_{\sigma_g(i)}V$, with σ_g a permutation on $\{1 \dots D\}$. The representation of g in the basis of $\{h_1V, h_2V, \dots, h_DV\}$ must therefore be a complex permutation matrix; since this is true of all g, $\operatorname{ind}_A^H(\Pi,V)$ must be a complex permutation representation. Moreover, this complex permutation representation is transitive, since for any pair of basis vectors h_iV and h_jV , there exists $h_ih_j^{-1} \in H$ which relates the two vectors (modulo a phase) and therefore $[U(h_ih_j^{-1})]_{ij} \neq 0$.

From this equivalence, it follows that (i) a complex permutation representation of H (being a direct sum of transitive complex permutation representations) is equivalently (ii) a direct sum of representations of H (each induced from a 1D representation of a subgroup of H). (i) and (ii) may be taken as equivalent definitions of a monomial representation of H.

4. Direct-product groups that are monomial

As a reminder, a *monomial group* is a group for which all irreducible representations (irreps) are monomial. For example,

Abelian finite groups are monomial because all their irreps are 1D.

Lemma for monomial direct-product groups. For H a group and A an Abelian group, H is monomial if and only if $H \times A$ is monomial.

Proof of lemma. It is well-known that *all* irreducible representations of a direct product (of two groups) are obtained by the tensor product of irreps of the individual groups [5]. In our application, A being Abelian implies it has only one-dimensional irreps which we label by η : any $a \in A$ is mapped to complex phase factor $\eta(a) \in U(1)$. We label an irrep of H by D, which maps $h \in H$ to a unitary matrix D(h). Any irrep of $H \times A$ can then be labeled by (D, η) and maps $(h, a) \in H \times A$ to the unitary $\eta(a)D(h)$.

Let us first prove the forward direction of the lemma: H monomial $\Rightarrow H \times A$ monomial. By assumption, for any irrep D of H, there exists a basis for D such that D(h) is a complex permutation matrix for all $h \in H$. The tensor product of such a basis with η gives a basis for (D, η) where $\eta(a)D(h)$ is a complex permutation matrix for all $(h, a) \in H \times A$. This is because any complex permutation matrix that is multiplied by a complex number [here, $\eta(a)$] remains a complex permutation matrix. Since the above holds for all irreps of $H \times A$, we deduce that $H \times A$ is monomial.

Lastly, we will prove the backward direction, which is contrapositively restated as H not monomial $\Rightarrow H \times A$ not monomial. By assumption, there exists at least one irrep D (of H) having no basis in which D(h) is a complex permutation matrix for all $h \in H$. This implies, for a being the identity element $e \in A$, that no basis exists for (D, η) where $\eta(e)D(h) = D(h)$ is a complex permutation matrix for all $\{(h, e)|h \in H\}$. Consequently, no basis exists for which $\eta(a)D(h)$ is a complex permutation matrix for all $(h, a) \in H \times A$; hence (D, η) is a nonmonomial irrep of $H \times A$, which completes the proof.

APPENDIX C: PROOF OF CRYSTALLOGRAPHIC SPLITTING THEOREM

This Appendix contains the proof of the crystallographic splitting theorem for monomial BRs, as stated in Sec. IV B. Below, steps 1–3 outline the proof of the forward arrow (existence of splitting satisfying (A-B) $\Rightarrow P$ is a monomial BR of G), and 4 the backward arrow.

- (1) In Sec. C 1, we prove the existence of a splitting $P = \bigoplus_i P^{(i)}$ (the sum over i is finite), with each $P^{(i)}$ a single orbit under G. By this, we mean that (a) $P^{(i)}$ is a direct sum of a subset of $\{P_j\}_{j=1}^N$, (b) $P^{(i)}$ forms a representation of G, and (c) the action of G on members of $P^{(i)}$ is transitive: for any $P_j, P_{j'}$ in the direct sum of $P^{(i)}$, there exists $g \in G$ such that $gP_jg^{-1} = P_{j'}$.
- (2) Since each unit-rank P_j is analytic with trivial first Chern class, it has a Wannier representation with a corresponding Wannier center (defined up to lattice translations). By Wannier center, we mean the expected position of a Wannier function in a Wannier basis for P_j . It is possible that the Wannier centers for different P_j (contained in the same orbit) are identical. We will show in Sec. C 2 that for each orbit, the number of distinct Wannier centers (A) divides the rank of $P^{(i)}$. This means that there are (in each unit cell) the

same number (M) of Wannier functions with the same Wannier center (denoted as $\boldsymbol{\varpi}_{\alpha}$, with $\alpha=1,\ldots,A$); we introduce $\mu=1,\ldots,M$ as an additional label to distinguish Wannier functions centered at the same position. It follows from this discussion that we can always decompose

$$P^{(i)} = \bigoplus_{\alpha=1}^{A} \bigoplus_{u=1}^{M} P_{\alpha,u}^{(i)}, \tag{C1}$$

such that $P_{\alpha,\mu}^{(i)}$ has unit rank and projects to Wannier functions indexed by (α,μ) . $P_{\alpha,\mu}^{(i)}$ then gives us a convenient relabelling of P_i .

- (3) In Sec. C3, we construct a rank-N Wannier basis by induction from a single Wannier function arbitrarily chosen from $P_{\alpha,\mu}^{(i)}$; the choice of $P_{\alpha,\mu}^{(i)}$ among $\{P_{\alpha,\mu}^{(i)}\}_{\alpha,\mu}$ is also arbitrary. It will be proven that this Wannier basis spans $P^{(i)}$, and is induced from a mononimal representation of a site stabilizer under G. Having thus proven that $P^{(i)}$ is a monomial BR (of G) completes the proof of the forward direction.
- (4) In the proof of the backward arrow, we then assume that P is a representation of G induced from a monomial representation D of a site stabilizer G_{ϖ_1} . We then choose a basis for the representation space of D such that each $g \in G_{\varpi_1}$ is represented as a complex permutation matrix. We will demonstrate that this basis gives a splitting of P into single-rank projectors which are permuted by any element of G, thus proving the backward direction.

1. Partitioning of band into space-group orbits

We would like to decompose the band projected by P into subbands which are individually invariant under G. For this purpose, it is useful to define H as the group of all symmetries (contained in G) that has a trivial action on each of P_i :

$$H = \{g \in G | \forall j \in \{1...N\}, \sigma_g(j) = j\} < G.$$
 (C2)

Let us prove that H, as defined in Eq. (C2), is a normal subgroup of G.

Proof of normality. By definition of H,

$$\forall h \in H, \quad \forall j = 1, ..., N, \quad [h, P_i] = 0.$$
 (C3)

Since h commutes with the right-hand side of

$$gP_ig^{-1} = P_{\sigma_\sigma(i)},\tag{C4}$$

it follows that

$$[h, gP_ig^{-1}] = 0 \Rightarrow [g^{-1}hg, P_i] = 0.$$
 (C5)

Since the above is true for all j = 1, ..., N, $g^{-1}hg$ must act as the trivial permutation, and therefore belongs in H. This holds for all $g \in G$ and $h \in H$; therefore, gH = Hg as desired.

Since H is a normal subgroup, the quotient G/H is a group whose order |G/H| is defined as the *index* of H. Let each equivalence class in G/H be represented by an element $f_i \in G$, such that

$$G/H = \{ [f_1 = e], [f_2], \dots [f_{|G/H|}] \};$$
 (C6)

e above is the identify element in G, so [e] consists of all elements in H. Because H acts as the trivial permutation, $\sigma_f = \sigma_{[f]}$ depends only on the equivalence class of G/H. It is useful to view σ_f as defining a group action for G/H on $\{P_i\}_i$, with [e] acting trivially, and the compatibility condition

given by

$$P_{\sigma_{f_2f_1}(j)} = \hat{f}_2 \hat{f}_1 P_j (\hat{f}_2 \hat{f}_1)^{-1}$$

= $\hat{f}_2 (\hat{f}_1 P_j \hat{f}_1^{-1}) \hat{f}_2^{-1} = P_{\sigma_{f_2} \sigma_{f_1}(j)}.$ (C7)

The *orbit* of P_j is defined as the subset of $\{P_j\}_{j=1}^N$ to which P_j can be moved by elements in G/H:

$$G/H \cdot P_i := \{ P_{\sigma_{(f)}(i)} | [f] \in G/H \}.$$
 (C8)

The set of orbits of $\{P_j\}_{j=1}^N$ under G/H (a group) form a partition of $P = \bigoplus_i P^{(i)}$ (a grouping of $\{P_j\}_{j=1}^N$ into nonempty subsets $P^{(i)}$, such that each element of $\{P_j\}_{j=1}^N$ is included in one and only one subset). Every orbit is an invariant subset on which G/H acts transitively, i.e., for every pair $P_{j'}$, P_j in the orbit, there exists $[f] \in G/H$ such that $\sigma_f(j') = j$).

Let us focus on one orbit in the partition $P = \bigoplus_{i=1} P^{(i)}$ with rank $N^{(i)}$. Since the following proof would be valid for any orbit, we may simplify notation by dropping the orbit index (i): without loss of generality, we relabel $P = \bigoplus_{j=1}^{N} P_j$ as the projector for a *single* orbit under G.

2. Lemma on the group action on Wannier centers

Since each of P_j is analytic with trivial first Chern class, it must be localizable, i.e., it has a Wannier representation—with a corresponding Wannier center that is uniquely determined modulo lattice translations. Since P_j is invariant under H [cf. Eq. (C2)], P_j must be a BR of H (according to the unit-rank splitting theorem) and its associated Wannier center is invariant (modulo lattice translations) under H. It is possible that the Wannier centers of distinct P_j are equivalent (modulo lattice translations); this defines a surjection $P_j \mapsto \boldsymbol{\varpi}_{S(j)}$, with $j=1,\ldots,N,S(j)=1,\ldots,A$, and $A\leqslant N$.

Lemma 1. There exists a group action of G/H on the set of single-rank projectors and the set of Wannier centers (defined modulo lattice translations), i.e., for any $[g] \in G/H$,

$$g: (\boldsymbol{\varpi}_{\alpha}, P_{i}) \mapsto (\boldsymbol{\varpi}_{g \cdot \alpha}, P_{\sigma_{\sigma}(i)}),$$
 (C9)

with $g \cdot \alpha$ a permutation on $\alpha \in \{1 \dots A\}$, defined through

$$\boldsymbol{\varpi}_{g\cdot\alpha} \equiv g \circ \boldsymbol{\varpi}_{\alpha}.$$
 (C10)

The group action of Eq. (C9) is transitive and satisfies

$$g \cdot (S(j)) = S(\sigma_g(j)), \quad \text{for } j = 1, \dots, N.$$
 (C11)

From this, we will show that A divides N.

Proof of Lemma 1. Since P_j is localizable, so would be gP_jg^{-1} for any $g \in G$. This is because any crystallographic symmetry acts as an isometry in real space: $\mathbf{r} \to g \circ \mathbf{r}$, and therefore cannot change the exponential decay of Wannier functions. Consequently, if P_j has a Wannier center $\mathbf{w}_{\alpha=S(j)}$, gP_jg^{-1} would have the Wannier center $g \circ \mathbf{w}_{\alpha}$. We write this as in Eq. (C9). Since G has an action on $\{P_j\}_j$, and $\{P_j\}_j$ a surjection to $\{\mathbf{w}\}_{\alpha}$, it must be that $g \circ \mathbf{w}_{\alpha} \equiv \mathbf{w}_{\alpha'}$ for the unique $\alpha' \in \{1, \ldots, A\}$, satisfying $\alpha' = S(\sigma_g(j))$. We define the permutation g through Eq. (C10), so that Eq. (C11) follows immediately.

Now we would show that g defines a group action of G/H on $\{\boldsymbol{\varpi}_{\alpha}\}_{\alpha}$. Indeed, the identity element $[e] \in G/H$ includes all $h \in H$, and $h \circ \boldsymbol{\varpi}_{\alpha} \equiv \boldsymbol{\varpi}_{\alpha}$ because H trivially permutes $\{P_j\}_j$

[cf. Eq. (C2)]. The compatibility axiom is also satisfied:

$$\boldsymbol{\varpi}_{(g_1g_2)\cdot\alpha} \equiv (g_1g_2)\circ\boldsymbol{\varpi}_{\alpha} = g_1\circ(g_2\circ\boldsymbol{\varpi}_{\alpha}) \equiv \boldsymbol{\varpi}_{g_1\cdot(g_2\cdot\alpha)}.$$
(C12)

Let us show that g is transitive as a group action, i.e., for any $\boldsymbol{\varpi}_{\alpha}$ and $\boldsymbol{\varpi}_{\alpha'}$, there exists $[g] \in G/H$ such that $\alpha' = g \cdot \alpha$. This g is determined (possibly nonuniquely) by the transitive group action of G/H on $\{P_j\}_j$. To clarify, if $S(j) = \alpha$ and $S(j') = \alpha'$, then we determine g through $\sigma_g(j) = j'$.

Finally, we apply the transitivity property to prove that A divides N. Indeed, suppose S maps M elements (denoted $\{j_1, j_2, \ldots, j_M\}$) to a single element α . By the transitivity property, for any element α' distinct from α , there exists a nontrivial element $[p] \in G/H$ such that $p \cdot \alpha = \alpha'$. By the condition of Eq. (C11),

$$S: \{\sigma_p(j_1), \dots, \sigma_p(j_M)\} \mapsto \alpha'.$$
 (C13)

Crucially, $\{\sigma_p(j_1), \ldots, \sigma_p(j_M)\}$ must not intersect $\{j_1, \ldots, j_M\}$, because the two sets map to distinct elements under S. If we repeat the logic for all other distinct elements of $\{\boldsymbol{\varpi}_{\alpha}\}_{\alpha=1}^{A}$, we conclude that for any element α'' (distinct from α and α'), there corresponds M elements in $\{1, \ldots, N\}$ which do not intersect with $\{j_1, \ldots, j_M\}$ or $\{\sigma_p(j_1), \ldots, \sigma_p(j_M)\}$. It follows that if $\{\boldsymbol{\varpi}_{\alpha}\}_{\alpha=1}^{A}$ has A distinct elements, then N = MA as desired. This completes the proof of the lemma.

a. Implications of Lemma 1

Here we collect some useful implications of the lemma and introduce the definitions of certain stabilizer groups, as will be applied in Sec. C 3.

The lemma implies that we are able to decompose P (of a single orbit) into a sum of single-rank projectors $P_{\alpha,\mu}$ [cf. Eq. (C1)], with $P_{\alpha,\mu}$ a relabelling of P_j ; we remind the reader that the orbit index i has been dropped for notational simplicity.

Due to the transitivity of the group action [cf. Eqs (C9) and (C10)], for any pair $P_{\alpha,\mu}$, $P_{\alpha',\mu'}$, there must exist $[p] \in G/H$ such that

$$pP_{\alpha,\mu}p^{-1} = P_{\alpha',\mu'}, \quad p \circ \boldsymbol{\varpi}_{\alpha} = \boldsymbol{\varpi}_{\alpha'}$$
 (C14)

holds. In particular, for $\alpha = \alpha' = 1$,

$$g_{\mu}P_{1,1}g_{\mu}^{-1} = P_{1,\mu}, \quad g_{\mu} \circ \boldsymbol{\varpi}_1 = \boldsymbol{\varpi}_1,$$
 (C15)

defines g_{μ} ; if more than one element of G satisfies Eq. (C15), then we may arbitrarily denote one representative as g_{μ} , and we may as well take g_1 to be the identify operation. The second equality in Eq. (C15) identifies g_{μ} as an element in the site stabilizer:

$$G_{\overline{\boldsymbol{w}}_1} := \{ g \in G \mid g \circ \overline{\boldsymbol{w}}_1 = \overline{\boldsymbol{w}}_1 \}. \tag{C16}$$

Similarly, restricting Eq. (C14) to $\mu = \mu' = 1$,

$$p_{\alpha}P_{1,1}p_{\alpha}^{-1} = P_{\alpha,1}, \quad p_{\alpha} \circ \boldsymbol{\varpi}_{1} = \boldsymbol{\varpi}_{\alpha}$$
 (C17)

defines p_{α} , with p_1 the identity operation. Due to the assumed transformation of the Wannier center $p_{\alpha} \circ \boldsymbol{w}_1 = \boldsymbol{w}_{\alpha}$, it must be that

$$p_{\alpha}P_{1,\mu}p_{\alpha}^{-1} = P_{\alpha,p_{\alpha}\cdot\mu},\tag{C18}$$

with $p_{\alpha} \cdot \mu$ a permutation on the μ index; $p_{\alpha} \cdot 1 = 1$ according to Eq. (C17).

It will be useful to define $G_{\alpha,\mu}$ as the stabilizer of $P_{\alpha,\mu}$ under G,

$$G_{\alpha,\mu} := \{ g \in G \mid [g, P_{\alpha,\mu}] = 0 \},$$
 (C19)

and the site stabilizer of $\boldsymbol{\varpi}$ under $G_{\alpha,\mu}$ as

$$G_{\alpha,\mu,\boldsymbol{\varpi}} := \{ g \in G_{\alpha,\mu} \mid g \circ \boldsymbol{\varpi} = \boldsymbol{\varpi} \}.$$
 (C20)

It follows from Eq. (C18) that the stabilizers $G_{1,\mu}$ and $G_{\alpha,p_{\alpha}\cdot\mu}$ are conjugate:

$$G_{\alpha, p_{\alpha} \cdot \mu} = p_{\alpha} G_{1, \mu} p_{\alpha}^{-1}. \tag{C21}$$

Combining the above equation with $p_{\alpha} \circ \boldsymbol{\varpi}_1 = \boldsymbol{\varpi}_{\alpha}$, we derive a conjugacy condition on the site stabilizers:

$$G_{\alpha, p_{\alpha} \cdot \mu, \overline{\boldsymbol{w}}_{\alpha}} = p_{\alpha} G_{1, \mu, \overline{\boldsymbol{w}}_{1}} p_{\alpha}^{-1}. \tag{C22}$$

3. Inducing Wannier basis for single-orbit band

Beginning from $P_{1,1}$ that represents $G_{1,1}$ [the stabilizer of $P_{1,1}$ under G; cf. Eq. (C19)], we will deduce the existence of a one-dimensional Wannier representation of the site stabilizer $G_{1,1,\varpi_1}$ [cf. Eq. (C20) above and Eq. (C24) below]. This one-dimensional representation will be induced to an M-dimensional monomial representation of G_{ϖ_1} [cf. Lemma 2 below], which is then induced to an infinite-dimensional representation of G – we will identify the latter as P for a single orbit under G. This would complete the proof of the forward arrow.

Since $P_{1,1}$ is a unit-rank representation of $G_{1,1}$, with assumed analytic projector and trivial first Chern class, $P_{1,1}$ must be a BR of $G_{1,1}$, according to our unit-rank splitting theorem. There must therefore exist a locally symmetric Wannier basis $\{W_{1,1,R}\}_{R\in\mathcal{T}}$ for $P_{1,1}$, a BR of $G_{1,1}$. We remind the reader (cf. Appendix A 3 b) that being locally symmetric means that $W_{1,1,R}$ has a Wannier center at $\boldsymbol{\varpi}_1 + \boldsymbol{R}$ and forms a one-dimensional representation of the site stabilizer $G_{1,1,\boldsymbol{\varpi}_1+\boldsymbol{R}}$ [cf. Eq. (C20)] for all \boldsymbol{R} . In particular,

$$\forall g \in G_{1,1,\varpi_1}, \quad g|W_{1,1,0}\rangle = \rho(g)|W_{1,1,0}\rangle,$$
 (C23)

with $\rho(g)$ a unimodular phase factor.

A set of M Wannier functions (lying in P) may be defined by

$$|W_{1,\mu,\mathbf{0}}\rangle := g_{\mu}|W_{1,1,\mathbf{0}}\rangle, \quad \mu = 1, \dots, M,$$
 (C24)

with g_{μ} defined through Eq. (C15).

Lemma 2. With $|W_{1,\mu,0}\rangle$ given by Eq. (C24), (a) $\{W_{1,\mu,0}\}_{\mu=1...M}$ forms an orthonormal basis for a monomial representation of G_{ϖ_1} , and (b) each $W_{1,\mu,0}$ is a 1D representation of the site stabilizer G_{1,μ,ϖ_1} , as defined in Eq. (C20).

Lemma 2 is proven below; let us first finish the proof of the forward direction of the crystallographic splitting principle.

By application of lattice translations in \mathcal{T} and the symmetry transformation p_{α} [defined in Eq. (C17)], we generate a set of Wannier functions from $W_{1,\mu,0}$:

$$|W_{\alpha, p_{\alpha} \cdot \mu, \mathbf{R}}\rangle := (\mathbf{R}|e)p_{\alpha}|W_{1, \mu, \mathbf{0}}\rangle \in P_{\alpha, p_{\alpha} \cdot \mu}.$$
 (C25)

That $|W_{\alpha,p_{\alpha}\cdot\mu,\mathbf{0}}\rangle$ belongs in $P_{\alpha,p_{\alpha}\cdot\mu}$ follows from Eq. (C18); that $|W_{\alpha,p_{\alpha}\cdot\mu,\mathbf{R}\neq\mathbf{0}}\rangle$ also belongs in $P_{\alpha,p_{\alpha}\cdot\mu}$ follows from $\mathcal{T}(< G)$ being a subgroup of $G_{\alpha,p_{\alpha}\cdot\mu}$ [the stabilizer defined in Eq. (C19)].

Since the band spanned by $\{W_{\alpha,p_{\alpha},\mu,R}\}_{(R|e)\in\mathcal{T}}$ is of unit rank, and so is $P_{\alpha,p_{\alpha},\mu}$ by assumption, we may identify

 $P_{\alpha,p_{\alpha}\cdot\mu} = \sum_{\mathbf{R}} |W_{\alpha,p_{\alpha}\cdot\mu,\mathbf{R}}\rangle\langle W_{\alpha,p_{\alpha}\cdot\mu,\mathbf{R}}|$. In combination, we have thus found a Wannier basis $\{W_{\alpha,\mu,\mathbf{R}}\}_{\alpha,\mu,(\mathbf{R}|e)\in\mathcal{T}}$ for the entirety of P (corresponding to a single orbit).

We now conclude that P spans a monomial BR of G, induced from a finite-dimensional monomial representation of G_{ϖ_1} spanned by $\{W_{1,\mu,0}\}_{\mu}$ [the representation in terms of complex permutation matrices is explicitly given in Eq. (C34)]. This is because the induction procedure (to derive a monomial BR) consists of defining new Wannier functions through Eq. (C25), where $\{p_{\alpha}\}_{\alpha}$ are representatives of the following coset decomposition:

$$G/(\mathcal{T} \rtimes G_{\overline{\boldsymbol{\omega}}_1}) = \{ [p_{\alpha}] | \alpha = 1, \dots, A \}. \tag{C26}$$

We briefly review how Eq. (C26) arises: $\mathcal{T} \rtimes G_{\varpi_1}$ is the subgroup of G that trivially maps ϖ_1 (modulo lattice translations). Since the orbit of ϖ_1 under G comprises A Wannier centers (modulo lattice translations), $G/(\mathcal{T} \rtimes G_{\varpi_1})$ must have A elements, each represented by p_α that maps $\varpi_1 \mapsto \varpi_\alpha$.

This finishes the proof of the forward direction of the crystallographic splitting principle.

Proof of Lemma 2

Proof of statement (a) in Lemma 2. The orthonormality condition $\langle W_{1,\nu,0}|W_{1,\nu',0}\rangle=\delta_{\nu\nu'}$ follows from $P_{1\nu}P_{1\nu'}=P_{1\nu}\delta_{\nu\nu'}$. Recall that G_{ϖ_1} has a transitive action on $\{P_{1,\mu}|\mu=1,\ldots,M\}$, which is therefore an orbit (of any of its elements) under G_{ϖ_i} :

$$Orb[P_{1,1}] = \{P_{1,\mu} | \mu = 1, \dots, M\}.$$
 (C27)

Since $G_{1,1}$ is the stabilizer of $P_{1,1}$ under G, it follows that $G_{1,1,\varpi_1}$ is the stabilizer of $P_{1,1}$ under G_{ϖ_1} :

$$Stab[P_{1,1}] = G_{1,1,\varpi_1}.$$
 (C28)

By the orbit-stabilizer theorem:

$$\frac{|G_{\varpi_1}|}{|\text{Stab}[P_{1,1}]|} = |\text{Orb}[P_{1,1}]| = M. \tag{C29}$$

There must therefore be M elements in the coset

$$G_{\overline{w}_1}/G_{1,1,\overline{w}_1} = \{[g_{\mu}]| \mu = 1, \dots, M\}.$$
 (C30)

To prove that each element can be represented by $g_{\mu} \in G_{\overline{w}_1}$ defined in Eq. (C15), it suffices to show that g_{μ} and $g_{\mu'}$ lie in different equivalence classes if $\mu \neq \mu'$. (Supposing the contrary, there would exist $g_{1,1} \in G_{1,1,\overline{w}_1}$ such that

$$g_{\mu} = g_{\mu'}g_{1,1} \implies P_{1,\mu} = g_{\mu}P_{1,1}g_{\mu}^{-1} = P_{1,\mu'},$$
 (C31)

which contradicts our assumption that $P_{1\mu}P_{1\mu'}=0$.) It follows from Eq. (C30) that the following coset decomposition holds:

$$G_{\overline{w}_1} = \bigcup_{\mu=1}^{M} g_{\mu} G_{1,1,\overline{w}_1}.$$
 (C32)

Now we derive the desired representation: consider that for any $g \in G_{\overline{w}_1}$

$$g|W_{1,\mu,\mathbf{0}}\rangle = gg_{\mu}|W_{1,1,\mathbf{0}}\rangle. \tag{C33}$$

Since $g_{\mu} \in G_{\overline{w}_1}$, the closure property of groups ensures $gg_{\mu} \in G_{\overline{w}_1}$. We may therefore apply the coset decomposition of Eq. (C32) to express $gg_{\mu} = g_{\mu'}g_{1,1}$, for some $\mu' = 1, \ldots, M$ and some $g_{1,1} \in G_{1,1,\overline{w}_1}$. Consequently,

$$g|W_{1,\mu,\mathbf{0}}\rangle = g_{\mu'}g_{1,1}|W_{1,0,\mathbf{0}}\rangle = \overline{\rho(g_{1,1})}^{s(g_{\mu'})}|W_{1,\mu',\mathbf{0}}\rangle, \quad (C34)$$

where $\overline{a}^{s(g)} = \overline{a}$ (the complex conjugate of a) if g is antiunitary, and otherwise $\overline{a}^{s(g)} = a$. Eq. (C34) defines a unitary representation of G_{ϖ_1} where each $g \in G_{\varpi_1}$ is mapped to a complex permutation matrix, with nonzero matrix elements given by the unimodular phase factor: $\overline{\rho}^s$. We thus conclude that $\{W_{1,\mu,0}\}_{\mu=1...M}$ spans a complex permutation representation of G_{ϖ_1} or, equivalently, a monomial representation of G_{ϖ_1} ; this equivalence has been proven in Appendix B 2.

Proof of statement (b) in Lemma 2. It follows from Eq. (C15) that $W_{1,\mu,0}$ lies in the vector space projected by $P_{1,\mu}$. By definition of the stabilizer $G_{1,\mu}$ [cf. Eq. (C19)], $P_{1,\mu}$ is a representation of $G_{1,\mu}$. This implies that for any $g_{1,\mu,\varpi_1} \in G_{1,\mu,\varpi_1} < G_{1,\mu}$ [cf. Eq. (C20)], $g_{1,\mu,\varpi_1} | W_{1,\mu,0} \rangle$ remains in $P_{1,\mu}$ and is therefore orthogonal to $W_{1,\mu'\neq\mu,0}$. Further applying that $g_{1,\mu,\varpi_1} \in G_{1,\mu,\varpi_1} < G_{\varpi_1}$, and that $\{W_{1,\mu,0}\}_{\mu}$ forms a complex permutation representation of G_{ϖ_1} [cf. Eq. (C34)], we deduce that

$$g_{1,\mu,\boldsymbol{\varpi}_1}|W_{1,\mu,\boldsymbol{0}}\rangle = \rho(g_{1,\mu,\boldsymbol{\varpi}_1})|W_{1,\mu,\boldsymbol{0}}\rangle,$$
 (C35)

with ρ a unimodular phase factor. Since this is true for any $g_{1,\mu,\varpi_1} \in G_{1,\mu,\varpi_1}$, we arrive at the desired claim.

Proof of backward arrow of crystallographic splitting principle. Suppose we have a BR of G induced from a complex permutation representation D of the site stabilizer G_{ϖ_1} , with the Wyckoff position ϖ_1 having multiplicity A. Let $\{W_{1\mu}\}_{\mu=1...M}$ be basis vectors of the representation space of D, such that

$$\forall h \in G_{\overline{\omega}_1}, \quad h|W_{1\mu}\rangle = \rho(h;\mu)|W_{1,h\cdot\mu}\rangle, \tag{C36}$$

with ρ a unimodular phase factor, and $h\cdot$ a permutation on the μ index.

Given the coset decomposition in Eq. ($\mathbb{C}26$), we define a set of A Wannier functions by

$$|W_{\alpha,\mu}\rangle := p_{\alpha}|W_{1\mu}\rangle, \quad \alpha = 1...A,$$
 (C37)

and the unit-rank projection to their Bravais-lattice translates

$$P_{\alpha\mu} := \sum_{(\mathbf{R}|e)\in\mathcal{T}} (\mathbf{R}|e)|W_{\alpha,\mu}\rangle\langle W_{\alpha,\mu}|(\mathbf{R}|e)^{-1}.$$
 (C38)

Since each Wannier function is assumed to be exponentially localized, each projector $P_{\alpha\mu}$ must be analytic with trivial first Chern class [76,77] and gives a splitting for

$$P = \bigoplus_{\alpha=1}^{A} \bigoplus_{\mu=1}^{M} P_{\alpha,\mu}.$$
 (C39)

Let us prove that $\{P_{\alpha,\mu}\}_{\alpha,\mu}$ is permuted by each element of G, which would complete the proof of the backward arrow.

Proof of permutation. The action of g on $P_{\alpha,\mu}$ is

$$gP_{1\mu}g^{-1} = \sum_{(\boldsymbol{R}|e)\in\mathcal{T}} g(\boldsymbol{R}|e)|W_{\alpha,\mu}\rangle\langle W_{\alpha,\mu}|(\boldsymbol{R}|e)^{-1}g^{-1}. \quad (C40)$$

Utilizing the coset decomposition in Eq. (C26), any $g \in G$ can be expressed as $g = (\mathbf{R}'|e)p_{\alpha'}h'$, for one $h' \in G_{\overline{w}_1}$, one $\alpha' \in \{1 \dots A\}$, and one $(\mathbf{R}'|e) \in \mathcal{T}$. It follows that

$$g(\mathbf{R}|e)|W_{\alpha\mu}\rangle = (p_{\alpha'}h' \circ \mathbf{R} + \mathbf{R}'|e)p_{\alpha'}h'p_{\alpha}|W_{1\mu}\rangle.$$
 (C41)

Since $p_{\alpha'}h'p_{\alpha} \in G$, it also has the coset decomposition:

$$p_{\alpha'}h'p_{\alpha} = (\mathbf{R}''|e)p_{\alpha''}h''. \tag{C42}$$

Substituting the above equation into Eq. (C41), we derive

$$g(\mathbf{R}|e)|W_{\alpha\mu}\rangle = (p_{\alpha'}h' \circ \mathbf{R} + \mathbf{R}' + \mathbf{R}''|e)\rho(h'';\mu)|W_{\alpha'',h''\cdot\mu}\rangle.$$
(C43)

Substituting the above equation into Eq. (C40), and applying that $p_{\alpha'}h' \circ \mathbf{R} + \mathbf{R}' + \mathbf{R}''$ is a Bravais-lattice vector, we derive the desired claim:

$$gP_{\alpha\mu}g^{-1} = P_{\alpha'' \in \{1...A\}, h'' \cdot \mu \in \{1...M\}}.$$
 (C44)

APPENDIX D: METHODS OF SYMMETRIC SPLITTING

Let *P* project to a rank-*N* representation of a space group *G*; in this section, we shall not distinguish between between space groups, magnetic space groups, and double space groups.

We define a symmetric splitting with respect to G as a splitting $P=\bigoplus_{j=1}^N P_j$ into single-rank projectors satisfying the symmetry condition (B) of the splitting theorem, namely, that for all $g\in G$, $g:P_j\to P_{\sigma_g(j)}$ with σ_g a permutation on $\{1,\ldots,N\}$.

Given a symmetric splitting, the splitting theorem states that if $P_j(\mathbf{k})$ is analytic in \mathbf{k} (over the Brillouin torus) and has trivial first Chern class, then P is a monomial BR of G. Beside offering a method to prove band representability, a symmetric splitting automatically gives a set of Wannier functions which are permuted by the space group.

For a given *P*, there is no unique symmetric splitting, but we will describe two methods which involve diagonalizing various operators: (i) the projected symmetry operator in Sec. D 1 and (ii) the projected position operator in Sec. D 2.

1. The projected symmetry method

We have exemplified the projected symmetry method for fragile obstructed insulators in Sec. III. Here we describe our method in greater generality: Suppose we are given a tight-binding Hamiltonian h(k) defined with respect to a Löwdin-orthonormalized [173,174] basis of Wannier functions. h(k) is assumed to have the symmetry of a space group G,

$$g \in G$$
, $\hat{g}h(\mathbf{k})\hat{g}^{-1} = h(g \circ \mathbf{k})$, (D1)

with \hat{g} the matrix representation of g in the Wannier basis. We define the Wannier-center operator \hat{r} as a diagonal matrix with each diagonal element equal to the central position of each Wannier function, such that

$$h(\mathbf{k} + \mathbf{G}) = e^{-i\mathbf{G}\cdot\hat{\mathbf{r}}}h(\mathbf{k})e^{i\mathbf{G}\cdot\hat{\mathbf{r}}}$$
 (D2)

for any reciprocal vector G. Finally, we assume that the real-space matrix elements of the tight-binding Hamiltonian decay exponentially; this guarantees that h(k) is analytic in k throughout the Brillouin torus [93]. Moreover, if a rank-N energy band of h(k) is spectrally isolated (i.e., separated by all other energy bands by a nonzero spectral gap at each k), it is guaranteed that the rank-N projector p(k) is also analytic in k throughout [77,98]. Our goal is to symmetrically decompose p(k).

We would like to identify a Hermitian operator \tilde{s} (in the tight-binding basis of Wannier functions), such that the eigenbands of the $\tilde{s}_k := p(k)\tilde{s}p(k)$ give a symmetric splitting with respect to G. \tilde{s}_k is the *projected symmetry operator*; by construction it is Hermitian and analytic throughout the Brillouin

torus. It is necessary that \tilde{s}_k has the same translational property [cf. Eq. (D2)] as h(k), so we impose $[\tilde{s}, e^{iG\cdot\hat{r}}] = 0$ for every reciprocal vector G. We further impose that for any $g \in G$, \hat{g} commutes or anticommutes with \tilde{s} ; in the former case \hat{g} trivially permutes the eigenspaces of \tilde{s} , and

$$\hat{g}\tilde{s}_k\hat{g} = \tilde{s}_{g\circ k}; \tag{D3}$$

in the latter case,

$$\hat{g}\tilde{s}_{k}\hat{g} = -\tilde{s}_{g \circ k},\tag{D4}$$

and \hat{g} interchanges the eigenspaces of \tilde{s} that have nonzero eigenvalues.

In some models, \tilde{s} is simply obtained by deforming the eigenvalues of one of the unitary symmetry operators \hat{g} . An example of this kind, with g the fourfold rotation, was provided in our case study of fragile obstructed insulators in Wigner-Dyson class AI (cf. Sec. III). Generally, \tilde{s} need *not* correspond to a symmetry of h(k), as we exemplify below.

We define the eigenvalue problem

$$[\tilde{s}_{k} - \lambda_{j}(k)]|u_{j}(k)\rangle = 0$$
, with $\lambda_{1}(k) \geqslant \lambda_{2}(k) \geqslant \dots$ (D5)

for all k. Generically, the band dispersion λ_j should be non-degenerate except on a zero-measure set of k, e.g., at a conical (Dirac-Weyl) band touching. If each band is spectrally isolated, then we have obtained a symmetric splitting $P=\bigoplus_{i=1}^N P_j$ with respect to G, with each $P_j(k)$ being analytic throughout the Brillouin torus; note $P_j(k)$ is the projector to the Bloch state $e^{ik\cdot(\hat{r}+R)}|u_j(k)\rangle$. Furthermore, if each P_j has trivial first Chern class, then P must be a monomial BR, according to our splitting theorem.

On the other hand, if $P = \bigoplus_j P_j$ is not a monomial BR, then either (a) there exists $P_j(k)$ that is nonanalytic at a set of k where λ_j is degenerate or (b) each P_j is analytic throughout the Brillouin torus, and at least one of $\{P_j\}$ must have a nontrivial Chern class. Colloquially speaking, \tilde{s}_k is the Hamiltonian of either a topological semimetal or a Chern insulator. Note if each λ_j is nondegenerate for all k, then case (b) is implied; however, the converse statement—namely, that (b) implies nondegeneracy—is not generally valid.

Except for certain double space groups with cubic point groups (cf. Sec. IV), not being a monomial BR means that P is an obstructed representation.

Example: \mathbb{Z}_2 topological insulator in Wigner-Dyson class AII. Let P project to the filled, rank-two band of the Kane-Mele \mathbb{Z}_2 topological insulator [32,33] with space group. $\mathcal{T}_2 \times$ \mathbb{Z}_4^T . Following Prodan [75], one may pick $\tilde{s} = \vec{n} \cdot S$, with S the spin operator and \vec{n} an arbitrary directional vector. Since time reversal inverts S, the bands of $\tilde{s}(k)$ would be nontrivially permuted by T. Thus $\underline{\tilde{s}} = \vec{n} \cdot S$ gives a symmetric splitting with respect to $\mathcal{T}_2 \times \mathbb{Z}_4^T$, despite not generally being a symmetry of the Hamiltonian. If \tilde{s}_k were spectrally gapped at each k, then P being an obstructed representation guarantees that the two bands of \tilde{s}_k have opposite and nonzero first Chern numbers—this is nothing more than the spin Chern number formulated for infinite samples by Prodan [75]. Our projected symmetry method may be viewed as the generalization of Prodan's projected spin method to include crystallographic space-group symmetry within class AII, and also to go beyond symmetry class AII. An example of the latter—a symmetric splitting in class AI—has been given in Sec. III C. To exemplify the former, we consider the Kane-Mele *honeycomb* model, whose symmetry is the double-group extension of $p6mm \times \mathbb{Z}_2^T$, which we will denote by \tilde{G}_6 . While $\tilde{s} = \vec{n} \cdot S$ no longer gives a symmetric splitting of \tilde{G}_6 for arbitrary \vec{n} , $\vec{n} = \vec{z}$ (the out-of-plane direction) would give the desired splitting. The reason is that S_z commutes with all rotations in \tilde{G}_6 , and anticommutes with all reflections.

2. Symmetric splitting by the projected position operator

We have proven in Sec. VB that the splitting $P = \bigoplus_{j=1}^N P_j^x$ into bands of the projected position operator [cf. Eqs. (10) and (11)] is symmetric with respect to certain two-space-dimensional space groups [satisfying conditions (i) and (2) in *Lemma 1* of Sec. VB]. In this Appendix section, we will prove a statement in Lemma 1 that is needed to derive the Zak winding theorem (cf. Sec. VB), namely, that each P_j^x is analytic throughout the Brillouin zone.

By analyticity throughout the Brillouin zone, we mean that the restriction of P_i^x to k,

$$P_j^x := \int \frac{d^2k}{(2\pi)^2} P_j^x(\mathbf{k}), \quad P_j^x(\mathbf{k}) := \left| \psi_{j\mathbf{k}}^x \right| \left| \psi_{j\mathbf{k}}^x \right|, \tag{D6}$$

is both analytic in k (for all k in the Brillouin zone), and periodic in reciprocal lattice translations $k \to k + G$. The Bloch function ψ_{jk}^x is obtained by 1D Fourier transform of the eigenfunctions of the projected position operator [cf. Eq. (10)]:

$$\psi_{jk}^{x} = \sum_{R \in \mathbb{Z}} e^{ik_{x}R} h_{j,k_{y},R}.$$
 (D7)

a. Proof of analyticity

Given that P has trivial first Chern class, a basis for the Bloch functions $\{\psi_{nk}\}_{n=1}^{N}$ exist that is analytic in k throughout the Brillouin torus, and is periodic under translation by any reciprocal vector: $\psi_{nk} = \psi_{nk+G}$; a review of this well-known fact may be found in Appendix A 1.

Since both $\{\psi_{nk}\}_{n=1}^{N}$ and $\{\psi_{jk}^{x}\}_{j=1}^{N}$ [cf. Eq. (D7)] span the same rank-N band P, there exists a U(N) transformation Q(k) that relates the two sets of Bloch functions:

$$\psi_{jk}^{x} = e^{-ik_{x}x_{j}(k_{y})} \sum_{n=1}^{N} [Q(k)]_{nj} \psi_{nk}.$$
 (D8)

As shown in Appendix D of Ref. [20], the columns of Q(k) are given by the eigenvectors of the Wilson loop W(k), which is defined as a path-ordered exponential of the Berry connection [cf. Eq. (6) with $u_{nk} = e^{-ik \cdot r} \psi_{nk}$]:

$$W(\mathbf{k}) = \mathcal{P}\exp\left[i\int_{k_x}^{k_x+2\pi} A_x(s, k_y)ds\right].$$
 (D9)

The above integral is over a k loop with base point (k_x, k_y) and end point $(k_x, k_y + 2\pi)$. [$\mathcal{W}(k)$ slightly differs in definition from $\mathcal{W}(\mathcal{C})$ in Eq. (7).] Q in Eq. (D8) is the unitary transformation that diagonalizes the Wilson loop,

$$W(\mathbf{k}) = Q(\mathbf{k})D(k_{v})Q(\mathbf{k})^{-1}, \tag{D10}$$

with D a diagonal matrix equal to

$$D(k_{v}) = \text{diag}[e^{i2\pi x_{1}(k_{y})}, \dots, e^{i2\pi x_{N}(k_{y})}].$$
 (D11)

 $2\pi x_j$ is referred to as a Zak phase [cf. Eq. (8)] and depends only on k_y ; this dependence is because for a given k loop, the spectrum of \mathcal{W} is independent of the base point [20].

While we have flippantly claimed the columns of Q(k) are the eigenvectors of W(k), beware that an eigenvector, if nondegenerate in eigenvalue, is only defined up to a phase. (If $x_j = x_{j'}$ is degenerate at isolated k_y , then the the two eigenvectors associated to x_j and x_j' can still be defined up to a phase by continuity in k_y .) This phase ambiguity is reduced by the following procedure: Since there is no topological obstruction to analyticity of an eigenvector over the base space S^1 , each column of $Q(0, k_y)$ can be made analytic and periodic in k_y . Moreover, from Eqs. (D9) and (D10), one deduces that $Q(k_x, k_y)$ and $Q(0, k_y)$ can always be related by a Wilson line [20]:

$$Q(k_x, k_y) = \mathcal{P}\exp\left[i\int_0^{k_x} A_x(s, k_y) ds\right] Q(0, k_y).$$
 (D12)

These conditions on Q are henceforth adopted.

Analytic properties of the Q matrix. The analyticity of ψ_{nk} implies that the Berry connection $A_x(k)$ is also analytic in k. Since $Q(0, k_y)$ is analytic in k_y and Eq. (D12) holds as well, we deduce that Q(k) is analytic in k. The periodicity of $\psi_{nk} = \psi_{nk+G}$ implies $A_x(k) = A_x(k+G)$. The periodicity of A_x , combined with the periodicity of $Q(0, k_y)$ in k_y , implies that Q(k) in Eq. (D12) is periodic in k_y . However, Q is generically aperiodic in k_x , i.e., $Q(k_x + 2\pi, k_y) = \mathcal{W}(k)Q(k)$.

Analytic properties of the Zak phase. The analyticity and periodicity of A(k) imply that W(k) is likewise analytic and periodic. This implies that the spectrum $\{e^{i2\pi x_j(k_y)}\}_{j=1}^N$ of W(k) is analytic and periodic. If we further assume the Zak permutation order $Z_{2\pi e_x} = 1$, then each eigenvalue $e^{i2\pi x_j(k_y)}$ can be made analytic and periodic, too. Beware, however, that $2\pi x_j$ can wind with respect to k_y ; the associated Zak winding number $W_{j,2\pi e_x}$ has been defined in Eq. (9).

Given the above-stated analytic properties of Q, x_j , and ψ_{nk} , we are then able to deduce the analytic properties of ψ_{jk}^x , as defined in Eq. (D8). Namely, ψ_{jk}^x is analytic in k throughout the Brillouin zone, periodic in k_x [20] but aperiodic in k_y if the Zak winding number $W_{j,2\pi e_x}$ [cf. Eq. (9)] is nonzero:

$$\psi_{j,k_x+2\pi,k_y}^x = \psi_{j,k_x,k_y}^x, \quad \psi_{j,k_x,k_y+2\pi}^x = e^{-ik_xW_{j,2\pi e_x}}\psi_{j,k_x,k_y}^x.$$
 (D13)

An alternative (and numerically motivated) construction of such a basis is described in Ref. [44], where it is referred to as a 'cylindrical gauge. While ψ_{jk}^x is possibly aperiodic under $k_y \to k_y + 2\pi$, one deduces from Eq. (D13) that the projector $P_j^x(k) = |\psi_{jk}^x\rangle\langle\psi_{jk}^x|$ is always periodic. Combining this with the analyticity of ψ_{jk}^x , we derive that $P_j^x(k)$ is both periodic and analytic throughout the Brillouin zone.

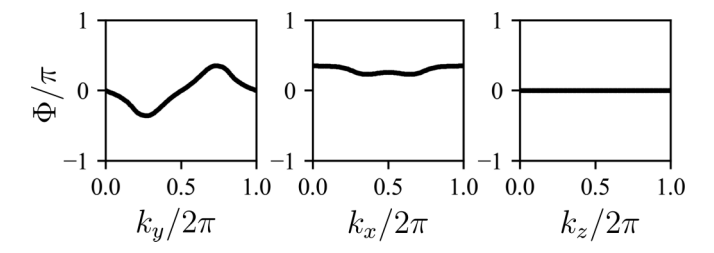


FIG. 10. Zak phase (divided by π) of the lowest band of the projected symmetry operator in three independent planes ($k_z = \pi$, $k_y = 0$ and $k_x = 0$ from left to right) in the Brillouin zone.

APPENDIX E: PROVING THE FRAGILITY OF ROTATION-INVARIANT TOPOLOGICAL CRYSTALLINE INSULATORS

1. Fragility of tetragonal TCI

Fu's tight-binding Hilbert space [55] for the $\mathcal{T}_3 \rtimes C_{4v} \times$ \mathbb{Z}_2^T -symmetric TCI is spanned by two pairs of p_x , p_y orbitals in each unit cell. The reduced real-space coordinates of the two pairs of orbitals are (0,0,0), in an orthogonal basis of Bravais lattice vectors. To remove the symmetry obstruction of the filled rank-two band, a unit-rank BR [induced by an s orbital at (0.5, 0.5, 0.0) is introduced to the model. The original parameters in Ref. [55] are adopted. Additionally, the on-site energy of the s orbital is set to -4.0, in units where the nearest-neighbor hopping between p orbitals (in the x-yplane) equals 1; this ensures that the s-type BR lies below the energy gap. The hopping between the s orbital and the two p_x orbitals in the home unit cell is continuously increased to 0.375, with all other hoppings determined by translational symmetry and C_{4v} . During this interpolation, the bulk gap never closes.

Before the introduction of the s-like BR, the spectrum of the projected symmetry operator is gapless along a nodal line, as illustrated in Fig. 2(a). Upon the introduction of the s-like BR, the projected symmetry operator consists of three bands whose dispersion are nondegenerate throughout the Brillouin zone [cf. Fig. 2(b)]. Each unit-rank band has trivial first Chern class, as verified by computing the winding of the Zak phase in three independent k-directions. For illustration, the Zak phase of the lowest band (of the three) is presented in Fig. 10.

2. Fragility of hexagonal TCI

In Ref. [36], a $\mathcal{T}_3 \times C_{3v} \times \mathbb{Z}_2^T$ -symmetric topological insulator was proposed on a triangular Bravais lattice with primitive vectors: $\boldsymbol{a}_1 = (1,0,0)$, $\boldsymbol{a}_2 = (-1/2,\sqrt{3}/2,0)$ and $\boldsymbol{a}_3 = (0,0,1)$, and with the following tight-binding model Hamiltonian:

$$H(\mathbf{k}) = \left[\frac{5}{2} - \cos(k_1 + 2\pi/3) - \cos(k_2 + 2\pi/3) - \cos(k_1 + k_2 - 2\pi/3) - \cos(k_3) \right] \Gamma_{30}$$

$$+ \{ 0.3 [e^{i\pi/3} \cos(k_1) + e^{-i\pi/3} \cos(k_2) - \cos(k_1 + k_2)] \Gamma_{1+} + h.c. \} + \sin(k_3) \Gamma_{20}.$$
 (E1)

Here, $k_j = \mathbf{k} \cdot \mathbf{a}_j$ for j = 1, 2, 3, $\Gamma_{ij} = \sigma_i \otimes \tau_j$ (with σ_i and τ_j being two sets of Pauli matrices), and $\Gamma_{1+} = \sigma_1 \otimes (\tau_1 + i\tau_2)$.

The tight-binding basis for the above Hamiltonian is given by two sets of $p_x \pm ip_y$ orbitals, both located at (0, 0, 0).

TABLE II. Hoppings between the *s* orbital and other orbitals in the format of $\langle 0m|H|Rs\rangle$, where *R* is a three-element vector denoting the unit cells of the *s* orbital and $m \in \{1, 2\}$ is an index for the *p* orbital. $p_{\pm}^{(2)}$, for example, denotes the $p_x \pm ip_y$ for the second set of *p* orbitals.

R	m	Hopping
[1,0,0]	$p_{+}^{(2)}$	<i>i</i> /6
	$p^{(2)}$	i/6
[1, 1, 1]	$p_+^{(1)}$	-0.116667 - 0.202073i
	$p^{(1)}$	0.233333
[1, -1, 1]	$p^{(2)}$	0.4
[1, 2, 0]	$p_+^{(1)}$	-i/6

The low-energy band of the above model is an obstructed representation of $\mathcal{T}_3 \rtimes C_{3v} \times \mathbb{Z}_2^T$, as deducible from the nontrivial Zak phase described in Ref. [69]. Associated to this obstruction is an integer-valued topological invariant χ —the halved-mirror chirality—which equals 1 in this model. The obstruction also manifests in the projected C_3 -rotation operator as a nodal line in the spectrum, as illustrated in the left panel of Fig. 11(a).

To break the symmetry obstruction on Wannier functions, we add to the low-energy subspace a unit-rank BR induced by an s orbital at the Wyckoff position (0, 0, 0), with the tight-binding hoppings tabulated in Table II. The projected C_3 operator now consists of three unit-rank bands whose dispersions are nondegenerate throughout the Brillouin zone [cf. right panel of Fig. 11(a)]; each band has trivial first Chern class [cf. Fig. 11(b)].

APPENDIX F: PROOF THAT CERTAIN POINT GROUPS ARE MONOMIAL

Here we show that the following point groups are monomial:

- (1) 32 crystallographic point groups [5]
- (2) 27 noncubic double point groups,
- (3) OR Grey magnetic point group generalizations of (1) and (2) (which correspond to the Wigner-Dyson symmetry classes AI and AII, respectively).

Noncubic point groups are crystallographic point groups that are neither tetrahedral nor octahedral, i.e., they are not any of T, T_h , T_d , O, and O_h . Grey crystallographic point groups are of the form $\mathcal{P} \times \mathbb{Z}_2^T$ where \mathcal{P} is a point group in (1), and \mathbb{Z}_2^T is a cyclic group of order two generated by time-reversal symmetry; grey double point groups are the double covers of $\mathcal{P} \times \mathbb{Z}_2^T$.

Bacry *et al.* [175] claimed that all 32 crystallographic point groups, i.e., the point groups in (1), are monomial, but did not provide a reference or proof. We have not seen the claim (or proof) of monomiality for point groups in (2) or (3) anywhere in the literature.

The rest of Appendix F is organized as follows.

(i) We begin in Appendix F 1 by reviewing Huppert's theorem [176], which gives sufficient conditions for a finite group

to be monomial; we will prove two corollaries of Huppert's theorem that are useful for point groups.

- (ii) Basic properties of the crystallographic point groups are reviewed in Sec. F2. Each class of point groups labeled (1)–(3) will further be divided into subclasses:
 - (A) Proper rotation groups
 - (B) Improper rotation groups with inversion
 - (C) Improper rotation groups without inversion

Proper rotation groups consist purely of rotations, while improper rotation groups include at least one reflection or inversion element.

- (iii) This subclassification was used by Altmann [177] to show that every crystallographic point group in (1) can be written as a triple semidirect product of a normal, Abelian subgroup and two cyclic subgroups (any one of which might be trivial). Altmann's result, together with the two previously mentioned corollaries and Wigner's theorem [104], allow us to prove the monomiality of (1)–(3) in Appendixes F3, F4, and F5, respectively.
- (iv) Finally, in Appendix F6, we show that the five double cubic point groups are not monomial, and exemplify a non-monomial representation for the double tetrahedral group.

1. Huppert's theorem for monomial groups, and two corollaries

To prepare the reader for Huppert's theorem, we briefly review the standard definitions of solvability, supersolvability and Sylow subgroups.

A finite group *G* is *solvable* if there exists a series of normal groups, i.e.,

$$C_1 = G_0 \triangleleft G_1 \triangleleft G_2 \dots \triangleleft G_k = G \tag{F1}$$

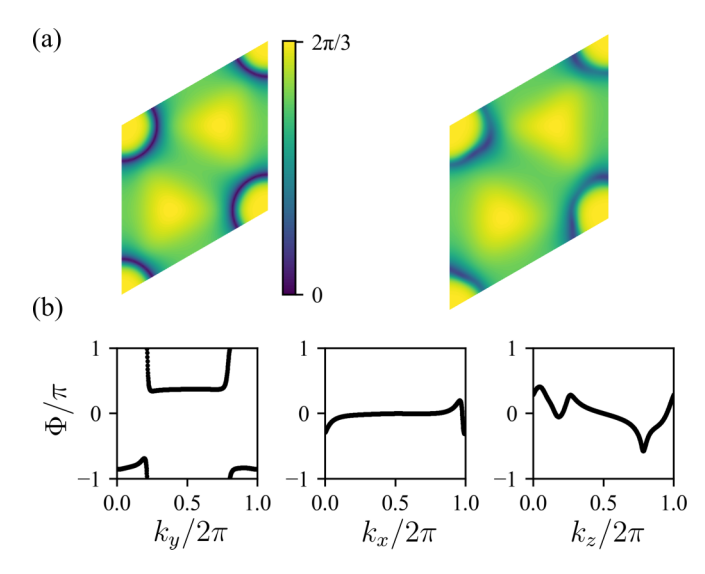


FIG. 11. (a) Left panel: Half the spectral gap between the two bands of the projected C_3 -rotation operator. Right panel: The spectral gap between the lowest band and middle band of the projected C_3 -rotation operator. (b) Zak phase (divided by π) for the lowest band of the projected C_3 operator, for three independent k planes ($k_x = 0$, $k_y = 0$, and $k_z = 0$ from left to right) in the Brillouin zone.

for a $k \ge 1$, such that G_{j+1}/G_j is Abelian for all $j = 1, \ldots, k-1$. Here, $G_j \triangleleft G_{j+1}$ means that G_j is normal in G_{j+1} .

G' is *supersolvable* if there exists a series of normal groups, i.e.,

$$C_1 = G'_0 \triangleleft G'_1 \triangleleft G'_2 \dots \triangleleft G'_n = G'$$
 (F2)

for $n \ge 1$, such that $G'_j \triangleleft G'$ and G'_{j+1}/G'_j is cyclic. Supersolvability is a stronger condition than solvability.

A p group is a group for which every element has order equal to an integer power of a prime p. A maximal subgroup of a group G'' is a subgroup that is not contained in any larger subgroup (that is not G'' itself). Lastly, a Sylow subgroup of G'' is a maximal p group.

Huppert's theorem. Let H' be a finite group with normal, solvable subgroup N', and with supersolvable quotient group H'/N'. If all subgroups of N' that are Sylow are also Abelian, then H' is monomial.

Corollary 1. If a finite group H has a decomposition $H = N \rtimes C^{(1)} \rtimes C^{(2)} \rtimes \ldots \rtimes C^{(n)}$ for a $n \geqslant 1$, where $C^{(j)}$ are cyclic subgroups, N is an Abelian normal subgroup of H, and \rtimes is associative, then H is monomial.

× being associative means that

$$A \rtimes B \rtimes C \rtimes D = A \rtimes (B \rtimes C \rtimes D)$$
$$= (A \rtimes B) \rtimes (C \rtimes D) = (A \rtimes B \rtimes C) \rtimes D,$$
(F3)

which implies A, $A \rtimes B$, and $A \rtimes B \rtimes C$ are all normal subgroups of $A \rtimes B \rtimes C \rtimes D$.

Proof of Corollary 1. Any Abelian group N is also solvable, because there exists a normal series $C_1 \triangleleft N$ with $N/C_1 = N$ that is Abelian. Furthermore, $H/N = C^{(1)} \rtimes C^{(2)} \rtimes \ldots \rtimes C^{(n)}$ has the normal series given in Eq. (F2), with the identifications $G'_j = C^{(1)} \rtimes \ldots \rtimes C^{(j)}$ and $G' = G'_n = H/N$. The associativity of \rtimes implies that $G'_j \triangleleft H/N$ for any $j = 1, \ldots, n$. Furthermore, $G_{j+1}/G_j = C^{(j+1)}$ is cyclic. Finally, since N is Abelian, all its subgroups are Abelian; therefore, if N has Sylow subgroups, such subgroups must also be Abelian. In combination of the above facts, we find that H and N satisfy all conditions of H' and N' in Huppert's theorem, respectively; hence H is monomial.

Corollary 2. If a finite group H has an Abelian, normal subgroup N, such that H/N is a cyclic subgroup of H, then H is monomial.

Proof of Corollary 2. Since *N* is Abelian, *N* is solvable (see beginning of Proof of Corollary 1). Furthermore, H/N is supersolvable, i.e., it has a normal series $C_1 \triangleleft H/N$ such that $(H/N)/C_1 = H/N$ is cyclic. Because H/N is Abelian, all its Sylow subgroups are also Abelian; therefore, Huppert's theorem applies. ■

2. Review of proper versus improper point groups

Here, we elaborate on the subclassification of point groups given in point (ii) of the outline of Appendix F.

A review of crystallographic point groups [class (1)] is given here, with emphasis on its subclassification into proper rotation groups [A], improper rotation groups with inversion symmetry [B], and improper rotation groups without inversion symmetry [C]. Class and subclass labels will be combined

TABLE III. Improper point groups without inversion $(\mathcal{P}_{\neg i};$ first column) can be constructed from proper rotation groups $(\mathcal{P};$ second column) and an index-2 subgroup $(H < \mathcal{P};$ third column).

$\mathcal{P}_{\neg i}$	${\cal P}$	Н
$\overline{C_s}$	C_2	e
S_4	C_4	C_2
C_{3h}	C_6	C_3
C_{2v}	D_2	C_2
C_{3v}	D_3	C_3
C_{4v}, D_{2d}	D_4	C_4, D_2
C_{6v}, D_{3h}	D_6	C_6, D_3
T_d	O	T

as (1)A, (1)B, (1)C. The subclassification cubic double crystallographic point groups will be described subsequently in Appendix F4, after we clarify the meaning of a double group.

There are 11 crystallographic point groups which consist only of rotations [class (1)A]: the trivial point group C_1 , the cyclic groups $\{C_n\}_{n=2,3,4,6}$, the dihedral groups $\{D_n\}_{n=2,3,4,6}$, the tetrahedral group T, and the octahedral group O.

Class (1)B consists of improper rotation groups with inversion which can be constructed by direct products of the above 11 proper rotation groups \mathcal{P} with \mathbb{Z}_2^i – the order-two group generated by inversion i; we denote these by $\mathcal{P}_i = \mathcal{P} \times \mathbb{Z}_2^i$. The direct-product structure reflects that inversion squares to identity and commutes with every point-group operation. The 11 point groups constructed in this way are S_2 , C_{2h} , C_{3i} , C_{4h} , C_{6h} , D_{2h} , D_{3d} , D_{4h} , D_{6h} , T_h , and O_h . Here, and throughout this work, we employ the standard notation for point groups that is reviewed in Ref. [5].

The remaining crystallographic point groups in class (1)C are improper rotation groups without inversion, and will be denoted by $\mathcal{P}_{\neg i}$. Such groups may be constructed from eight out of the 11 proper rotation groups [(1)A] which have at least one index-2 subgroup. The three (1)A groups without index-two subgroups are the trivial group C_1 , C_3 and T. D_4 and D_6 each has two index-two subgroups, as given in the third column of Table III. All other (1)A groups have exactly one index-two subgroup [cf. Table III]. Denoting a (1)A group by \mathcal{P} and its index-two subgroup by H, a (1)C group is constructed as $\mathcal{P}_{\neg i} = H + i \mathcal{P} \backslash H$, where $\mathcal{P} \backslash H$ denotes all elements of \mathcal{P} that are not in H. Two 1(C) groups can be constructed from $\mathcal{P} = D_4$ (and also D_6), which has two indextwo subgroups. Altogether there are ten (1)C groups which we tabulate in Table III.

We will eventually use that $\mathcal{P}_{\neg i}$ is isomorphic to \mathcal{P} . The proof is as follows. First note that H is both a subgroup of \mathcal{P} and $\mathcal{P}_{\neg i}$. We define a map $\varphi: \mathcal{P} \to \mathcal{P}_{\neg i}$ that is the identity map on $H < \mathcal{P}$, and maps an element $p \in \mathcal{P} \setminus H$ bijectively onto $ip \in \mathcal{P}_{\neg i}$. Since i squares to the identity and commutes with all point-preserving spatial isometries (including all elements in H and \mathcal{P}), the bijection φ preserves the multiplication rule, and hence constitutes a group isomorphism.

3. Crystallographic point groups are monomial

To show that crystallographic point groups [class (1)] are monomial, we will apply Altmann's semidirect-

product decomposition [178] of the crystallographic point groups.

Review of the semidirect product. $N \rtimes C$ is a group that is constructed from two groups N and C for which C acts on N by conjugation, i.e., $n \to cnc^{-1}$, for all $n \in N$ and $c \in C$. As a set, $N \rtimes C = N \times C$; as a group, elements in $N \rtimes C$ are multiplied as $(n, c) \cdot (n', c') = (n \, cn' c^{-1}, cc')$. The subgroup $N \times C_1$ – henceforth referred to as N – is a normal subgroup of $N \rtimes C$; the subgroup $C_1 \times C$ – simply denoted by C – is generally just a subgroup of $N \rtimes C$.

Altmann showed that all crystallographic point groups can be expressed as $\mathcal{P} = N \rtimes C$, where N is a maximal normal subgroup of \mathcal{P} and C a cyclic subgroup. Both N and C are subgroups of the group O(3) of isometries in 3D real space, so the action of C on N is uniquely defined within O(3) <.

For 28 of the 32 crystallographic point groups that are not $\{T_h, T_d, O_h, O\}$, N can further be shown to be Abelian. Let us give an example for each subclass of (1): in class (1)A, $\mathcal{P} = D_n$, $N = C_n$, $C = C_2'$ (C_2' is generated by a twofold rotation with rotational axis perpendicular to the rotational axis defined for C_n); in class (1)B, $\mathcal{P} = C_{4h}$, $N = C_4$, $C = \mathbb{Z}_2^i$; in class (1)C, $\mathcal{P} = C_{4v}$, $N = C_4$, $C = C_s'$ (C_s' is generated by a mirror plane which is parallel to the rotational axis of N, and thus acts trivially on N). To recapitulate, each of these 28 crystallographic point groups is an extension of an Abelian group (C) by an Abelian group (C); such groups are called *metabelian*, and it is known that all metabelian groups are monomial [179].

For the four remaining crystallographic point groups— T_h , T_d , O_h , and O—all maximal normal subgroups N are non-Abelian [180] See p. 222 of Ref. [177]. But since every such N is also a crystallographic point group, it has itself a decomposition $N = N' \rtimes C'$ with C' cyclic and N' a maximal normal subgroup of N. Altmann [177] showed that every crystallographic point group $\mathcal{P} = N \rtimes C$ for which $N = N' \rtimes C'$ is non-Abelian, has a decomposition with N' Abelian and \rtimes associative [cf. Eq. (F3)]. The latter also implies that N' is a normal subgroup of \mathcal{P} .

Example of triple semidirect product: $O = T \times C_2'' = D_2 \times (C_3' \times C_2'')$ [177]. In review, the octahedral group O consists of the orientation-preserving symmetries of a cube. Let the x, y, and z axes go through the center of the three faces of the cube; these three axes also define the axes of the twofold rotational symmetries, which generate the subgroup D_2 . A cube also has a threefold rotational axis going through the corner (1,1,1) of the cube; this threefold rotational symmetry generates the group C_3' . (Incidentally, $D_2 \times C_3' = T$ are the orientation-preserving symmetries of a tetrahedron.) Finally, the cube has another twofold rotational symmetry with axis going through the center of the vertex (1,1,0). This twofold rotational symmetry generates C_2'' . Altogether, the mirror, threefold, and twofold rotational symmetries generate the group O.

To recapitulate, for all crystallographic point groups \mathcal{P} , there exists an Abelian normal subgroup N' of \mathcal{P} such that $\mathcal{P} = N' \rtimes (C' \rtimes C)$ where C, C' are cyclic subgroups of \mathcal{P} ; C or C' may be the trivial subgroup [181] See p. 228 of Ref. [177]. Therefore, Corollary 1 of Appendix F1 implies that \mathcal{P} is monomial.

4. Noncubic double point groups are monomial

In this Appendix section, we will apply Corollary 2 of Appendix F1 to prove that all 27 noncubic double point groups [class (2)] are monomial. Given also that the five cubic double point groups are nonmonomial (as proven in Appendix F6), we conclude that a double crystallographic point group is monomial if and only if it is noncubic.

After giving a brief review of double crystallographic point groups in Appendix F4a, we tackle the proof of monomiality for class (2)A, (2)B, and (2)C separately, in Appendixes F4b, F4c, and F4d.

a. Review of double point groups

It is well known from the study of angular momentum that the double cover of SO(3) is SU(2). SU(2) may be viewed as the unsplit central extension of SO(3) by \mathbb{Z}_2 . The \mathbb{Z}_2 group is generated by \tilde{e} , which commutes with every element in SU(2), and has the physical interpretation of a 2π rotation. SU(2) being a double cover means there exists a 2-1 surjection ϕ : $SU(2) \rightarrow SO(3)$.

Analogously, for each of the 11 proper rotation point groups (denoted \mathcal{P}) that are subgroups of SO(3), the double cover $\tilde{\mathcal{P}} = \phi^{-1}(\mathcal{P})$ is a subgroup of SU(2). The identity $e \in \mathcal{P}$ lifts (via ϕ^{-1}) to two elements in $\tilde{\mathcal{P}} - e$ and $\tilde{e} \neq e$ – which both commute with all elements in $\tilde{\mathcal{P}}$, and satisfy $\tilde{e}^2 = e$. For any $g \in \mathcal{P}$, there exist two corresponding elements, g and $\tilde{g} = g\tilde{e}$, in $\tilde{\mathcal{P}}$. The multiplication rule of any two elements in $\tilde{\mathcal{P}}$ is determined by the multiplication rule of the same elements in SU(2).

More generally, the double covers of the crystallographic point groups $(\mathcal{P}, \mathcal{P}_i, \mathcal{P}_{\neg i})$ are referred to as the *double crystallographic point groups*, and denoted by $(\tilde{\mathcal{P}}, \tilde{\mathcal{P}}_i, \tilde{\mathcal{P}}_{\neg i})$. We shall only concern ourselves with half-integer-spin representations of the double crystallographic point groups, in which \tilde{e} is represented by -1 times the identity matrix.

b. Proof for proper double point groups

Of the 11 proper double crystallographic point groups, only two of them $(\tilde{T} \text{ and } \tilde{O})$ are cubic. The remaining nine groups form class (2)A, and are proven here to be monomial.

The double covers of C_n for n = 1, 2, 3, 4, 6 are still cyclic but with twice as many elements, i.e., $\tilde{C}_n \cong \mathbb{Z}_{2n}$. This reflects that a 2π rotation is not the identity element but a 4π rotation is (cf. Appendix F4a). Abelian groups such as \mathbb{Z}_{2n} are monomial because all their irreps are 1D (and 1D irreps are trivially induced from 1D irreps of the group itself).

The only remaining double proper crystallographic point groups are the double covers (\tilde{D}_n) of $D_n = C_n \rtimes C_2'$, where n=2,3,4,6 and the C_2' axis is perpendicular to the C_n axis. The generators of C_2' and C_n are denoted c_2' and c_n , respectively. As an element of \tilde{D}_n , c_n generates a subgroup isomorphic to \mathbb{Z}_{2n} . This subgroup is normal in \tilde{D}_n because $c_2'c_nc_2'^{-1}=c_n^{-1}$ (recall here that c_2' inverts the C_n axis) and the quotient group $\tilde{D}_n/\mathbb{Z}_{2n}=\{[e],[c_2']\}$ is cyclic and isomorphic to \mathbb{Z}_2 ; note that $c_2''=\tilde{e}\in\mathbb{Z}_{2n}$ lies in [e]. Therefore, \mathbb{Z}_{2n} is an Abelian and normal subgroup of \tilde{D}_n with cyclic quotient group \mathbb{Z}_2 . Corollary 2 then implies that \tilde{D}_n is monomial.

c. Proof for improper double point groups with inversion

The nine groups (denoted $\tilde{\mathcal{P}}_i$) in class (2)B are obtained by including inversion symmetry (i) for each of the nine groups (denoted $\tilde{\mathcal{P}}$ in class (2)A. i squares to the identity and commutes with all double point-group operations [8,182]; we have the direct-product form $\tilde{\mathcal{P}}_i = \tilde{\mathcal{P}} \times \mathbb{Z}_2^i$. We have already proven in Appendix F 4 b that all \mathcal{P} in class (2)A are monomial; then, according to the *Lemma for monomial direct-product groups* in Appendix B 4, $\tilde{\mathcal{P}}_i = \tilde{\mathcal{P}} \times \mathbb{Z}_2^i$ must also be monomial.

d. Proof for improper double point groups without inversion

Of the ten improper double crystallographic point groups without inversion, only one of them (\tilde{T}_d) is cubic, and the rest have the denotation $\tilde{\mathcal{P}}_{\neg i}$ and form class (2)C.

To prove the monomiality of $\tilde{\mathcal{P}}_{\neg i}$, we first prove its isomorphism with $\tilde{\mathcal{P}}$ in class (2)A (cf. Appendix F4b). $\tilde{\mathcal{P}}_{\neg i} \cong \tilde{\mathcal{P}}$ will be derived from the isomorphism $\mathcal{P}_{\neg i} \cong \mathcal{P}$, for \mathcal{P} a proper, noncubic crystallographic point group having an index-two subgroup H. To clarify, of the nine noncubic proper crystallographic point groups, two of them $[C_1 \text{ and } C_3]$ have no index-two subgroups, for two of them $[D_4 \text{ and } D_6]$ each has two index-two subgroups, while the rest each has one index-two subgroup. This means that the nine groups in class (2)C will be shown to be isomorphic to seven groups in class (2)A.

We remind the reader of the set decompositions $\mathcal{P}=H+\mathcal{P}\backslash H$ and $\mathcal{P}_{\neg i}=H+i\mathcal{P}\backslash H$, as reviewed in Appendix F 2. Under the 2-1 surjection $\phi:SU(2)\to SO(3)$, the preimage of H is a subgroup of both $\tilde{\mathcal{P}}$ and $\tilde{\mathcal{P}}_{\neg i}$. On the other hand, $\phi^{-1}(\mathcal{P}\backslash H)$ is a subset of \mathcal{P} , while $i\phi^{-1}(\mathcal{P}\backslash H)$ is a subset of $\tilde{\mathcal{P}}_{\neg i}$. There is therefore a bijection of group elements between $\tilde{\mathcal{P}}$ and $\tilde{\mathcal{P}}_{\neg i}$, where in the direction $\tilde{\mathcal{P}}_{\neg i}\to \tilde{\mathcal{P}}$ one merely drops the i label. Moreover, this bijection preserves the multiplication rule, because i commutes with every point-group operation [8,182].

Now we combine the just-stated isomorphism with a result established in Appendix F 4 b, namely, that all *noncubic* double proper rotation groups $[\tilde{\mathcal{P}}$ in class (2)A] are monomial. Since each noncubic double improper rotation group without inversion $[\tilde{\mathcal{P}}_{\neg i}]$ in class (2)A] is isomorphic to one of $\tilde{\mathcal{P}}$ in class (2)A, we deduce that $\tilde{\mathcal{P}}_{\neg i}$ must also be monomial. This follows because if two groups $A \cong B$ are isomorphic, then A is monomial if and only if B is monomial. Indeed, every representation of A gives a representation of B via the group isomorphism, and vice versa. So if all representations of A are induced from 1D irreps of subgroups of A, so must all representations of B be induced from 1D irreps of subgroups of B, and vice versa.

5. Grey magnetic point groups and grey magnetic double point groups are monomial

Here we prove that all 32 grey magnetic point groups (denoted \mathcal{P}_T), and all 27 grey magnetic noncubic double point groups ($\tilde{\mathcal{P}}_T$) are monomial.

Our proof relies on Wigner's seminal result [104], namely, that *all* irreps of $\mathcal{P}_T = \mathcal{P} \times \mathbb{Z}_2^T$ are induced from irreps of the crystallographic point group \mathcal{P} . Similarly, *all* half-integer-spin irreps of $\hat{\mathcal{P}}_T$ (the double-group extension of $\mathcal{P} \times \mathbb{Z}_2^T$) are

induced from irreps of the double point group $\tilde{\mathcal{P}}$. [In fact, Wigner goes further to show that a representation D of \mathcal{P} is either (a) compatible with time-reversal T symmetry, or (b) incompatible with T symmetry, but $D \oplus D^*$ [D^* being the complex conjugate of D] is compatible. Which case holds depends on whether D is an integer-spin or half-integer-spin representation, and whether D is real, complex, or quaternionic. Such considerations, however, lie outside the scope of our proof.]

Since any irrep (denoted D_T) of \mathcal{P}_T is induced from an irrep (D) of \mathcal{P} , the question of whether D_T is monomial reduces to the question of whether D is monomial. In other words, if D is induced from a one-dimensional representation of a subgroup $H < \mathcal{P}$, then it follows that D_T is also induced from the same one-dimensional representation of $H < \mathcal{P} < \mathcal{P}_T$. Such a one-dimensional representation always exists for any representation D of \mathcal{P} , because of our previously-established result that all 32 crystallographic point groups are monomial; cf. Appendix F 3. Thus we conclude that all 32 grey magnetic point groups are also monomial.

By similar reasoning, one concludes that all 27 grey magnetic noncubic double point groups are monomial, based on our result that all 27 double noncubic point groups are monomial; cf. Appendix F 4.

6. Double cubic point groups are nonmonomial

We will show that the double-group extensions of the cubic crystallographic point groups T, T_d, T_h, O, O_h are nonmonomial.

 \tilde{T} and \tilde{O} are standard examples of *non*monomial groups [183].

Example of nonmonomial irrep of double cubic point group \tilde{T} . Let us consider the nonmonomial [184] 2D irrep \bar{E} of double group \tilde{T} . In a representation basis with spin quantization axis that is parallel to the C_2 axis, the three generators of \tilde{T} are represented as

$$C_2 = e^{-\pi i \sigma_z/2}, \quad C_2' = e^{-\pi i \sigma_x/2}, \quad C_3' = e^{-\pi i (\sigma_x + \sigma_y + \sigma_z)/(3\sqrt{3})}.$$

 C_2 and C_2' are complex permutation matrices but C_3' is not; an analogous statement holds in an eigenbasis of C_2' . In a basis where $C_3' = \mathrm{e}^{-\pi i \sigma_z/3}$ is diagonal, we find instead that $C_2 = \mathrm{e}^{-\pi i (-\sigma_x + \sigma_y - \sigma_z)/(2\sqrt{3})}$ is not a complex permutation matrix

Of the three remaining double cubic point groups, two have the direct-product form: $\tilde{T}_h = \tilde{T} \times \mathbb{Z}_2^i$ and $\tilde{O}_h = \tilde{O} \times \mathbb{Z}_2^i$. (The direct-product structure was explained in Appendix F4.) Since \tilde{O} and \tilde{T} are nonmonomial, it follows that \tilde{O}_h and \tilde{T}_h must also be nonmonomial, according to the *Lemma for monomial direct-product groups* in Appendix B 4.

Finally, to show that \tilde{T}_d is nonmonomial, we will use that double-group extensions of isomorphic crystallographic point groups are also isomorphic and monomiality (as well as nonmonomiality) is preserved by group isomorphisms—both of these claims have been proven in Appendix F 4 d. Thus, $T_d \cong O$ implies their double-group extensions are also isomorphic: $\tilde{T}_d \cong \tilde{O}$; moreover, since \tilde{O} is known to be nonmonomial, so must \tilde{T}_d be nonmonomial.

APPENDIX G: TIGHTLY BOUND BRS AND THE EXISTENCE OF THE SYMMETRIC TIGHT-BINDING LIMIT

We have used inSecs. V and IX that every BR has a symmetric tight-binding limit to a tightly bound BR. We remind the reader that a tightly bound BR is a BR for which all Wannier functions are one-site localized. The goal of this Appendix is to describe tightly bound BRs in the language of *G*-vector bundles (in Appendix G 2), so as to rigorously prove the existence of a symmetric tight-binding limit for any BR (in Appendix G 3). In Appendix G 1, we provide definitions for *G*-vector bundles and discuss their applications in tight-binding lattice models.

1. G-vector bundles and tight-binding lattice models

We have heuristically introduced (complex) vector bundles in Appendix A 1 from the perspective of band theory. Here, we review some basic bundle notions from the mathematical perspective, and describe their application to tight-binding lattice models.

A complex vector bundle is a continuous surjection $p: E \to B$ from a (topological) space E, called total space, to a (topological) space E, called base space. Furthermore, it has a local trivialization: For every $b \in B$ there exists a neighbourhood $U_b \subset B$ and a continuous bijection $h_b: p^{-1}(U_b) \to U_b \times \mathbb{C}^N$ with continuous inverse such that $h_b|_{p^{-1}(b)}$ is a linear isomorphism of vector spaces. $E_b = p^{-1}(b)$ is called the fiber over E, and E the vector bundle.

The total space E can also be viewed as a disjoint union of all fibers, i.e., $E \equiv \sqcup_{b \in B} E_b$. The local trivialization implies that every fiber of a complex rank-N vector bundle is isomorphic to \mathbb{C}^N .

The notion of isomorphism for vector spaces is well known, e.g., any complex N-dimensional vector space is isomorphic to \mathbb{C}^N . There is an analogous notion of isomorphism for vector bundles:

For two vector bundles E, E' over the same base space B, a *vector bundle isomorphism* is a continuous bijection $f: E \to E'$ with continuous inverse such that $f|_{E_b}$ is a linear isomorphism from the fiber E_b to the fiber E_b' for all $b \in B$.

For example, a vector bundle that has nontrivial first Chern class is not isomorphic a *product bundle*; the latter has total space $BZ \times V$, with BZ the Brillouin zone and V an N-dimensional complex vector space.

Let us apply these bundle notions to *tight-binding lattice models*. A tight-binding lattice model corresponds to a finite-dimensional vector space (in each unit cell indexed by Bravais-lattice vector \mathbf{R}) spanned by N_{tot} tight-binding basis functions $\vec{\phi}_{\alpha,\mathbf{R}}$, indexed by $\alpha=1,\ldots,N_{\text{tot}}$. The Fourier transforms of tight-binding basis functions span the fibers of a vector bundle with total space E_{TB} over B=BZ (the Brillouin zone). Since tight-binding basis functions are, by definition, one-site localized, their Fourier transforms are \mathbf{k} independent; hence, the fibers are \mathbf{k} -independent N_{tot} -dimensional complex vector spaces, denoted V_{TB} and $E_{\text{TB}} = \text{BZ} \times V_{\text{TB}}$.

Any rank-N vector bundles E over the BZ—with $1 \le N \le N_{\text{tot}}$ —can be embedded in this tight-binding product bundle E_{TB} with N_{tot} large, as exemplified by a rank-N energy band

of a tight-binding Hamiltonian. Then each fiber E_k is spanned by N vectors which we denote as $\vec{\mathfrak{V}}_n(k) = (\mathfrak{V}_n(k)^\alpha)_{\alpha=1}^{N_{tat}}$ with $n=1,\ldots,N$. It is assumed that $\{\vec{\mathfrak{V}}_n(k)\}_{n=1}^N$ are periodic over the Brillouin torus; these vectors span the fiber E_k at each k. If the vector bundle is topologically trivial (in spatial dimension $d \leq 3$, topological triviality is equivalent to having trivial first Chern class), then each $\vec{\mathfrak{V}}_n(k)$ can be chosen to be a periodic and analytic function of k. The Fourier transform of each such $\vec{\mathfrak{V}}_n(k)$ defines a set of Wannier functions related by Bravais-lattice translations. Especially, if E is spanned by one-site localized Wannier functions, then $\vec{\mathfrak{V}}_n(k)$ can be chosen k independent, and E is a product bundle.

Space-group symmetries $g \in G$ provide additional structure to vector bundles. Especially, the total space E and the base space B are G spaces.

For a topological group G and a topological space X, called a G space, a continuous action of G on X is given by a continuous map $\circ: G \times X \to X$ such that $e \circ x = x$ and $(gh) \circ x = g \circ (h \circ x)$ for all $x \in X$ and all $g, h \in G$.

In band theory, G acts on the BZ by $g: k \to \check{g}k$ (modulo reciprocal lattice vectors) and acts fiberwise on E by a unitary matrix $U_g(k)$ that is sometimes called the sewing matrix:

$$\hat{g}: \vec{\mathfrak{V}}_n(\mathbf{k}) \in E_{\mathbf{k}} \mapsto \sum_{n'=1}^N [U_g(\mathbf{k})]_{n'n} \vec{\mathfrak{V}}_{n'}(\check{g}\mathbf{k}) \in E_{\check{g}\mathbf{k}}.$$
 (G1)

(A space group G is a topological group using the discrete topology.) In fact, E is a G bundle, defined as follows.

Definition G.1. For G spaces E and B, a G-vector bundle is a vector bundle for which $p: E \to B$ is a G-map, and the fiberwise action $g: E_b \to E_{gb}$ is a linear isomorphism for all $b \in B$.

For p to be a G-map means that gp(e) = p(ge) for all $e \in E$ and $g \in G$.

Two G-vector bundles E, E' over the same base space B are G-isomorphic if there exists a complex vector bundle isomorphism $f: E \to E'$ that is also a G map.

Note the notational difference between an isomorphism (as a complex vector bundle) and a G isomorphism.

2. BRs and tightly bound BRs as G-vector bundles

We now discuss how BRs and tightly bound BRs can be expressed as *G*-vector bundles.

For simplicity, let us consider a rank-N BR(G, ϖ , D). Then there always exists a basis $\{\vec{\mathfrak{V}}_n(k)\}_{n=1}^N$ of each fiber E_k that is analytic in $k \in BZ$ (e.g., Ref. [80], Sec. I. B). Their continuity and linear independence at each $k \in BZ$ implies that there exists an isomorphism (as complex vector bundles) from E to the rank-N product bundle (cf. Ref. [53], p. 8).

For a BR(G, $\boldsymbol{\varpi}$, D), the action of G on E is referred to as a (G, $\boldsymbol{\varpi}$, D) *action*, which we define by Eq. (G1) with $U_g(\boldsymbol{k})$ having the following canonical form (cf. Ref. [17]):

$$[U_g(\mathbf{k})]_{n'n} = e^{-is_g \check{\mathbf{g}} \mathbf{k} \cdot \Delta_{g,n',n}} [U_g(\mathbf{0})]_{n'n}.$$
 (G2)

Here, n' is uniquely defined by the Wannier center $\boldsymbol{\varpi}_{n'}$ and by a Bravais lattice vector $\Delta_{g,n',n}$ such that $g \circ \boldsymbol{\varpi}_n = \boldsymbol{\varpi}_{n'} + \Delta_{g,n',n}$. Furthermore, $U_g(\mathbf{0})$ is determined by $D(\check{g}_{n'}^{-1}\check{g}\check{g}_n)$, as

explained in detail in Ref. [80], Appendix A. To recapitulate, a BR(G, ϖ , D) forms a G-VB E with a (G, ϖ , D) action. (Implicit in this definition is that E is vector bundle isomorphic to the product bundle.)

A tightly bound BR(G, ϖ , D) is a BR(G, ϖ , D) with the additional property that (i) it is subbundle of a tight-binding lattice model (given by E_{TB} over BZ) and (ii) it is a G-product bundle with (G, ϖ , D) action. (ii) implies there exists a k-independent basis for the k-independent fibers; the Fourier transform of this basis gives one-site localized Wannier functions.

3. Existence of symmetric tight-binding limit

A BR and a tightly bound BR with the same $(G, \boldsymbol{\varpi}, D)$ action are G isomorphic.

Proof. Here we prove the more general claim that any two G-vector bundles E and E' of the same rank and with the same $(G, \boldsymbol{\varpi}, D)$ -action are G-isomorphic. In particular, this holds for E a rank-N BR with $(G, \boldsymbol{\varpi}, D)$ action and for E' a rank-N tightly bound BR with the same $(G, \boldsymbol{\varpi}, D)$ action.

Let E and E' be two G-vector bundles of the same rank and with the same $(G, \boldsymbol{\varpi}, D)$ action. Their fibers at $\boldsymbol{k} \in BZ$ are spanned by $\{\vec{\mathfrak{V}}_n(\boldsymbol{k})\}_{n=1}^N$ and $\{\vec{\mathfrak{V}}_n'(\boldsymbol{k})\}_{n=1}^N$, respectively. By definition, E and E' are isomorphic as complex vector bundles, which means there exists a linear isomorphism \mathcal{I} from the fibers of E and to those of E' (cf. Ref. [53], p. 8):

$$\mathcal{I}(\mathbf{k}, \vec{\mathfrak{V}}_n(\mathbf{k})) = (\mathbf{k}, \vec{\mathfrak{V}}'_n(\mathbf{k})). \tag{G3}$$

To show that \mathcal{I} is also a G isomorphism, it suffices to prove that \mathcal{I} is a G map:

$$\hat{g}\mathcal{I}(\boldsymbol{k}, \vec{\mathfrak{V}}_{n}(\boldsymbol{k})) = \hat{g}(\boldsymbol{k}, \vec{\mathfrak{V}}'_{n}) = \left(\check{g}\boldsymbol{k}, \sum_{n'=1}^{N} [U_{g}(\boldsymbol{k})]_{n'n} \vec{\mathfrak{V}}'_{n'}(\boldsymbol{k})\right)$$

$$= \sum_{n'=1}^{N} [U_{g}(\boldsymbol{k})]_{n'n} (\check{g}\boldsymbol{k}, \vec{\mathfrak{V}}'_{n'}(\boldsymbol{k}))$$

$$= \sum_{n'=1}^{N} [U_{g}(\boldsymbol{k})]_{n'n} \mathcal{I}(\check{g}\boldsymbol{k}, \vec{\mathfrak{V}}_{n'}(\check{g}\boldsymbol{k})))$$

$$= \mathcal{I}\left(\check{g}\boldsymbol{k}, \sum_{n'=1}^{N} [U_{g}(\boldsymbol{k})]_{n'n} \vec{\mathfrak{V}}_{n'}(\check{g}\boldsymbol{k})\right)$$

$$= \mathcal{I}(\hat{g}(\boldsymbol{k}, \vec{\mathfrak{V}}_{n}(\boldsymbol{k}))). \tag{G4}$$

For the equality in the second row, we used the linearity of the fibers of E', whereas for the first equality in the fourth row we used the linearity of \mathcal{I} and the linearity of the fibers of E.

Let us discuss a physical interpretation of the above G isomorphism, in the case that E and E' are subbundles of a larger rank- N_{tot} G-vector bundle E_{TB} , with E corresponding to a nontightly bound BR, E' to a tightly bound BR, and E_{TB} the vector bundle of a tight-binding lattice model (as introduced in Appendix G 1). The universal G-vector bundle theorem [139] states that the proven G isomorphism between E and E' corresponds bijectively to a G homotopy, i.e., a continuous, symmetric deformation from E to E'.

For a fixed tight-binding lattice model E_{TB} and a subbundle E that transforms as a nontightly bound $BR(G, \varpi, D)$, the G-vector bundle E' of a tightly bound $BR(G, \varpi, D)$ may not be a subbundle of E_{TB} . In this case, the BR would have a *symmetric tight-binding obstruction*, as defined in Sec. IX. To construct a G-symmetric homotopy between E and E', it is sufficient to enlarge the tight-binding lattice model as $E_{TB} \to E_{TB} \oplus E'$, as exemplified numerically in Ref. [62].

APPENDIX H: LEMMA FOR ZAK PHASES OF TIGHTLY BOUND BAND REPRESENTATIONS

We will prove a lemma stated in Sec. V A, namely, that for the rank-N projector P to a tightly bound BR, the Zak phase $2\pi x_j(k_y)$ for a set of loops $C(k_y)$ (given by varying k_x at fixed k_y) is independent of k_y , for all $j = 1 \dots N$. (As in Sec. V A, we will simplify notation by assuming a rectangular real-space lattice with lattice periods set to one.)

It is sufficient to prove the lemma for the tightly bound $BR(G, \varpi_1, D)$, with the understanding that a general tightly bound BR is a direct sum of tightly bound BRs with Wyckoff positions that are possibly symmetry inequivalent.

The Wannier centers of the tightly bound $BR(G, \varpi_1, D)$ are given by $\{\varpi_n + R\}_{n=1...M,R\in BL}$, with M the number of distinct Wannier centers in one unit cell, and BL shorthand for the Bravais lattice. The projector to this tightly bound BR can be decomposed as a sum of projectors to a finite number A of Wannier functions on each site: $P = \sum_{n=1}^{M} \sum_{R\in BL} P_{nR}$. We assume that the real-space support of Wannier functions on different sites do not intersect. (This is certainly true of tight-binding Wannier functions which are one-site localized.) Then the projected position operator simplifies to a sum of commuting operators:

$$P\hat{x}P = \sum_{n\mathbf{R}} P_{n\mathbf{R}} \hat{x} P_{n\mathbf{R}}. \tag{H1}$$

The eigenproblem for each commuting operator should then be independently solved,

$$\left(P_{nR}\hat{x}P_{nR} - \bar{x}_{nR}^{\alpha}\right)\left|W_{nR}^{\alpha}\right\rangle = 0,\tag{H2}$$

giving the complete spectrum of the projected position operator:

$$\operatorname{spec} P \hat{x} P = \left\{ \bar{x}_{nR}^{\alpha} \right\}_{\alpha = 1 \dots A, n = 1 \dots M, R \in \operatorname{BL}}.$$
 (H3)

Observe that $\bar{x}_{nR}^{\alpha} := \bar{x}_{nR_{\chi}}^{\alpha}$ is independent of R_{y} , owing to the y-translational symmetry of PxP and the spatial localization of the Wannier functions. Indeed, supposing $|W_{nR}^{\alpha}\rangle$ is an eigenstate of P_{nR} with eigenvalue \bar{x}_{nR}^{α} [cf. Eq. (H2)], $\widehat{(e_{y}|e)}|W_{nR}^{\alpha}\rangle$ must be an eigenstate of $P_{nR+e_{y}}$ with the same eigenvalue.

It follows that any linear combination of $\{W_{nR}^{\alpha}\}$ with the same $\{n, R_x, \alpha\}$ label remains an eigenstate of $P\hat{x}P$,

$$\left(P\hat{x}P - \bar{x}_{nR_x}^{\alpha}\right) \sum_{R_y} f(R_y) |W_{nR}^{\alpha}\rangle = 0, \tag{H4}$$

with f an arbitrary function. In particular, if we choose f to be the plane-wave phase factor $e^{ik_yR_y}$, then the sum can be identified as the hybrid function $|h_{j,k_y,R_x}\rangle$ in Eq. (10) with $j:=(\alpha,n)$, and $\bar{x}_{nR_x}^{\alpha}$ can be identified as the eigenvalue

 $(x_j(k_y) + R_x)$ in Eq. (10). We thus derive the desired result that $x_j(k_y)$ is independent of k_y for all j.

APPENDIX I: PROOF OF LOCALIZATION OBSTRUCTION LEMMA

In this Appendix, we prove the localization obstruction lemma of Sec. VI A.

Let P be a representation of a space-group G with translational subgroup \mathcal{T}_d . If the Wannier functions spanning P are all one-site localized, then the set of all Wannier functions $\{W_{1,0}^{\alpha}\}_{\alpha=1}^{A}$ lying on a Wyckoff position ϖ_1 must form a representation of the site stabilizer G_{ϖ_1} . Indeed, since any $g \in G_{\varpi_1}$ acts in real space as an isometry, $\hat{g}W_{1,0}^{\alpha}$ must also be one-site localized to ϖ_1 , and therefore has zero overlap with any Wannier function that is not one of $\{W_{1,0}^{\alpha}\}_{\alpha=1}^{A}$. On the other hand, $\hat{g}W_{1,0}^{\alpha}$ must belong in P which represents G. Thus for any $g \in G_{\varpi}$, $\langle W_{1,0}^{\alpha}|\hat{g}W_{1,0}^{\beta}\rangle$ is a A-dimensional unitary matrix in the indices α and β .

To finish the proof, if $\boldsymbol{\varpi}_1$ is the Wannier center of precisely A linearly independent Wannier functions $\{|W_{1,\boldsymbol{0}}^{\alpha}\rangle\}_{\alpha=1}^{A}$ in P, then for any representatives of the coset: $G/(\mathcal{T}_d \rtimes G_{\varpi_1}) = \{[g_1 = e], [g_2], ..., [g_M]\}$ (with $M = |G/(\mathcal{T}_d \rtimes G_{\varpi_1})|$), the real-space position $\boldsymbol{\varpi}_n = g_n \circ \boldsymbol{\varpi}_1$ must likewise be the Wannier center for the A linearly-independent Wannier functions:

 $\{\hat{g}_n|W_{1,0}^{\alpha}\}_{\alpha=1}^A$ in P. This is because P is assumed to be invariant under all elements of G. Using once again that g acts as a real-space isometry, and that all Wannier functions are one-site localized, it follows that any Wannier function in P with Wannier center $\boldsymbol{\varpi}_n$ belongs to the span of $\{\hat{g}_n|W_{1,0}^{\alpha}\}_{\alpha=1}^A$, which forms an A-dimensional representation of $G_{\varpi_n} = g_n G_{\varpi_1} g_n^{-1}$. Finally, for any $(\mathbf{R}|e) \in \mathcal{T}_d$, $\{W_{n,\mathbf{R}}^{\alpha} :=$ $(R|e)W_{n,0}^{\alpha}\}_{\alpha}$ must also form an A-dimensional representation of the site stabilizer of $\boldsymbol{\varpi}_n + \boldsymbol{R}$. With this, all conditions are satisfied for $\{W_{n,R}^{\alpha}\}_{\alpha,n,R}$ to be a locally-symmetric Wannier basis [cf. Appendix A 3 b] for a BR of G with Wyckoff position $\boldsymbol{\varpi}_1$. (A stronger statement can be made if there exists a basis of Wannier functions where $\langle W_{1,0}^{\alpha} | \hat{g} W_{1,0}^{\beta} \rangle$ is a complex permutation matrix (for any g in the site stabilizer), namely, that $\{W_{n,R}^{\alpha}\}_{\alpha,n,R}$ would span a monomial BR of G. However, our proof more generally applies to nonmonomial BRs as

If $\{W_{n,R}^{\alpha}\}_{\alpha,n,R}$ spans P then the proof is complete, otherwise there must exist other Wannier functions that lie at G-inequivalent Wyckoff positions. By iterating the above argument for the remaining Wannier functions, one would generally conclude that P is a direct sum of BRs of G, possibly with Wyckoff positions that are not related by G symmetry. Finally, P being a BR contradicts our initial assumption that P is an obstructed representation.

- [1] E. Fermi, Z. Phys. 36, 902 (1926).
- [2] P. A. M. Dirac, Proc. R. Soc. Lond A 112, 661 (1926).
- [3] F. Bloch, Z. Phys. **52**, 555 (1929).
- [4] L. Brillouin, *Die Quantenstatistik und ihre Anwendung auf die Elektronentheorie der Metalle* (J. Springer, Berlin, 1931).
- [5] M. Tinkham, Group Theory and Quantum Mechanics (Dover, New York, 2003).
- [6] L. C. L. Y. Voon and M. Willatzen, *The* $k \cdot p$ *Method: Electronic Properties of Semiconductors* (Springer, Berlin, 2009).
- [7] L. P. Bouckaert, R. Smoluchowski, and E. Wigner, Phys. Rev. 50, 58 (1936).
- [8] V. Heine, *Group Theory in Quantum Mechanics* (Pergamon Press, New York, 1977).
- [9] J. Kruthoff, J. de Boer, J. van Wezel, C. L. Kane, and R.-J. Slager, Phys. Rev. X 7, 041069 (2017).
- [10] B. Bradlyn, L. Elcoro, J. Cano, M. G. Vergniory, Z. Wang, C. Felser, M. I. Aroyo, and B. A. Bernevig, Nature 547, 298 (2017).
- [11] H. C. Po, A. Vishwanath, and H. Watanabe, Nat. Commun. 8, 50 (2017).
- [12] F. Hund, Zeitschrift für Physik 99, 119 (1936).
- [13] C. Herring, Phys. Rev. 52, 361 (1937).
- [14] C. Herring, Phys. Rev. 52, 365 (1937).
- [15] L. Michel and J. Zak, Phys. Rev. B 59, 5998 (1999).
- [16] B. Bradlyn, J. Cano, Z. Wang, M. G. Vergniory, C. Felser, R. J. Cava, and B. A. Bernevig, Science 353, aaf5037 (2016).
- [17] J. Zak, Phys. Rev. B 20, 2228 (1979).
- [18] J. Zak, Phys. Rev. B 23, 2824 (1981).
- [19] L. Elcoro, B. Bradlyn, Z. Wang, M. G. Vergniory, J. Cano, C. Felser, B. A. Bernevig, D. Orobengoa, G. de

- la Flor, and M. I. Aroyo, J. Appl. Crystallogr. **50**, 1457 (2017).
- [20] A. Alexandradinata, X. Dai, and B. A. Bernevig, Phys. Rev. B 89, 155114 (2014).
- [21] J. Höller and A. Alexandradinata, Phys. Rev. B 98, 024310 (2018).
- [22] M. Atala, M. Aidelsburger, J. T. Barreiro, D. Abanin, T. Kitagawa, E. Demler, and I. Bloch, Nat. Phys. 9, 795 (2013).
- [23] T. Li, L. Duca, M. Reitter, F. Grusdt, E. Demler, M. Endres, M. Schleier-Smith, I. Bloch, and U. Schneider, Science 352, 1094 (2016).
- [24] J. Zak, Phys. Rev. Lett. 62, 2747 (1989).
- [25] L. Fu and C. L. Kane, Phys. Rev. B 74, 195312 (2006).
- [26] R. Yu, X. L. Qi, A. Bernevig, Z. Fang, and X. Dai, Phys. Rev. B 84, 075119 (2011).
- [27] A. M. Turner, Y. Zhang, and A. Vishwanath, Phys. Rev. B **82**, 241102(R) (2010).
- [28] T. L. Hughes, E. Prodan, and B. A. Bernevig, Phys. Rev. B 83, 245132 (2011).
- [29] A. Alexandradinata, T. L. Hughes, and B. A. Bernevig, Phys. Rev. B 84, 195103 (2011).
- [30] Z. Huang and D. P. Arovas, Phys. Rev. B 86, 245109 (2012).
- [31] B. Bradlyn, Z. Wang, J. Cano, and B. A. Bernevig, Phys. Rev. B 99, 045140 (2019).
- [32] C. L. Kane and E. J. Mele, Phys. Rev. Lett. 95, 226801 (2005).
- [33] C. L. Kane and E. J. Mele, Phys. Rev. Lett. 95, 146802 (2005).
- [34] L. Fidkowski, Phys. Rev. Lett. 104, 130502 (2010).
- [35] T. H. Hsieh, H. Lin, J. Liu, W. Duan, A. Bansil, and L. Fu, Nat. Commun. 3, 982 (2012).

- [36] A. Alexandradinata, C. Fang, M. J. Gilbert, and B. A. Bernevig, Phys. Rev. Lett. 113, 116403 (2014).
- [37] C.-X. Liu, R.-X. Zhang, and B. K. VanLeeuwen, Phys. Rev. B 90, 085304 (2014).
- [38] Z. Wang, A. Alexandradinata, R. J. Cava, and B. A. Bernevig, Nature 532, 189 (2016).
- [39] A. Alexandradinata, Z. Wang, and B. A. Bernevig, Phys. Rev. X 6, 021008 (2016).
- [40] S. Satpathy and Z. Pawlowska, Phys. Status Solidi 145, 555 (1988).
- [41] N. Marzari and D. Vanderbilt, Phys. Rev. B 56, 12847 (1997).
- [42] A. A. Soluyanov and D. Vanderbilt, Phys. Rev. B 83, 235401 (2011).
- [43] A. A. Soluyanov and D. Vanderbilt, Phys. Rev. B 83, 035108 (2011).
- [44] A. A. Soluyanov and D. Vanderbilt, Phys. Rev. B 85, 115415 (2012).
- [45] G. W. Winkler, A. A. Soluyanov, and M. Troyer, Phys. Rev. B 93, 035453 (2016).
- [46] Essentially, this is the same method used by Po *et al.* in Refs. [62,66], where trial Wannier functions are validated by a symmetric, gapped interpolation.
- [47] A. Bouhon, A. M. Black-Schaffer, and R.-J. Slager, Phys. Rev. B 100, 195135 (2019).
- [48] J. Ahn and B.-J. Yang, Phys. Rev. B 99, 235125 (2019).
- [49] H.-X. Wang, G.-Y. Guo, and J.-H. Jiang, New J. Phys. **21**, 093029 (2019).
- [50] S.-S. Chern, Ann. Math. 47, 85 (1946).
- [51] D. J. Thouless, M. Kohmoto, M. P. Nightingale, and M. den Nijs, Phys. Rev. Lett. 49, 405 (1982).
- [52] F. J. Dyson, J. Math. Phys. 3, 1199 (1962).
- [53] A. Hatcher, Vector Bundles and K-Theory, May (Autoedición, 2009).
- [54] A. Kitaev, AIP Conf. Proc. 1134, 22 (2009).
- [55] L. Fu, Phys. Rev. Lett. **106**, 106802 (2011).
- [56] As another case in point, spacetime-inversion-symmetric bands can also have a fragile obstruction that is not identifiable by k-space representations [66].
- [57] T. Ochiai, Phys. Rev. A 96, 043842 (2017).
- [58] Y. Yang, Z. Gao, H. Xue, L. Zhang, M. He, Z. Yang, R. Singh, Y. Chong, B. Zhang, and H. Chen, Nature 565, 622 (2019).
- [59] A. Slobozhanyuk, S. H. Mousavi, X. Ni, D. Smirnova, Y. S. Kivshar, and A. B. Khanikaev, Nat. Photonics 11, 130 (2016).
- [60] M. B. de Paz, M. G. Vergniory, D. Bercioux, A. García-Etxarri, and B. Bradlyn, Phys. Rev. Research 1, 032005 (2019).
- [61] I. Souza, J. Íñiguez, and D. Vanderbilt, Phys. Rev. B 69, 085106 (2004).
- [62] H. C. Po, H. Watanabe, and A. Vishwanath, Phys. Rev. Lett. 121, 126402 (2018).
- [63] J. Cano, B. Bradlyn, Z. Wang, L. Elcoro, M. G. Vergniory, C. Felser, M. I. Aroyo, and B. A. Bernevig, Phys. Rev. Lett. 120, 266401 (2018).
- [64] D. V. Else, H. C. Po, and H. Watanabe, Phys. Rev. B 99, 125122 (2019).
- [65] J. Ahn, S. Park, and B.-J. Yang, Phys. Rev. X 9, 021013 (2019).
- [66] H. C. Po, L. Zou, T. Senthil, and A. Vishwanath, Phys. Rev. B 99, 195455 (2019).
- [67] Z. Song, Z. Wang, W. Shi, G. Li, C. Fang, and B. A. Bernevig, Phys. Rev. Lett. 123, 036401 (2019).

- [68] This can be inferred from the following observation: Intermediate between the two gapped phases is a Weylsemimetallic phase [36], where the energy gap closes at generic and mirror-invariant wave vectors. In the latter case, the gap closing is between Bloch states in the same mirror representation [36].
- [69] A. Alexandradinata and B. A. Bernevig, Phys. Rev. B 93, 205104 (2016).
- [70] The incompatibility is proven in Sec. V A.
- [71] For a tight-binding Hamiltonian whose real-space matrix elements decay exponentially, the projector (to a spectrally isolated band) is analytic [77,98].
- [72] This reflects the anomalous nature of TCI boundary states, namely, that they cannot be continuously deformed to the energy eigenstates of a Hamiltonian defined over 2D real space.
- [73] An equally natural Wannier splitting is given by $P_{a,E} = P_x + P_y$ corresponding to p_x and p_y orbitals on each site. One may also verify that each $g \in G$ permutes $\{P_x, P_y\}$, though a trivial permutation in the $P_{x,y}$ splitting may be nontrivial in the P_{\pm} splitting.
- [74] The proof is elementary: If there exists Wannier functions $\{W_{10,\dots},W_{N0}\}$ that represent $\{P_j=\sum_R|W_{jR}\rangle\langle W_{jR}|\}$ in the Wannier splitting $P=\sum_{j=1}^N P_j$, and if $\hat{g}|W_{j0}\rangle=\lambda_{g,j}|W_{\sigma_g(j),0}\rangle$, with λ a phase factor and σ a permutation on $\{1,\dots,N\}$, then $\hat{g}P_j\hat{g}^{-1}=P_{\sigma_e(j)}$.
- [75] E. Prodan, Phys. Rev. B 80, 125327 (2009).
- [76] C. Brouder, G. Panati, M. Calandra, C. Mourougane, and N. Marzari, Phys. Rev. Lett. 98, 046402 (2007).
- [77] G. Panati, Ann. Henri Poincaré 8, 995 (2007).
- [78] It is sufficient to calculate the first Chern number on three independent slices of the Brillouin zone: $k_x = 0$, $k_y = 0$, and $k_z = 0$. There are standard numerical techniques to calculate the Chern number, e.g., by calculating the winding of the Zak phase.
- [79] Z. Song, S.-J. Huang, Y. Qi, C. Fang, and M. Hermele, Sci. Adv. 5, eaax2007 (2019).
- [80] A. Alexandradinata and J. Höller, Phys. Rev. B 98, 184305 (2018).
- [81] We thank Barry Bradlyn for pointing us to this example.
- [82] This equivalence is valid for d = 2, 3 [76,77], which is assumed throughout this paper.
- [83] M. V. Berry, Proc. R. Soc. Lond A 392, 45 (1984).
- [84] Here we applied that there is no topological obstruction to analytic Bloch functions over the base space S^1 .
- [85] M. Taherinejad, K. F. Garrity, and D. Vanderbilt, Phys. Rev. B 89, 115102 (2014).
- [86] A. Alexandradinata and L. Glazman, Phys. Rev. B 97, 144422 (2018).
- [87] C. Wang, W. Duan, L. Glazman, and A. Alexandradinata, Phys. Rev. B **100**, 014442 (2019).
- [88] G. De Nittis and K. Gomi, J. Geom. Phys. 86, 303 (2014).
- [89] A. Alexandradinata, Z. Wang, B. A. Bernevig, and M. Zaletel, Phys. Rev. B 101, 235166 (2020).
- [90] B. J. Wieder and B. A. Bernevig, arXiv:1810.02373.
- [91] The Zak phase of the hexagonal *k* loops defined in Ref. [31] has a nonzero relative winding that is illustrated in the top-left corner of Fig. 8 in Ref. [31]. The illustrated Zak-phase degeneracies have unit codimension [87] owing to a Wilsonian C_3 -rotation symmetry [39] (visualized in bottom-left corner of Fig. 8 in Ref. [31]). Another way to deduce the obstruction

- is by verifying that the band's symmetry representation in k space is incompatible with any BR of $\tilde{P}3$ [157].
- [92] This follows from $\hat{T}^2 = -I$.
- [93] J. D. Cloizeaux, Phys. Rev. 135, A685 (1964).
- [94] D. J. Thouless, J. Phys. C: Solid State Phys. 17, L325 (1984).
- [95] G. Nenciu, Rev. Mod. Phys. 63, 91 (1991).
- [96] L. Chen, T. Mazaheri, A. Seidel, and X. Tang, J. Phys. A: Math. Theor. 47, 152001 (2014).
- [97] J. C. Budich, J. Eisert, E. J. Bergholtz, S. Diehl, and P. Zoller, Phys. Rev. B 90, 115110 (2014).
- [98] N. Read, Phys. Rev. B 95, 115309 (2017).
- [99] G. Panati and A. Pisante, Commun. Math. Phys. 322, 835 (2013).
- [100] J. Dubail and N. Read, Phys. Rev. B 92, 205307 (2015).
- [101] R. Winkler, Spin-Orbit Coupling Effects in Two-Dimensional Electron and Hole Systems, Springer Tracts in Modern Physics (Springer, New York City, 2003).
- [102] D. Hsieh, Y. Xia, D. Qian, L. Wray, J. H. Dil, F. Meier, J. Osterwalder, L. Patthey, J. G. Checkelsky, N. P. Ong, A. V. Fedorov, H. Lin, A. Bansil, D. Grauer, Y. S. Hor, R. J. Cava, and M. Z. Hasan, Nature 460, 1101 (2009).
- [103] J. C. Y. Teo, L. Fu, and C. L. Kane, Phys. Rev. B 78, 045426 (2008).
- [104] E. P. Wigner, Göttingen Nachr. 31, 546 (1932).
- [105] E. P. Wigner, Group Theory and Its Application to the Quantum Mechanics of Atomic Spectra (Academic Press Inc., New York, 1959).
- [106] In more detail, G_{rj} being isomorphic to G/\mathcal{T}_d means that each element of G_{rj} is a representative of an equivalence class in the coset G/\mathcal{T}_d ; distinct elements of G_{rj} correspond to different equivalence classes in the coset. Therefore, any element in G_{rj} is the composition of an element in G_{r1} with a Bravais-lattice translation; moreover, the extension of G_{rj} (by \mathcal{T}_d) is identical to the extension of G_{r1} ; this holds independent of f.
- [107] To prove this, it is convenient to set the spatial origin at $r_j = \mathbf{0}$, such that any element in G_{rj} is a point-preserving transformation ($\mathbf{0} | \check{g}$ without any translational component. Any element of $G = \mathcal{T}_d \rtimes G_{rj}$ can then be written as ($\mathbf{R} | \check{g}$ for some ($\mathbf{0} | \check{g} \in G_{rj}$ and some \mathbf{R} in the Bravais lattice. Assuming that ($\mathbf{0} | \check{g} | W_{j0} \rangle = \lambda_{\check{g}} | W_{j0} \rangle$ with $\lambda_{\check{g}} \in U(1)$, and applying further the translational property $|W_{jR}\rangle = (e|R)|W_{j0}\rangle$, it follows that $(R|\check{g})|W_{jR'}\rangle = \lambda_{\check{g}}|W_{j,R+R'}\rangle$. Finally, we obtain the desired result: $(R|\check{g})P_j(R|\check{g})^{-1} = \sum_{R'} |W_{j,R+R'}\rangle \langle W_{j,R+R'}| = P_j$. [108] Any element in G_j can be expressed as a product of an el-
- [108] Any element in G_j can be expressed as a product of an element of G_{j,ϖ_j} and a lattice translation. Therefore, Eq. (12) implies $\hat{g}\tilde{\psi}_{jk} = \mathrm{e}^{-is_g\bar{g}k\cdot(g\circ\varpi_j-\varpi_j)}\rho_{g,j} + \tilde{\psi}_{js_g\bar{g}k}$ for $g\in G_j$, which has been shown in Ref. [80] to be a sufficient condition for band representability.
- [109] R. D. King-Smith and D. Vanderbilt, Phys. Rev. B 47, 1651 (1993).
- [110] S. A. Parameswaran, A. M. Turner, D. P. Arovas, and A. Vishwanath, Nat. Phys. 9, 299 (2013).
- [111] H. C. Po, H. Watanabe, M. P. Zaletel, and A. Vishwanath, Sci. Adv. 2, e1501782 (2016).
- [112] H. Watanabe, H. C. Po, and A. Vishwanath, Sci. Adv. 4, eaat8685 (2018).
- [113] M. Hafezi, E. A. Demler, M. D. Lukin, and J. M. Taylor, Nat. Phys. 7, 907 (2011).

- [114] A. B. Khanikaev, S. Hossein Mousavi, W.-K. Tse, M. Kargarian, A. H. MacDonald, and G. Shvets, Nat. Mater. 12, 233 (2012).
- [115] T. Ma, A. B. Khanikaev, S. H. Mousavi, and G. Shvets, Phys. Rev. Lett. 114, 127401 (2015).
- [116] L.-H. Wu and X. Hu, Phys. Rev. Lett. 114, 223901 (2015).
- [117] D. S. Freed and G. W. Moore, Ann. Henri Poincare 14, 1927 (2013).
- [118] K. Shiozaki, M. Sato, and K. Gomi, Phys. Rev. B 95, 235425 (2017).
- [119] What is meant by preserving the symmetry is clarified in Sec. IX B.
- [120] V. Yannopapas, Phys. Rev. B 84, 195126 (2011).
- [121] R. Jackiw and C. Rebbi, Phys. Rev. D 13, 3398 (1976).
- [122] Jin Au Kong, Proc. IEEE 60, 1036 (1972).
- [123] For the E' and E'' notations, refer to the character table in the Appendix of Ref. [5].
- [124] This is demonstrated in Chap. 8 of Ref. [185].
- [125] H. Nielsen and M. Ninomiya, Phys. Lett. B 130, 389 (1983).
- [126] X. Wan, A. M. Turner, A. Vishwanath, and S. Y. Savrasov, Phys. Rev. B 83, 205101 (2011).
- [127] G. B. Halasz and L. Balents, Phys. Rev. B 85, 035103 (2012).
- [128] C. Fang, M. J. Gilbert, X. Dai, and B. A. Bernevig, Phys. Rev. Lett. 108, 266802 (2012).
- [129] S. Murakami, New J. Phys 9, 356 (2007).
- [130] L. Muechler, A. Alexandradinata, T. Neupert, and R. Car, Phys. Rev. X 6, 041069 (2016).
- [131] T. Ochiai, J. Opt. Soc. Am. B 35, 2642 (2018).
- [132] J. von Neumann and E. Wigner, Phys. Z. 30, 467 (1929).
- [133] Q. Yan, R. Liu, Z. Yan, B. Liu, H. Chen, Z. Wang, and L. Lu, Nat. Phys. 14, 461 (2018).
- [134] Y. Zhou, K. M. Rabe, and D. Vanderbilt, Phys. Rev. B 92, 041102(R) (2015).
- [135] W. A. Benalcazar, B. A. Bernevig, and T. L. Hughes, Science 357, 61 (2017).
- [136] Z. Song, Z. Fang, and C. Fang, Phys. Rev. Lett. 119, 246402 (2017).
- [137] F. Schindler, A. M. Cook, M. G. Vergniory, Z. Wang, S. S. P. Parkin, B. A. Bernevig, and T. Neupert, Sci. Adv. 4, eaat0346 (2018).
- [138] C. Callan and J. Harvey, Nuclear Phys. B 250, 427 (1985).
- [139] M. F. Atiyah, *K-theory* (W. A. Benjamin, New York, Amsterdam, 1967).
- [140] The universal bundle theorem in Ref. [139] applies to \mathcal{P} -vector bundles with finite group \mathcal{P} . For G-vector bundles with G a space group, we observe that the translation subgroup of G acts trivially on the bundle, hence we may directly apply the universal bundle theorem with \mathcal{P} identified as the (finite) point group of G.
- [141] Except for the term 2Q', H_b is identical to a model of an insulator-vacuum interface proposed in Ref. [186].
- [142] J. E. Moore, Y. Ran, and X.-G. Wen, Phys. Rev. Lett. 101, 186805 (2008).
- [143] A. Alexandradinata, A. Nelson, and A. A. Soluyanov, Teleportation of berry curvature on the surface of a Hopf insulator, arXiv:1910.10717.
- [144] L. Fu, C. L. Kane, and E. J. Mele, Phys. Rev. Lett. 98, 106803 (2007).
- [145] J. E. Moore and L. Balents, Phys. Rev. B **75**, 121306(R) (2007).

- [146] R. Roy, Phys. Rev. B 79, 195322 (2009).
- [147] D. Hsieh, D. Qian, L. Wray, Y. Xia, Y. S. Hor, R. J. Cava, and M. Z. Hasan, Nature 452, 970 (2008).
- [148] S.-Y. Xu, C. Liu, N. Alidoust, M. Neupane, D. Qian, I. Belopolski, J. D. Denlinger, Y. J. Wang, H. Lin, L. A. Wray, G. Landolt, B. Slomski, J. H. Dil, A. Marcinkova, E. Morosan, Q. Gibson, R. Sankar, F. C. Chou, R. J. Cava, A. Bansil, and M. Z. Hasan, Nat. Commun 3, 1192 (2012).
- [149] Y. Tanaka, Z. Ren, T. Sato, K. Nakayama, S. Souma, T. Takahashi, K. Segawa, and Y. Ando, Nat. Phys 8, 800 (2012).
- [150] K. Shiozaki, M. Sato, and K. Gomi, Phys. Rev. B 91, 155120 (2015).
- [151] C. Fang and L. Fu, Phys. Rev. B 91, 161105(R) (2015).
- [152] K. Shiozaki, M. Sato, and K. Gomi, Phys. Rev. B 93, 195413 (2016).
- [153] P.-Y. Chang, O. Erten, and P. Coleman, Nat. Phys. **13**, 794 (2017).
- [154] J. Ma, C. Yi, B. Lv, Z. Wang, S. Nie, L. Wang, L. Kong, Y. Huang, P. Richard, P. Zhang, K. Yaji, K. Kuroda, S. Shin, H. Weng, B. A. Bernevig, Y. Shi, T. Qian, and H. Ding, Sci. Adv. 3, e1602415 (2017).
- [155] X.-Y. Dong and C.-X. Liu, Phys. Rev. B 93, 045429 (2016).
- [156] M. G. Vergniory, L. Elcoro, C. Felser, N. Regnault, B. A. Bernevig, and Z. Wang, Nature 566, 480 (2019).
- [157] Z. Song, L. Elcoro, N. Regnault, and B. A. Bernevig, Phys. Rev. X 10, 031001 (2020).
- [158] J. May, Topol. Its Appl. 153, 605 (2005).
- [159] J. F. Adams, Stable Homotopy and Generalised Homology (University of Chicago Press, Chicago, 1974).
- [160] R. A. Evarestov and V. P. Smirnov, Phys. Stat. Sol 122, 231 (1984).
- [161] H. Bacry, Commun. Math. Phys. 153, 359 (1993).
- [162] L. Michel and J. Zak, Europhys. Lett. 50, 519 (2000).
- [163] D. Gresch, G. Autès, O. V. Yazyev, M. Troyer, D. Vanderbilt, B. A. Bernevig, and A. A. Soluyanov, Phys. Rev. B 95, 075146 (2017).
- [164] J. Ahn, D. Kim, Y. Kim, and B.-J. Yang, Phys. Rev. Lett. 121, 106403 (2018).
- [165] The symmetry must be antiunitary, square to the identity, and have a trivial action in k space.

- [166] It is worth remarking that having a nontrivial second Stiefel-Whitney class also does not generally obstruct band representability [66]—except for rank-two bands, which are better classified by the Euler class anyway [65,164].
- [167] M. Reed and B. Simon, Methods of Modern Mathematical Physics. IV, Analysis of Operators (Academic Press, San Diego, 1978).
- [168] See the Kato-Rellich theorem in Ref. [167].
- [169] H. Grauert, Math. Ann. 135, 263 (1958).
- [170] A. Huckleberry, arXiv:1303.6933.
- [171] C. J. Bradley and B. L. Davies, Rev. Mod. Phys. 40, 359 (1968).
- [172] H. G. Bray and M. Weinstein, *Between Nilpotent and Solvable* (Polygonal, Passaic, 1982), p. 231.
- [173] P.-O. Löwdin, J. Chem. Phys. 18, 365 (1950).
- [174] J. C. Slater and G. F. Koster, Phys. Rev. 94, 1498 (1954).
- [175] H. Bacry, L. Michel, and J. Zak, *Group Theoretical Methods in Physics*, Lecture Notes in Physics, Vol. 313 (Springer, Berlin, Heidelberg, 1988), p. 289.
- [176] The original work is found in Ref. [187]. An English translation and proof can be found in Theorem 3.10, Chap. 2 of Ref. [172].
- [177] S. L. Altmann and H.-R. William, Phil. Trans. Roy. Soc. London Ser. A 255, 216 (1963).
- [178] See pp. 220–222 of Ref. [177].
- [179] See Theorem 52.2 in Ref. [188].
- [180] See p. 222 of Ref. [177].
- [181] See p. 228 of Ref. [177].
- [182] G. F. Koster, Properties of the Thirty-two Point Groups (MIT Press, Boston, 1963).
- [183] See Example 5 on p. 57 of Ref. [172], where we used that *T* is isomorphic to the alternating group and *O* to the symmetric group of four elements.
- [184] See Example 2 on pp. 54–55 of Ref. [172].
- [185] B. A. Bernevig and T. L. Hughes, *Topological Insulators and Topological Superconductors* (Princeton University Press, Princeton, 2013).
- [186] L. Fidkowski, T. S. Jackson, and I. Klich, Phys. Rev. Lett. 107, 036601 (2011).
- [187] B. Huppert, Nagoya Math. J. 6, 93 (1953).
- [188] C. W. Curtis and I. Reiner, *Representation Theory of Finite Groups and Associative Algebras* (Interscience Publishers, New York, 1962).